PREPARATION, CHARACTERIZATION AND PERFORMANCE EVALUATION OF MONOLITH BASED ZEOLITE COATED CATALYST FOR THE CONVERSION OF METHANOL TO PROPYLENE

BY

Muhammad Haris

A Thesis Presented to the
DEANSHIP OF GRADUATE STUDIES

KING FAHD UNIVERSITY OF PETROLEUM & MINERALS

DHAHRAN, SAUDI ARABIA

In Partial Fulfillment of the
Requirements for the Degree of

MASTER OF SCIENCE

In

CHEMICAL ENGINEERING

December 2015

KING FAHD UNIVERSITY OF PETROLEUM & MINERALS

DHAHRAN- 31261, SAUDI ARABIA

DEANSHIP OF GRADUATE STUDIES

This thesis, written by **Muhammad Haris** under the direction his thesis advisor and approved by his thesis committee, has been presented and accepted by the Dean of Graduate Studies, in partial fulfillment of the requirements for the degree of **MASTER OF SCIENCE IN CHEMICAL ENGINEERING.**

Dr. Nadhir A.H. Al-Baghli
(Advisor)

Dr. Mohammed Ba-Shammakh
Department Chairman

Dr. Shakeel Ahmed
(Co Advisor)

Dr. Salam A. Zummo
Dean of Graduate Studies

Dr. Zuhair Omar Malaibari
(Member)

22/12/15
Date

Dr. Mohammad M. Hossain
(Member)

Dr. Basim Ahmed Abussaud
(Member)

This work is dedicated to my beloved parents, brothers, teachers and children (Aisha binte Haris & Muhammad Qasim)

ACKNOWLEDGMENTS

"In the name of Allah, the Most Merciful and the Most Gracious"

All praise and thanks to Almighty Allah who provided me the opportunity, ability and knowledge to complete the master degree in Chemical Engineering. I am greatly thankful to Chemical Engineering department of King Fahd University of Petroleum and Minerals for providing me the scholarship and research facility to carry out this work.

I would like to extend my sincere thanks and appreciations to Dr. Nadhir A.H. Baghli who supported as my thesis advisor and his helpful guidance to the accomplishment of this research. I acknowledge the sincere efforts of my co-advisor Dr. Shakeel Ahmed for teaching me the philosophy of research and his technical support. I am greatly thankful to Dr. Zuhair Omer Malaibari for his valuable contribution throughout this research. I am also obliged to Dr. M. Mozahar Hossain for giving access to his lab facility and his valuable time. I must also gratitude to Dr. Basim Ahmed Abussaud for his support and guidance.

I would like to thank Dr. Mohammad Ashraf Ali for his help during the initial phase of installation & commissioning of fixed bed reactor system and providing the financial assistance in this research. I am also thankful to Mr. Yasir Khan, Mr. Uwais and Mr. Nisar for helping me in lab work.

My sincere admiration is devoted to my mother (May Allah grant her peace and give her blessings, Ameen). The moral support and back-up support received from my family in the duration of my studies at KFUPM are deeply appreciated.

TABLE OF CONTENTS

LIST OF TABLES

LIST OF FIGURES

LIST OF ABBREVIATIONS

MTH	:	Methanol-to-Hydrocarbons
MTG	:	Methanol-to-Gasoline
MTO	:	Methanol-to-Olefin
MTP	:	Methanol-to-Propylene
WHSV	:	Weight Hourly Space Velocity
TOS	:	Time on Stream
BTX	:	Benzene, Toluene and Xylene
SEM	:	Scanning Electron Microscopy
EDX	:	Energy Dispersive X-ray
XRD	:	X-Ray Diffraction
TGA	:	Thermo-Gravimetric Analysis
BET	:	Braunauer – Emmett – Teller
TPD	:	Temperature Program Desorption
HTP	:	High Temperature Peak
LTP	:	Lower Temperature Peak
FCC	:	Fluidized Catalytic Cracking
DME	:	Dimethyl Ether
FBR	:	Fixed Bed Reactor
GC	:	Gas Chromatograph
TCD	:	Thermal Conductivity Detector
FID	:	Flame Ionization Detector
DI	:	Deionized

ABSTRACT

Full Name : Muhammad Haris

Thesis Title : Preparation, Characterization and Performance Evaluation of Monolith based Zeolite Coated Catalyst for the Conversion of Methanol to Propylene.

Major Field : Chemical Engineering

Date of Degree : December 2015

Propylene was produced from methanol using both pelletized and monolith coated ZSM-5 with silica to alumina (SiO_2/Al_2O_3) molar ratio of 30, 50, 80, 280, and 410. Reaction data was collected using a fixed bed reactor at 1 atm, 500 $^{\circ}$C, and weight hourly space velocity (WHSV) of 11, 15, and 19 h^{-1}. The results reveal that the yield and the selectivity of propylene ranged from 9 to 20% and 25 to 48%, respectively. The maximum yield and selectivity of propylene were obtained for the pelletized ZSM-5 with SiO_2/Al_2O_3 molar ratio of 280. The ZSM-5 with SiO_2/Al_2O_3 molar ratio of 280 was coated with 2 wt. % binder through dip coating method. The results indicate considerable improvements in both the yield and the selectivity of propylene. The surface properties of the pelletized and the prepared monolith catalysts were characterized using the NH_3-Temperature Program Desorption (NH_3-TPD), the Scanning Electron Microscope (SEM), the X-Ray Diffraction (XRD), the Energy Dispersed X-Ray Spectroscopy (EDX), the N_2 Adsorption/ Desorption, and the Thermogravimetric Analysis (TGA). The NH_3-TPD results showed that the acidity decreases by increasing the silica to alumina ratio. The XRD analysis of the coated monolith catalyst confirmed that the crystallinity of ZSM-5 is preserved during the coating process. The SEM images revealed a uniform catalyst coating in the channels of the

monolith structure. The high yield and selectivity of propylene on the monolith catalyst are attributed to the reduction of internal mass transfer resistances in the monolith; which consequently accelerated the rate of desorption of propylene and other olefins. The fast desorption of the products also reduced the coke formation on the catalyst.

ملخص الرسالة

الاسم الكامل: محمد حارث

عنوان الرسالة: تحضير وتشخيص وتقييم كفاءة المنليث المغلف بمحفر الزيوليت لتحويل الميثانول للبروبالين.

التخصص: الهندسة الكيميائية

تاريخ الدرجة العلمية: ربيع الاول – ١٤٣٧

تم انتاج البروبالين من الميثانول باستخدام حفاز ال ZSM-5 بصيغته الاصلية بنسب سيلكا الي امونيا تراوحت من 30 الى 410. تم تجميع معلومات التفاعل من مفاعل ثابت تحت ضغط جوي واحد ودرجة حرارة 500 درجة موية وسرعة تدفق وزنية 11, 15, و 19 1/ساعة. اظهرت النتائج ان معدل انتاج البروبالين تراوحت بين 9 الى 20 بالمئة بينما تراوحت معدلات الانتقائية من 25 الى 48%. كما اظهرت النتائج ان الحد الاقصى لأنتاج وانتقائية البروبالين كان للحفاز المحتوي على 280 جزيء سيلكا لكل جزيء المنيوم. تم طلاء هذا الحفاز بلاصق بنسبة مؤية 2%. اظهرت النتائج تحسن واضح في قيم الانتاج والانتقائية للبربيلين للحفاز المطلي بنسبة الى الحفاز غير المطلي. تم فحص الخصائص السطحية لجميع الحفازات المحضرة باستخدام تقنيات (NH_3- TPD) (SEM) (XRD) (EDX) و (الادمصاص النيتروجيني) و (TGA) . اظهرت نتائج فحص الي (NH_3-TPD) ان حامية السطع تقل عند زيادة نسبة السيليكا للألومينا في جميع العينات. كما اكدت نتائج فحص ال XRD بوضوح انه تم خفض بلورية الزيرلات المطلي. كذلك عكست النتائج فحص SEM تناسق الطلاء خلال قنوات الحفاز المطلي . اثبتت النتائج ان زيادة معدل الانتاج والانتقائية يؤدي لخفض المقاومة الداخلية لانتقال المادة خلال فتحات الحفاز المطلي وكان لهذا دور بارز في تسارع عملية تفريغ البروبلين عند انتاجه على سطح الحفاز.

CHAPTER 1

INTRODUCTION

Propylene and Ethylene have a dominant position in chemical industry, they are major building block for the modern petrochemical industry. The demand for these light olefins is increasing globally day by day which results in increase in prices [1]. The majority of olefins consumption is driven by the production of polymers including polyethylene and polypropylene in addition to other important derivatives such as ethylene dichloride, ethylene oxide, propylene oxide, polystyrene, acrylic acid and acrylonitrile. The foremost use of propylene is in production of polypropylene which is actually the two-third of global consumption of propylene. Polypropylene is mainly consumed in production of plastics which is necessity in almost every field; form the beverages we drink to the clothes we wear [2,3]. In application of chemical industry, the global consumption of propylene is projected to increase by 4.5 % annually, global propylene market is expected to grow by 33 million metric ton by year 2021. On purpose propylene production are the newly developed methods for the production of propylene. These newly developed commercial methods for propylene production will supply 25% of global propylene by 2021. Production of on purpose propylene is filling the gap between projected demand and generation which is shown in Figure 1.1 [4].

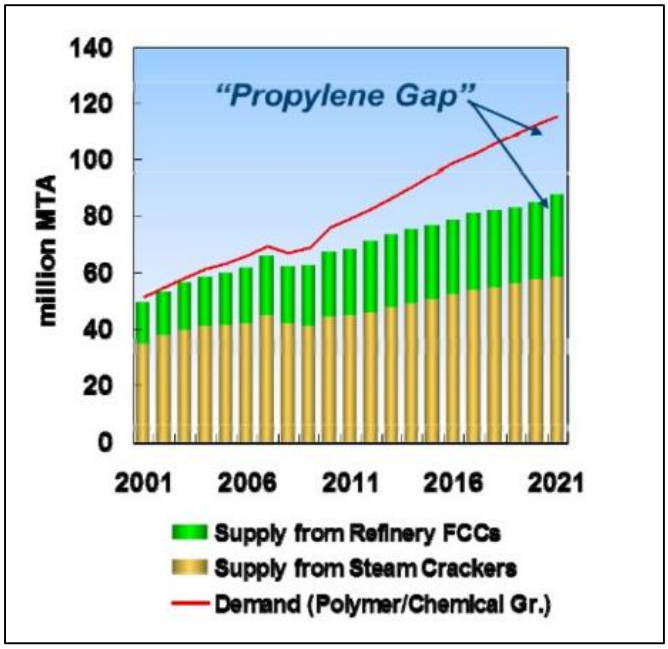

Figure 1-1: Global propylene supply & demand [4]

Steam cracking produces propylene as a byproduct which contributes to 66% of worldwide propylene production. In addition to that, 32% of propylene production is supplied by fluidized catalytic cracking (FCC) [5]. The primary product produced by FCC units is gasoline while propylene is produced as a by-product. The rest of 2% of the propylene is produced from propane dehydrogenation or metathesis [5]. The global propylene production is currently about half that of ethylene production [5,6]. Demand for these light olefins is predicted to be increased in coming decades. The demands for ethylene and propylene increase at dissimilar rates. Globally, the propylene demand is predicted to increase by 6 to 8% per year, which exceeds the predicted growth in global ethylene demand of 4 to 6% per year [5,6]. As the predicted rate in ethylene growth is lower than that in propylene growth, the conventional steam cracking technology itself will not be able to meet the demand for propylene. It is estimated that 10% of propylene produced,

equivalent to 10 million tons, will have to come from other technologies [5]. In this respect, methanol conversion will act as an important alternative for on-purpose propylene production.

Methanol is the simplest alcohol, with a chemical formula of CH_3OH. Methanol can be produced by synthesis gas, which is basically produced by steam reforming of natural gas or it can also be produced by the gasification of carbonaceous materials including coal, recycled plastics, municipal wastes, or other organic materials [7]. Direct use of methanol is commercially common in blending with gasoline or methanol is also used as a potential motor fuel, this direct use of methanol is not economical because it requires a heavy investment to deal with the problems related to processing [8].

The discovery of methanol-to-hydrocarbons (MTH) reaction was accidental, one group at Mobil was working to use ZSM-5 catalyst to convert methanol to other oxygen-containing compounds, and they obtained unexpected hydrocarbons. Independently, another Mobil group was also trying for the alkylation of isobutene with methanol by using ZSM-5 catalyst, they observed that isobutane was completely unreactive, and a mixture of paraffins and aromatics in the gasoline boiling range was solely formed from methanol [9]. There are some insufficiencies in the existing technologies for the conversion of Methanol to light olefins, The catalyst like SAPO-34 used in Hydro Methanol-to-Olefin (MTO) technology has very narrow opening due to which ethylene selectivity increases as compared to propylene and it gives the higher deactivation rate [8]. In most of the catalytic process shape and size selectivity is the dynamic consideration. Normally, selectivity based on either the shape or size of the reactants or products. Catalyst having the uniform pores with molecular dimension can provide such shape/size selective behavior. Zeolite are

highly ordered structure which gives the uniform porosity. They have such a crystalline network that adsorbs the specific molecules and exclude the others [10].

To achieve good mass transfer small crystal size of zeolites can be used. Although, reduced size of crystal pellets increase the mass transfer, it can result in higher pressure drop in the reactor. This problem can be overcomed by using macroporous support coated with the zeolite. Shape of the catalyst affects the residence time distribution of the catalyst which results in change in catalyst selectivity. A well designed structured catalyst results in a more stable and better selectivity of the catalyst system [11]. Many types of structured support materials have been used depending upon the reaction types and objective. Support material affects the mass and heat transfer properties, pressure drop and conversion. Inert structure are coated by depositing the zeolite particles to obtain an active catalyst. Main types of coating techniques used for the deposition of zeolite are dip coating, spin coating and slip coating [12,13].

In overall reaction path of the methanol conversion, methanol is first converted into dimethyl ether which then reacts further to produce olefins, alkanes, aromatics and water as shown in the following reaction scheme.

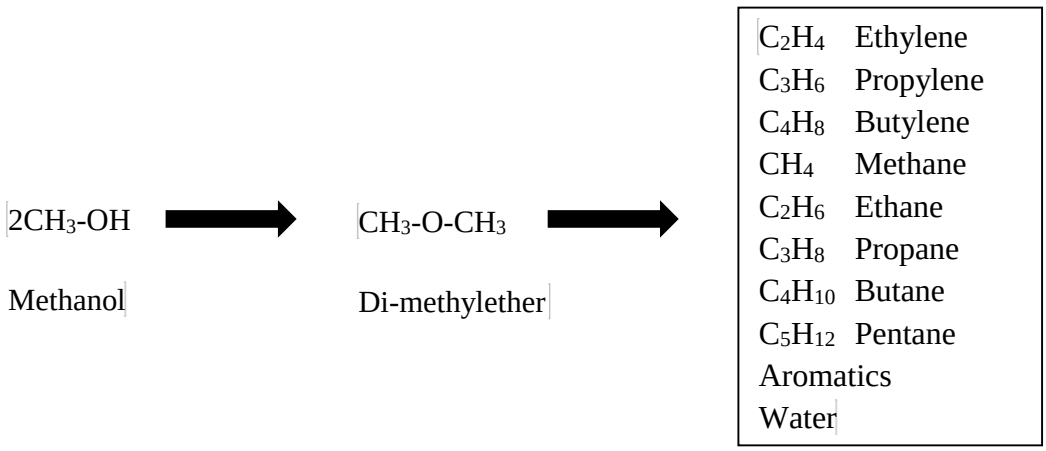

1.1 Research Strategy

The focus of thesis will be to provide an insight about the properties of structured catalysts that are involved in the production of light olefins particularly propylene. For this purpose, ZSM-5 zeolites with different SiO_2/Al_2O_3 ratios were characterized and evaluated in a fixed bed flow reaction system. ZSM-5 zeolite catalyst of specific SiO_2/Al_2O_3 ratio which gives higher propylene selectivity was further coated on a cordierite monolith structure. The synthesized ZSM-5 monolith structure catalysts was characterized and evaluated for the methanol to propylene reaction in continuous flow mode.

To carry out this research work, initially a fixed bed reactor with online GC is installed and commissioned according to the requirements of methanol to propylene reaction system. ZSM-5 zeolite with SiO_2/Al_2O_3 of 30, 50, 80, 280 and 410 were characterized. Initials runs were carried out in a fixed bed flow reaction system coupled with online GC (FID-TCD). Catalyst performance was optimized through tuning the reaction conditions such as temperature, pressure, feed rate, cooling water temperature, carrier gas flow rates and catalyst weight/inert SiC ratio. ZSM-5 zeolite catalyst of a particular SiO_2/Al_2O_3 ratio was selected on the basis of higher propylene selectivity and conversion.

In the 2nd phase of this work the selected ZSM-5 was coated on cordierite monolith to produce hydrothermally and mechanically stable structured catalyst. The synthesis of this structure catalyst was carried out using the dip coating method followed by drying and calcination steps. ZSM-5 coated monolith structured catalyst was characterized and evaluated in the fixed bed flow reactor having the facility to deal with the structure of 22.5 inch diameter shaped catalyst. The synthesized catalyst was evaluated for the conversion

of methanol to propylene. Total effluent from the reactor was separated into gas and liquid streams and analyzed by online GC-TCD and FID system.

1.2 Objectives of the Study

The main objective of this study is to enhance the propylene production from methanol by using the diverse catalytic properties of ZSM-5 zeolite and its use as a coating on monolith structure.

The detailed objectives are:

- To evaluate ZSM-5 zeolite catalyst pellets with different SiO_2/Al_2O_3 ratios for the selection of the best catalyst on the basis of propylene selectivity.
- To prepare the coated structure catalyst on monolith using the best performing ZSM-5 SiO_2/Al_2O_3 ratio catalyst.
- To characterize the pelletized and structure coated catalyst using techniques such as XRD, NH_3- TPD, SEM, EDX, N_2 adsorption isotherm analysis and TGA.
- To evaluate performance of the structure coated catalysts for methanol to propylene conversion in a fixed bed flow reaction system.

CHAPTER 2

LITERATURE REVIEW

2.1 History

The catalysis of methanol-to-hydrocarbons (MTH) includes the processes to make hydrocarbon products from methanol. The conversion of Methanol to Hydrocarbon was discovered accidently by Mobil's research division in 1970, when they were working to produce high octane gasoline form methanol and isobutane over zeolite catalyst. They thought that highly branched higher alkanes were formed when methanol would be added to isobutane but they are surprised to see that a wide range of hydrocarbons were formed. [8,14,15]. Energy crisis at that time provided the favorable conditions for research in alternative fuels and chemicals, simulating the advancement on newly developed this methanol process [8]. Methanol-to-gasoline (MTG) catalysis was also one of the product of this research, it was first patented by Mobil Oil Corporation and accepted in 1976 [16] and released in peer-reviewed literature in 1977 [14]. Soon after the discovery, the development of the process have led to bench-scale and pilot-scale demonstration plants. Using Mobil's MTG process, the first plant was built by Mobil in New Zealand and commercialized in 1985, with production of 14500 barrels per day (about 30% of the country's need) of gasoline. In this commercialized process, methanol is mainly converted to gasoline range hydrocarbons (C5+) by using the medium pore zeolite H-ZSM-5 [15,17].

Methanol to Hydrocarbon process chemistry has been studied for decades over several zeolite and Zeotype materials. Depending on the catalyst topology and process parameters used, a wide range of product distribution could be obtained during the MTH reaction [17]. In this research area, the catalysis of methanol remained an important research topic. This has led to several articles and patents on methanol conversion over zeolite materials particularly Methanol to Olefins (MTO) process that has gained more interest in the industry due to world demand for polyolefin was increasing [15,17]. Figure 2.1 illustrates MTO production through upgrading of coal, natural gas and oil.

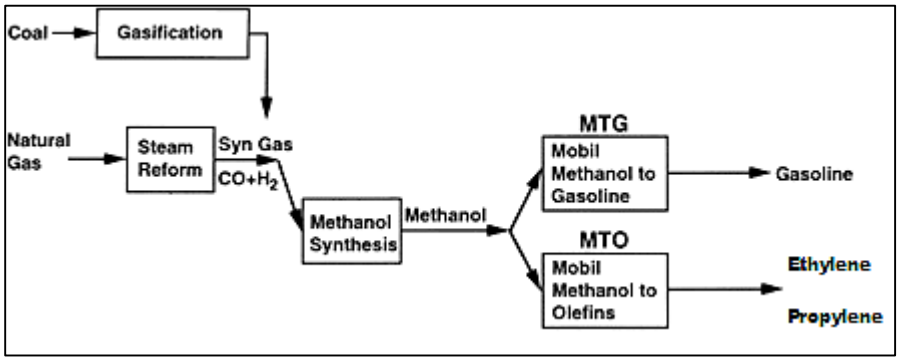

Figure 2-1: Olefins production route through methanol [9]

MTO process was successfully developed in 1990s by UOP in cooperation with Norsk Hydro by applying a small pore Zeotype material, SAPO-34 in a low pressure reactor. In this process methanol is converted to light alkenes, mainly ethylene and propylene. The narrow pores of the material restrict diffusion of large hydrocarbons. MTO favors the products propylene and ethylene as opposed to larger olefins like pentanes and aromatics

also. This technology utilizes methanol on acidic zeolites to produce olefin monomers. To accomplish this target, the reaction conditions are altered and the catalyst is switched.

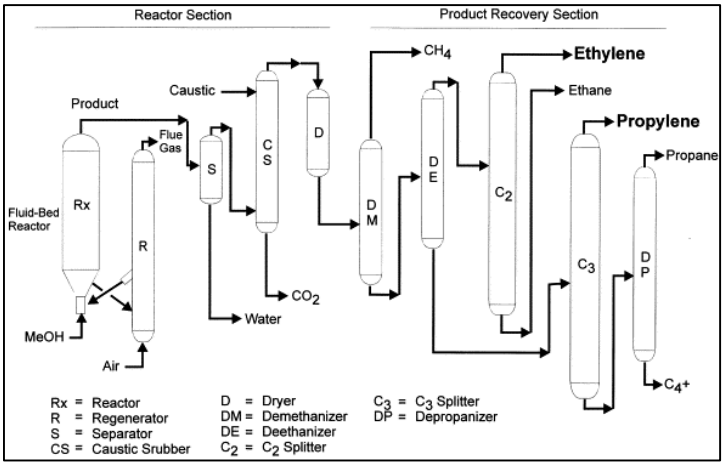

Figure 2-2: Process flow scheme of the UOP/Norsk Hydro MTO process [18]

2.2 Methanol Production

Methanol is produced by synthesis technology in which carbon sources like natural gas [19], coal [20] and biomass [21] can be used. Even CO_2 is also considered to be the future carbon source [22,23]. Methanol is produced from any of the carbon source mentioned above, it is the highly relevant chemical intermediate. Synthesis gas (syn gas) is the most common feedstock for the industrial production of methanol. Syn gas is a combination of carbon dioxide, hydrogen and carbon monoxide and it is formed by steam reforming of natural gas [3]. Worldwide methanol production is nearly 12 billion gallons, with roughly 10% produced in the United States [24].

2.3 Methanol to Propylene

The methanol to propylene (MTP) process is catalyzed using ZSM-5 catalyst. In this case, methanol is converted to propylene with some by-product gasoline and LPG type fuels. The selectivity of the process is optimized towards propylene by high temperature and low pressure employed during the reaction, as well as recycling of the heavier hydrocarbons [25].

H-ZSM-5 is used commercially in both MTG and MTP processes. As indicated by the process names, there is some variability in possible product distributions. Typically, reaction conditions for MTG involve “lower” temperatures (623-683 K) and a pressure of around 20 bar. MTP is performed at “higher” temperatures (733-753 K) and close to atmospheric pressure [26]. Lurgi developed H-ZSM-5 based fixed-bed MTP technology to maximize propylene production, whereas the development course of H-SAPO-34 based fluidized-bed MTO technologies for the production of both ethylene and propylene [27].

As shown in Figure 2-3, in the pre-reactor, methanol is partly dehydrated, the mixture of methanol and dimethyl ether is then fed into an adiabatic fixed-bed quench reactor via inter-stage feeding to control the temperature. Silicon rich H-ZSM-5 based catalyst was used to achieve the high selectivity to propylene. After conversion, the reactor effluent is fractionized in which undesired products like ethylenes, butylenes and higher aliphatic products were simply recycled to the methanol conversion reactor for further production of propylene. The production facility consists of three parallel fixed-bed reactors which enable intermittent regeneration [27].

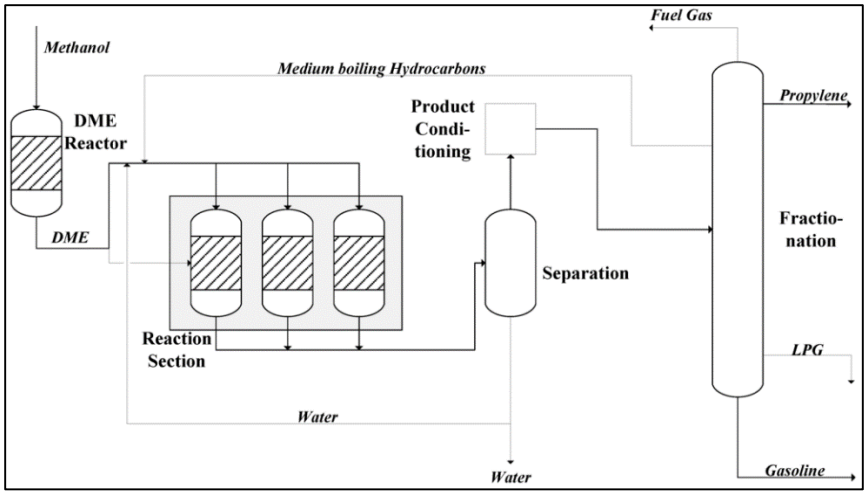

Figure 2-3: A simplified scheme of Lurgi's MTP process [26]

In 2010, the first MTP plant was brought on stream in China with an annual capacity of 500000 tons of propylene per year and 185000 tons gasoline per year as the main by-product [27]. By using ZSM-5 catalyst, Lurgi's process can get nearly 70% propylene selectivity from Dimethyl Ether (DME). Lurgi used fixed bed reactor in olefin synthesis reaction from DME. So, a large amount of heat of formation from exothermic reaction of methanol dehydration can be avoided by fixing methanol to dimethyl ether process. The commercial project with olefin yield of nearly 100,000 ton per year based on Lurgi's process has been constructed in Iran [28].

2.4 Zeolites

The zeolites are aluminosilicates, crystalline in nature having three-dimensional framework that consists of channels, pores, and cages which gives higher internal surface areas. The pore sizes ranges from 5-20 Å and this property makes them quite useful as

molecular sieves. In comparison to their amorphous counterparts, zeolites are highly uniform and this increases the stability and tolerance to high temperature especially in the presence of water [29]. About 170 different topologies are currently known but the new unique variations are frequently reported. Zeolites are known by their topologies which are designated by a three-letter framework type codes [30,31].

Figure 2-4 illustrates examples of selected zeolite structures along with their pore systems. The zeolite pore size is mainly determined by the number of T-atoms defining the entrance (ring-size) to the interior of the crystal. Zeolites can be distinguished on the basis of pore size, it has small pore surrounded by 8 T-atoms or medium, pore surrounded by 10 T-atoms, large pore surrounded by 12 atoms and extra-large pore structures which is surrounded by more than 12 T-atoms [32]. According to some, zeolites are known as mineral consisting of TO4 tetrahedral formed into frameworks with open cavities and according to others, only the structures consisting of Si and Al as true zeolites [33,34]. The pores in zeolites can be one-dimensional like ZSM-12 and ZSM-22 [35], two-dimensional like MCM-22 [30] or three dimensional like ZSM-5 and Faujasite [35]. The Crystal sizes play important role in application of zeolites as catalyst. For example, catalyst effectiveness for smaller crystals is higher but recovery of these smaller crystals would not be easy. Those catalytic reactions which are shape selective requires larger crystals but the deactivation may be severe and regeneration of used catalyst can be more difficult for larger crystal [36].

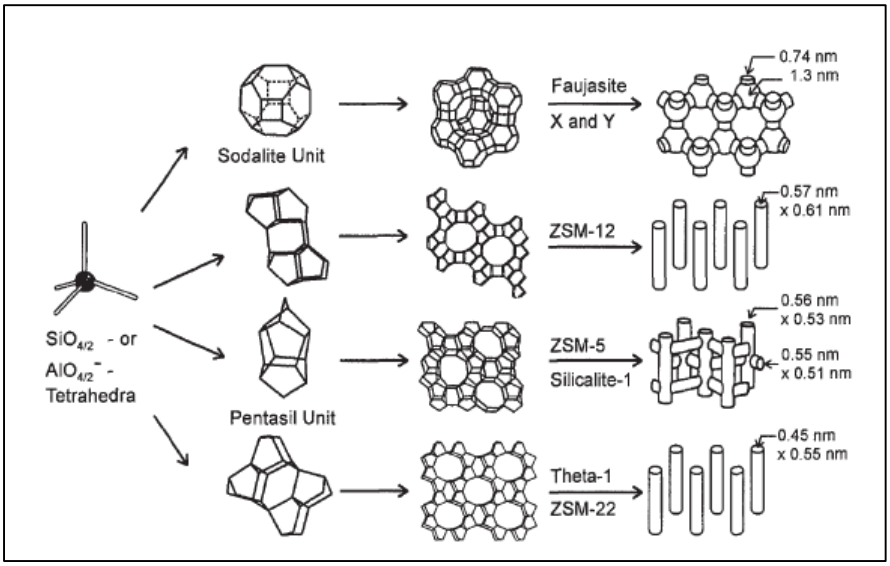

Figure 2-4: Structures of zeolites and their micropore system [35]

2.4.1 Zeolite Catalysts

Zeolite catalyst are used in oil refineries, gas separation, and ion exchange [37–40]. However, considering market values, the catalytic application of zeolites is the most important. The possibility of generating functionality within the zeolite pores make them attractive for wide range of applications. Such functionality may have acid, base, redox or bifunctional properties, and act as active site to catalyze numerous reactions [41]. The wide application of zeolites is due to its high surface area, defined crystal structures, high thermal stability, possibility of modulating active sites (including the incorporation of metal sites to the lattice) and the shape selectivity brought about by their pores of molecular dimensions. [42]

2.4.2 Shape selectivity by Zeolite

Shape selectivity is often divided into three types as shown schematically in Figure 2.5 Reactant selectivity occurs when reactants are too large to enter the channels of the zeolite, transition state prevents the formation of too large to exist inside the pore and product selectivity prevents the formation of too large to diffuse out of the crystal [43]. If the molecules formed inside the zeolitic pores are too large to diffuse out of them, these must react further to species that are able to leave the structure. It is important to keep in mind that the shape selectivity only occurs in the bulk volume of zeolitic material. It means that if the crystals are small and the shape selectivity is less effective, than the reactions takes place on the surface or in the pore mouths [44].

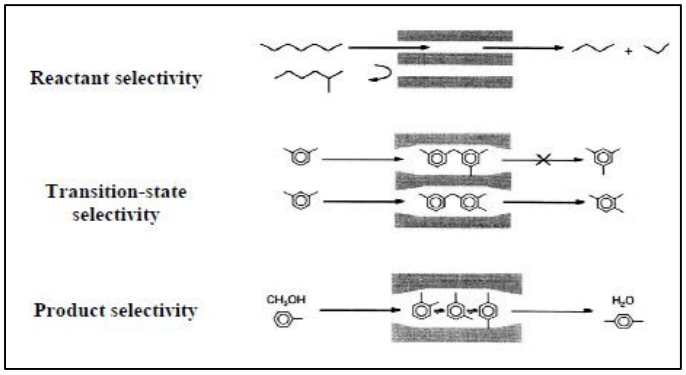

Figure 2-5: The three type of reaction selectivity imposed by zeolite [43]

2.4.3 Synthesis of Zeolite

Zeolites synthesis is carried out under hydrothermal conditions. The sources of silicon and aluminum dissolved in aqueous solution of alkali hydroxide and structure directing agent (SDA). Zeolites are metastable and the final synthesis product is determined by factors like

nature, concentrations of reactants and conditions in which it is to be synthesized like temperature, crystallization time, and pH. The hydrothermal synthesis of zeolites is often carried out in autoclave at elevated temperature and autogenous pressure. There is a consecutive steps for the nucleation of phase(s) through which crystallization normally occurs from the solution [46]. The final crystal size obtained depends upon the ratio between nuclei growth rate and the nucleation rate[36]. The zeolite crystallization process is dependent on a number of parameters such as: ageing of the synthesis gel [47], solubility of silicon [48], crystallization temperature [49], and addition of seed crystals [50].

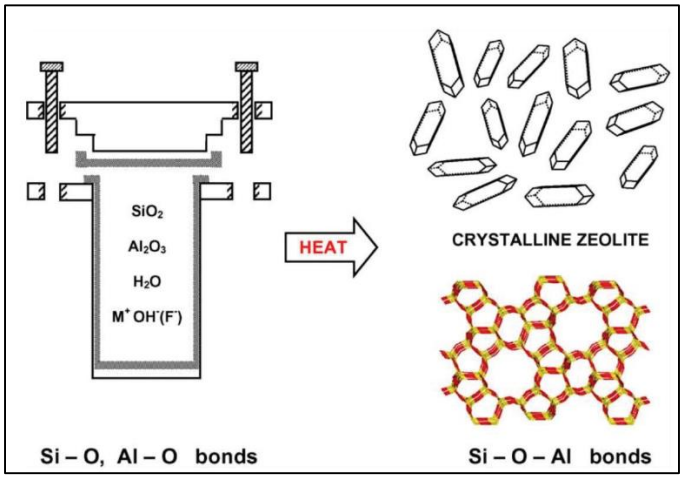

Figure 2-6: Illustration of hydrothermal zeolite synthesis [51]

2.4.4 ZSM-5

ZSM-5 is a synthetic zeolite with MFI topology. ZSM-5 is a three-dimensional medium-pore zeolite with 10 T-atom pores and two sets of channels that run perpendicular to one another. The channel diameter is large enough to easily accommodate diffusion of large molecule (see Figure 2.7). Acid site density can vary on ZSM-5, and is controlled by

altering the amount of aluminum available during synthesis. Commercially available from Zeolyst International, ZSM-5 can be purchased with aluminum contents ranging from SiO_2/Al_2O_3 = 30 to SiO_2/Al_2O_3 = 280. ZSM-5 is used in a variety of isomerization and disproportionation reactions, ZSM-5 has also been used to make synthetic gasoline [52,53].

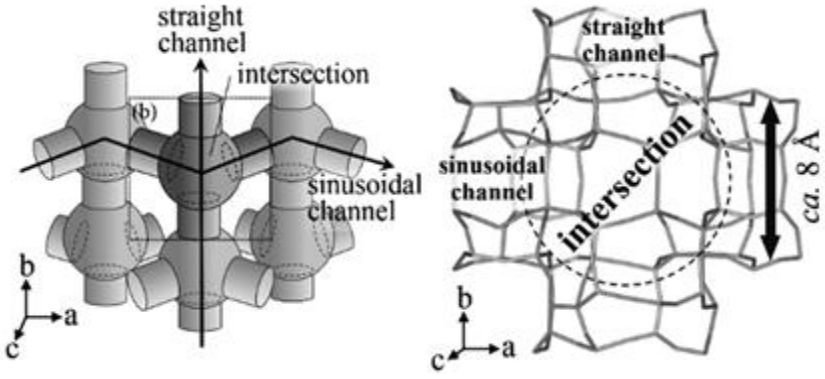

Figure 2-7: The channel system of MFI-type zeolite [54]

2.5 Structure Catalyst

Structure catalysts are introduced to obtain more efficient results from the catalytic process. In recent years, these type of catalysts are developed from the materials which has some special properties like good mechanical resistance and highly thermal conductive. Keeping in view the specific application of the structure catalyst, its materialistic properties and other factors are considered like thermal resistance, weight, heat management, cost and so on. They are actually solid structures for example foams, monolith or fibers upon which active catalytic phase is deposited. In this way, the structure actually make possible to overcome the draw backs involve in packed-bed reactors [55]. The traditional reactors can be replaced by using these structures which are beneficial to give high production in less

energy consumption in the processes [56]. Physical, chemical and geometrical properties of the supporting material are important features to be considered when selecting the structure support. Among physical properties the size of channels and pores is one of the important characteristics of material, through which the gaseous products and reactants passes [57].

2.6 Monolith

Monolithic reactor is most widely used structured catalytic system[58]. The Monoliths are structured materials composed of many straight and parallel channels. There are many applications of monolith among which the renowned one is in automotive catalytic convertors. The monolith are applied in industrial catalytic reactions, catalytic combustion and even in bio-chemical reactors also. Monoliths are honeycomb structured works as a supports for the catalyst upon which catalyst coating slurries are deposited, they have channels which are straight and parallel. They are of mainly two types of monolith structures. First is metallic monoliths and other ceramic monoliths normally made from cordierite (14 wt. % MgO, 36 wt. % Al2O3 and 50 wt. % SiO2,) [58,59]. Monoliths are characterized on the basis of their shape, channels, wall thickness and cell size as shown in Figure 2-8. All these monolith characterized parameters are controlled during the manufacturing process, these parameters affect the performance of the monolith and determine the cell density.

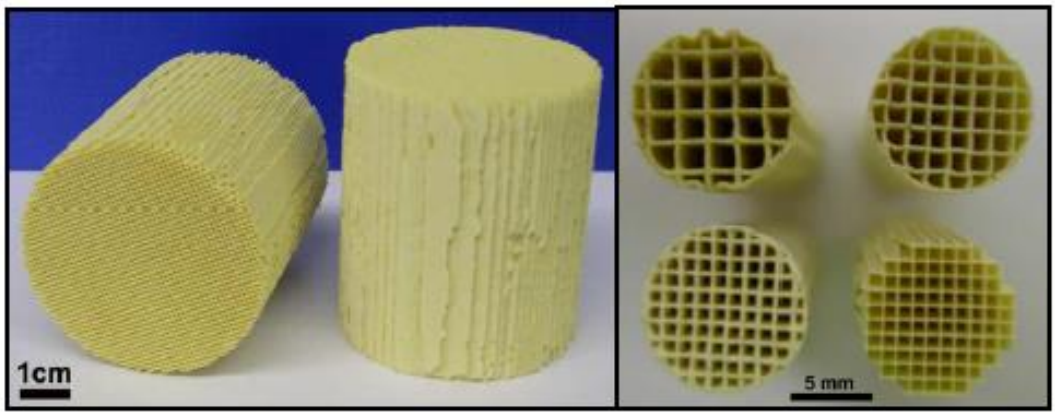

Figure 2-8: Ceramic honeycomb monoliths with different cell density [60]

2.6.1 Metal & Ceramic based Monoliths

Both types of metal-based and ceramic-based monolith catalysts have their advantages and disadvantages and the choice depends on the end application. Monolith catalysts with thin walls have low thermal capacity, which make them advantageous at reducing warm-up period [61,62].

Metallic monolith wall is thinners as compared to ceramic monolith. Thin wall thickness enable the structure to have short warm-up time period which results in better efficiency of the catalyst. Whereas if we talk about the cost then ceramic monoliths are cheaper then metallic monolith and having large pores which help in adsorbing the coating slurries and hence enhanced the coating adherence [63–65]

2.6.2 Monolith and Catalysis

Due to the high geometric surface area, thinner walls, low-pressure drop and ease of production of monolith when compared to conventional fixed bed reactors, monoliths have

also been developed as novel catalytic reactors in heterogeneous liquid phase and multiphase gas-liquid systems [66]. Monolithic catalysts are principally hierarchical organized structures. The use of appropriate wash-coats or catalysts (e.g. zeolites), also allowed the development of porosity on three different levels (micro-/meso-/macro-porosity), allowing for molecular sieving properties, extremely high surface areas and enhanced transport phenomena because of the combination of the benefits of each pore-size regime [67].

2.6.3 Monoliths vs. Packed Bed Catalyst Reactors

In heterogeneous catalysis, most of the catalysts used are in the form of pellets which are packed into the reactor volume in the fixed-bed configuration. For some applications and under specific conditions, the use of honeycomb structured catalysts allow for an improvement of the process [68,69]. Concerning mass- and heat-transfer, the radial movement inside a parallel-channel monolith (honeycomb) takes place exclusively by molecular diffusion. As axial dispersion is generally countered by the forced convection of the flow, also back-mixing occurs rarely and only at very low speeds. Due to the flow pattern in the channels, the honeycomb structure doesn't allow for the optimal radial mixing, which is generally a typical feature of pellets packings [70,71].

If powdered catalyst is used for the catalytic process, then catalyst bed formed can be easily plugged, whereas if pelletized catalyst bed is used, then this problem can be resolved somehow. But, in pelletized catalyst the active phase is only in a thin surface layer which results in the low product output [72]. Moreover, the monolithic reactor provides a higher

reaction rate than a fixed bed reactor with the similar external surface area. In terms of mass transfer and heat transfer features, the major issue of parallel channel monoliths are the laminar flow through the channels, the low interconnectivity among the channels and poor heat conductivity. On the other side, using appropriate channel geometry/design helps to overcome this limitation. Especially for gases, the molecular diffusion is fast enough to compensate the convection and to achieve an efficient radial transport [73].

2.6.4 Preparation/ Coating of Monolith Honeycomb Catalyst

Ceramic or metal are used in the preparation of monolithic honeycomb [57]. There are two different types of ceramic monoliths (I) low surface area monoliths and (II) high surface area monoliths, whose preparation paths are illustrated in Figure 2.10. The monoliths especially low surface area monoliths are made from ceramic materials like cordierite ($2MgO\text{-}2Al_2O_3\text{-}5SiO_2$) which are coated by washcoat. The high surface area monoliths are directly made from porous material which provides high internal surface area and this allows achieving higher amount of catalyst loading on the structure. Honeycomb monolith can be produced in different geometries depending on the applications [73].

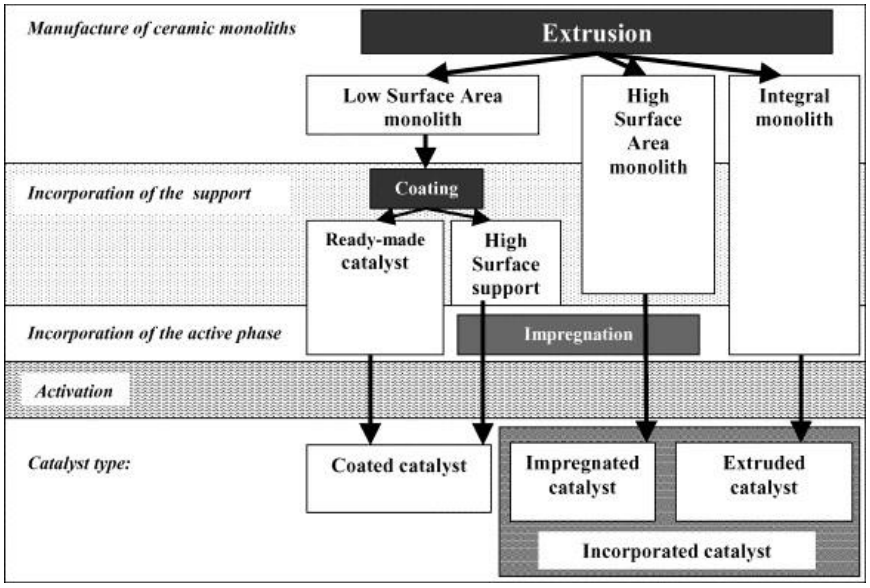

Figure 2-9: Preparation of ceramic monolithic catalysts [58]

The preparation of monolithic catalysts was basically divided in three preparation steps, (I) extrusion of the monolithic structure, (II) incorporation of the porous support and (III) incorporation of the active phase.

The most common method used to increase the internal surface area of low surface area monolithic carriers is the washcoating of porous particles by slurry. The advantages of this technique have small diffusion lengths, the possibility of direct coating of readymade catalysts and the high catalyst loading. Washcoat quality depends upon the solid and liquid properties, the mass fraction of solid in the suspension, the suspension viscosity and the calcination temperature [74]. Slurry for coating consists of a powder with a mean particle diameter of a few micro meters suspended in water. Sometimes binder for increasing the coating strength and acid for changing the pH of the suspension can be added. The monolith carrier is dipped in slurry of the porous particles for about 1 min. In this 1 min, the porous monolithic carrier absorbs water from the suspension and a cake of porous particles

develops on the walls. The excess slurry is removed gently by applying pressurized air. In the end, the coated monolith is dried at 100 ^{o}C and subsequently calcined. Typically, the calcination temperature is at least 500 ^{o}C. The calcination step is important because it binds the washcoat to the monolith walls. About 10 wt. % washcoat can be deposited on the walls per coating step. To achieve higher washcoat loadings, the coating procedure can be repeated [74,75].

The methods used for the absorption of active phase on the monolithic support are the same as applied in conventional catalysts in pellet or powder form. To distinguish the small catalyst support particles, we have to pay special attention in order to achieve an equal distribution of the active phase in the large structure of a monolithic catalyst. Especially for high cell densities, the impregnating solution surface tension can cause heterogeneous distribution of the active phase within the monolith channels. Many methods for incorporation of the active phase, e. g. impregnation, ion exchange, precipitation and crystallization are applied by the people [58,74].

To carry out the impregnation method, the metal precursor is dissolved in water and the porous support is dipped into this solution. The concentration of the precursor in the solution act as the loading of the active phase. Subsequently, the impregnated catalyst support will be dried at a temperature right below the boiling temperature of the solvent to prevent boiling. It is important that the drying procedure affects the distribution of the active material on the support. Freeze-drying or microwave drying could help to avoid redistribution of the active phase. The final step is the calcination of the precursor containing support. At temperatures of usually 500 ^{o}C the precursor salt is changed into a metal oxide and the interaction between the active phase and the support increases. The

impregnation procedure can be repeated to increase the active phase loading on the support [74,76].

2.7 Reaction Mechanism

Early efforts in mechanistic investigations of MTH process were strongly focused around the question of how the first C-C bond was formed [17,77]. Dessau and co-workers from Mobil proposed the alkene methylation or cracking mechanism for the MTH reaction illustrated in Figure 2.11 [78,79]. According to Dessuau's proposal, methanol is converted to hydrocarbons through repeated methylation of light alkenes to form higher alkenes which undergoes further methylation or cracking reactions. In addition, aromatic species formed during the MTH reaction are only presented as end products resulting from hydrogen transfer reactions [77].

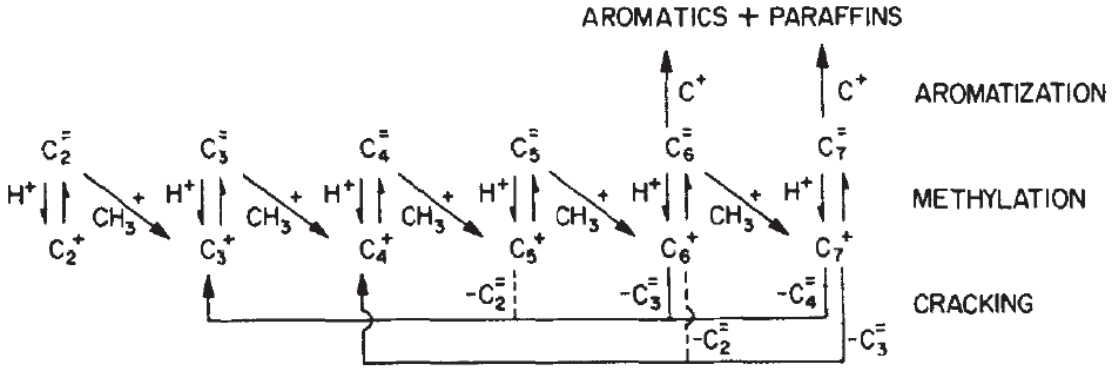

Figure 2-10: Dessau's scheme of a mechanism based on successive methylation and cracking [80]

Dahl and Kolboe proposed the "hydrocarbon pool mechanism" for the MTH reaction [80,81]. They carried out experiments by co-feeding olefin precursors (ethanol, propanol) and methanol. Analysis shows that the alkenes were inert and most of the products were formed exclusively from methanol under the applied reaction condition. Hence, a parallel indirect mechanism the “hydrocarbon pool” was proposed. According to the hydrocarbon pool mechanism, species trapped in the zeolite/zeotype materials act as reaction centers for methanol conversion [80,81].

Recently, the reaction mechanism study namely NMR (Nucleation magnetic resonance) presented that in first stage the complex molecules are formed which further cracked in next step to produce light olefins [81–85]. Kaarsholm’s had taken the experimental data from MTO reaction carried out over ZSM-5 catalyst modified by the phosphorous, his model was based on hydrocarbon pool mechanism [86]. Propylene formation over high silica HZSM-5 catalyst in a fixed bed reactor was studied by Wu [87]. In this study it was proposed that the main reaction mechanism is methylation-cracking in a typical methanol to propylene process. On the basis of methylation reaction from alkenes, he had presented a reaction scheme containing consecutive methylation from butane to pentene further upto heptene [87] . The schematic diagram of methylation – cracking mechanism projected by Wu is illustrated in Figure 2-12.

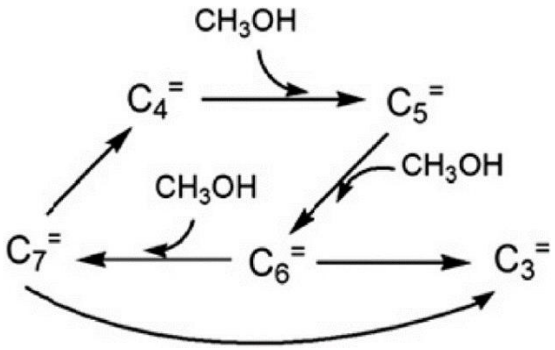

Figure 2-11: Reaction scheme for propylene formation in the MTP process [88]

2.7.1 Reactions involved in MTP process

In methanol to propylene reaction system, first of all the methanol is dehydrated to form olefins including butane, pentene, hexene and heptene. These higher olefins then undergo for the series of methylation reactions. The heavier components such as hexene and heptene cracked to form light olefins including ethylene and propylene. Furthermore, the heptene which is the heaviest component in the reaction system also generates the paraffins such as ethane, propane, butanes, pentanes and the aromatics. Methane was produced directly from methanol [88]. The reactions involved in MTP process includes:

$4\ CH_3OH \longrightarrow C_4H_8 + 4\ H_2O$

$5\ CH_3OH \longrightarrow C_5H_10 + 5\ H_2O$

$6\ CH_3OH \longrightarrow C_6H_{12} + 6\ H_2O$

$7\ CH_3OH \longrightarrow C_7H_{14} + 7\ H_2O$

$CH_3OH + C_4H_8 \longrightarrow C_5H_{10} + H_2O$

$CH_3OH + C_5H_{10} \longrightarrow C_6H_{12} + H_2O$

$CH_3OH + C_6H_{12} \longrightarrow C_7H_{14} + H_2O$

$C_6H_{12} \longrightarrow 2\ C_3H_6$

$C_6H_{12} \longrightarrow 3\ C_2H_4$

$C_6H_{12} \longrightarrow C_2H_4 + C_4H_8$

$C_7H_{14} \longrightarrow C_3H_6 + C_4H_8$

$2\ CH_3OH \longrightarrow CH_4 + Coke + H_2O$

$C_7H_{14} \longrightarrow$ Paraffins (C_2H_6, C_3H_8, C_4H_{10}, C_5H_{12})

$C_7H_{14} \longrightarrow$ Aromatics (Benzene, Toulene, Xylene)

CHAPTER 3

EXPERIMENTAL METHODS

This chapter gives an overview of the experimental setup and procedures adopted in carrying out this research work. Detailed description of the catalytic tests that were performed and the equipment utilized is also given herein. Experiments are planned in the following manner to achieve the stated objective of this study.

- Installation of experimental setup including fixed bed reactor with online GC.
- Carryout base experiments using zeolite catalyst and identification of the most suitable conditions for catalytic reactions. Conditions include the temperature, methanol flow rate, catalyst/inert ratio, nitrogen flow rate and TOS (time on stream).
- Characterisation of Zeolite catalyst (ZSM-5) consisting of SiO_2/Al_2O_3 ratios of 30, 50, 80, 280 and 410. Characterizations include XRD, SEM, EDX, NH_3-TPD and BET surface area, pore volume.
- Catalyst pellets (0.5 – 1.0 mm) are evaluated in fixed bed reactor, gases are analysed through online GC-TCD, whereas liquid product is first separated and then analysed.
- Based on the results of these catalysts, catalyst of a given SiO_2/Al_2O_3 ratio showing the best performance is selected and coated on cordierite monolith using the dip coating method.

- Coated monoliths are characterised and evaluated in a fixed bed reactor and its performance is analysed on the basis of propylene selectivity, conversion and stability.

3.1 Materials

Zeolite catalysts (ZSM-5) are purchased from Zeolyst possessing 30, 50, 80 and 280 SiO_2/Al_2O_3 molar ratios respectively. Powder catalysts are dried and then calcined at 450^oC for 3 hours prior to use. Powder catalyst was pelletized, crushed and sieved to provide 0.5-1.0 mm (Mesh size No. 35 – 18) size of the catalyst sample. Cordierite monolith of 25.5 cm length and 24.5 cm diameter is purchased from Applied Ceramics Inc, the monolith cell density was 400 per square inch. Monolith are grinded using sand paper to fit in the reactor tube which has a diameter of 22.4 mm.

Gas cylinders including Nitrogen, Hydrogen, Helium and Zero air are purchased from Air liquid. Methanol (CH_3OH, 99.9 wt. %) was purchased from Carlo Erba. Propanol ($(CH_3)_2CHOH$, 100 wt. %) was obtained from BDH Limited, and it was used in the calculations of internal standard method, Nitric Acid (HNO_3, 5wt %) is used for monolith cleaning before coating. Ludox® HS – 40 Colloidal Silica (40 wt. % suspension in H_2O) was used as a binder. All chemicals are used without any further treatment. Siemens ultra-clear system was used to obtain the pure Deionized (DI) water, DI water was used in the preparation of coating slurry and also used for the water circulation bath.

3.1.1 Pelletizing the Powder Catalyst

This was achieved by pressing the powder into tablets using Bench Top Laboratory Press. Once the required number of tablets have been pressed, the tablets were crushed using pestle and then sieved to produce a 0.5 – 1.0 mm fraction. Particles greater than 1.0 mm were again lightly ground and re-sieved. Particles smaller than 0.5 mm were again pressed to make pellets and the process was repeated to achieve the required sized particles.

3.2 Experimental Setup

For the evaluation of structured catalyst, a suitable fixed bed reaction system equipped with required features and facilities including online gas analysis is needed. Both the pelletized catalyst and the synthesized structure coated catalyst were evaluated for methanol to propylene conversion reaction in continuous flow mode. For this purpose, a fixed bed reactor with online GC was installed.

3.2.1 Fixed Bed Reactor

The schematic diagram of the experimental set-up for MTP process is shown in Figure 3.1. The actual setup in laboratory is shown in Figure 3.2. This reaction system was manufactured by Hi-Tech Engineering. The Fixed Bed Reactor unit consists of four different sections including Reactant gas flow control section, Reactant liquid flow control section, Reactor section and Product section. The system has been designed for working

conditions upto 500°C and 10 barg. In Gas feed section, the nitrogen gas flows through the mass flow controller and check valve. The inlet pressure of gases can be monitored through local pressure gauge. Reactor is equipped with one liquid inlet in which pure methanol is used as liquid feed. Liquid inlet is in lined with Feed tank, Filter, Ball valve, Pressure gauge, Liquid pump, Check valve, Pressure safety valve and Three way valve. After passing through liquid section, the feed enters into the vaporizer.

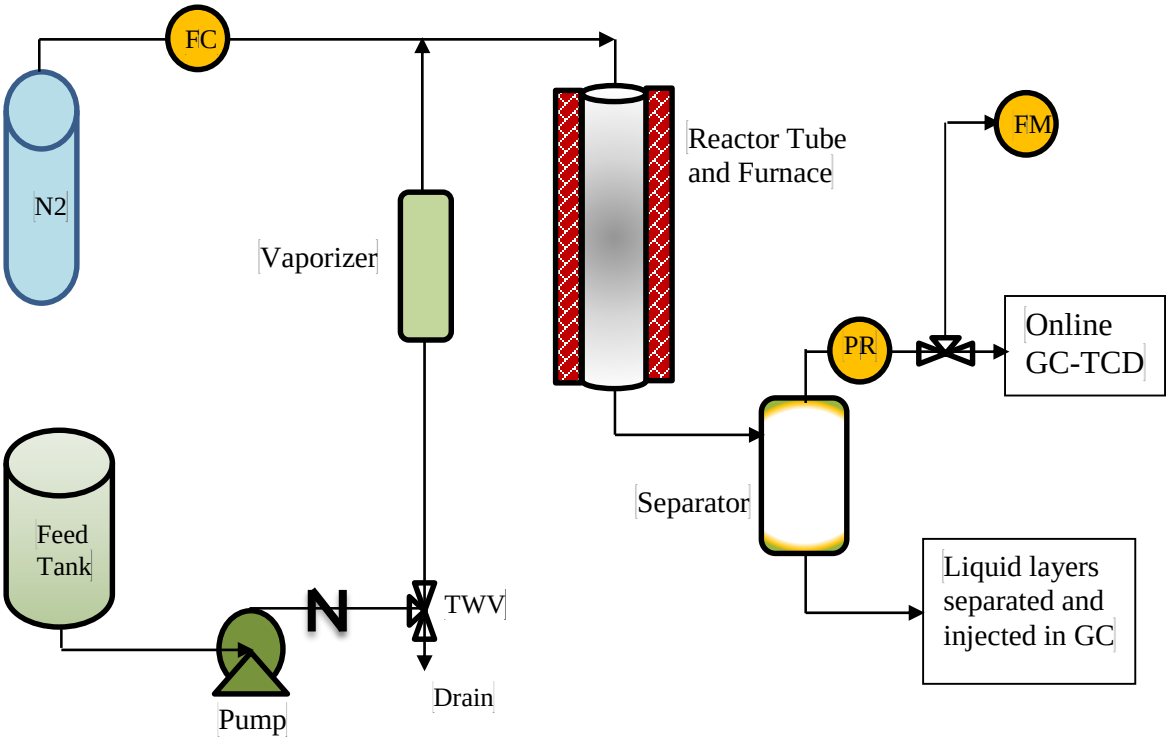

Figure 3-1: Schematic diagram of fixed bed reactor

Figure 3-2: Picture of the Fixed bed flow reaction system.

The reactor is designed to work in the down-flow mode. The mixed gases and vapors enter at the top of the reactor tube. The reactor tube is constructed using 316 L stainless steel with an approx. capacity of 185 cm^3. The dimensions of the tube are 22.4 mm Internal Diameter X 31.8 mm Outer Diameter and 470 mm Length. The reactor tube is heated with single zone furnace. The temperature control is based on skin of reactor tube. Reactor furnace heats a reactor tube at the desired temperature. Furnace temperature controlled either via single step directly or by a ramp step pattern programming. In product section, the liquid product is condensed and separated from the gas product. The separator is provided with a pressure control valve to control the reaction pressure. The gas is then sent to GC (Gas Chromatograph) for analysis.

3.2.2 Installation of the Reactor

During the installation of the fixed bed reactor, all the temperature controllers are verified, flow meters and pumps are calibrated, functioning of the pressure relieve valve at the outlet of pump is checked, gas circuit leakage is detected by holding the pressure of 5 bar for 12 hours accompanied by continuous examination for leakages.

3.2.3 Furnace

The reactor is provided with a single zone furnace, which is an electrically heated type furnace provided with a temperature controller and a temperature indicator. The furnace heater can be heated up either in a single step mode or by a ramp step pattern.

3.2.4 Gas Chromatograph

The Gas Chromatograph (GC) is supplied by Agilent (Model4890B), equipped with Flame ionized Detector (FID) and Thermal Conductivity Detector (TCD). Helium gas is used as the sample carrier gas while air and hydrogen are used as the gases for the FID detector. Online gas sample injection is in the back detector of GC. Liquid sample is manually injected in the inlet port of front detector. INNOWAX column (part # 113-4362) temperature range "0-260 ^{o}C" with dimensions of 30 m X 320 μm X 0.5 μm is connected with front detector for Liquid analysis samples. GASPRO column (part # 19091N-213) temperature range "0-260 ^{o}C" with dimensions of 60 m X 320 μm is connected with back detector for the gas sample analysis. A standard gas mixture calibration is conducted to determine the retention time of each component.

In the developed method of gas analysis, the GC column was maintained at a temperature of 35 ^{o}C for 4 min followed by a temperature increase from 35 ^{o}C to 110 ^{o}C then maintained at this temperature for 15 min, afterwards increase in temp upto 150 ^{o}C and then maintained at this temperature until the analysis was completed. For liquid sample analysis using a GC, 0.5 μm liquid sample is injected in the column. GC column was maintained at 35 ^{o}C for 1 min after which the temperature was increased to 60 ^{o}C at a rate of 5^{o}C/min.

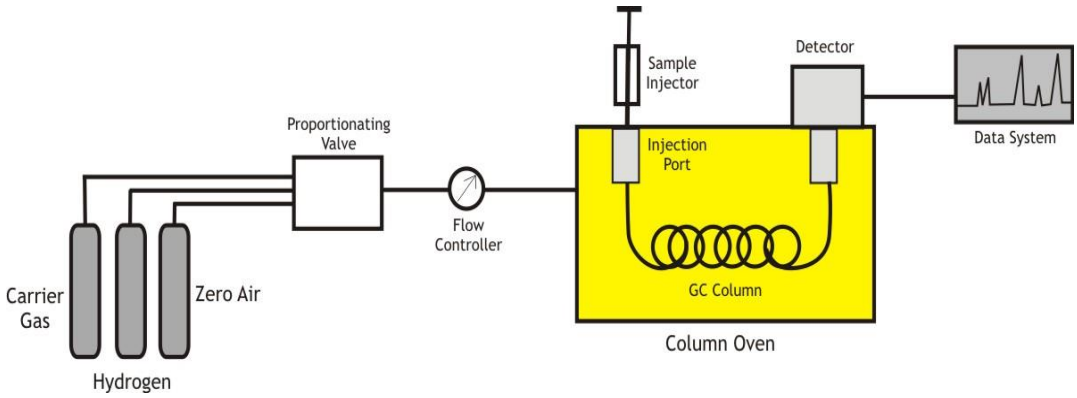

Figure 3-3: Schematic Diagram of the Gas chromatograph

GC Calibration

The calibration of GC is useful in identification and quantification of the product's chemical composition of methanol to propylene reaction system. The major products in the gaseous phase include alkanes and light olefins whereas in liquid phase the major components are aromatics, water and unreacted methanol. The gas separation in GC column depends upon the flow rate of carrier gas, temperature, the type of separation column used and the split ratio. For the calibration of GC, the first step is to determine the retention time of all compounds of interest employed in this work. For the gaseous phase a standard sample containing nitrogen, methane, propane, ethylene, propylene, butane, butylene and pentane was injected in TCD. The retention time and peaks were observed at different temperatures of oven, split ratio and flow rates. After the clear identification of peaks of standard gas sample, each of the gases products were quantified on the basis of their known mol %. In liquid phase the identification of unreacted methanol is our target to determine the conversion. For this purpose internal method calculation is used in which GC is calibrated for different composition of methanol and propanol.

3.3 Other Equipment Used in Research

Apparatus	Model or Specification	Manufacturer
Aluminium Hot Plate & Magnetic stirrer	AM4	Velp Scientifica
Hot Plate & Magnetic stirrer	MSH – 20D	Wise Stir
Bench Top Laboratory Press	Model C	Carver, Inc.
High temperature Chamber furnace	CWF	Carbolite
Balance	PA64	OHAUS
Oven	----	Fisher Scientific
Furnace	CWF1100	Carbolite
Furnace	P 330	Nabertherm
Ultrasonic bath	DR-P60	Derui

3.4 Preparation of Coated Structured Catalyst

The dip coating method is followed for the coating of zeolite on cordierite monolith in this work [89]. Honeycomb Cordierite monolith of 400 cpi is used as structured support for the coating of zeolite. The obtained zeolites are either in H-ZSM5 form or in NH_3- ZSM5 form. The NH_3-ZSM5 form catalyst is calcined at 550 ^oC for 4 hours. The dip coating procedure is followed in 3 steps. In the first step, cordierite is cleaned and calcined; in the 2nd step, zeolite catalyst slurry is prepared and in the 3rd step the monolith is coated and calcined.

3.4.1 Cordierite Monolith Cleaning

The cordierite monoliths are grinded cylindrically using sand paper to attain the required size equal to the reactor internal diameter. Afterwards these monoliths are dipped in 5 wt.% HNO_3 solution for 15 minutes to remove any traces of impurities if present .The soaked monolith are then washed thoroughly with DI water and then dried in an oven at 110 ^oC for 6 hours. The dried monoliths are then calcined at 500 ^oC at a heating rate of 10 ^oC/min and kept at 500 ^oC for 3 hours. As soon as the temperature reached bellow 110 ^oC during the cooling process, the monoliths were placed in a desiccator to remove the moisture coming from air. Finally, the dry weight of each monolith was recorded.

3.4.2 Preparation of ZSM-5 Coated Monolith Catalyst

The dip coating process of monoliths with ZSM-5 was performed by preparing a mixture of ZSM-5 crystals with a solvent and a binder. Dip coating slurry can be prepared with various composition by using either butyl acetate or DI water. In this research work, aqueous solutions were prepared with 20 wt. % ZSM-5 zeolite, using colloidal silica (Ludox AS-40, 40 wt. % colloidal suspension of silica in water) as a binder. The amount of binder used was1 wt. % of the total amount of catalyst for 20 wt. % ZSM-5 in solvent. To study the effect of binder [90], coating slurries were prepared in water without binder, with 1 wt. % binder and with 2 wt.% binder. To obtain a homogeneous mixture the slurry was stirred for 6 hours on a magnetic stirrer at 600 RPM at ambient temperature. Monolith were then dipped in selected ZSM-5 slurry for 3 min followed by ultra sonication to facilitate the penetration of slurry into the monolith channels. The excess slurry was then

removed by blowing pressurized air into the channels. ZSM-5 dip coated monoliths were dried for 12 hours at 110°C in a rotating oven at a heating rate of 1 ^{o}C/ min. Subsequently, the monoliths were calcined at 500 ^{o}C for 4 hours at a heating of 2 ^{o}C/ min. The weights of the zeolite coated monoliths were then recorded by using a physical balance.

3.4.3 Testing of Catalyst Coating Adhesion

To test the adhesion of ZSM-5 zeolite coating on monoliths; the as prepared coated monoliths were placed in an ultrasonic bath for 60 min at 25 ^{o}C. The samples were then dried for 24 hours at 110 ^{o}C after which the monoliths were weighed in order to determine any loss in weight. The difference in weight before and after the ultrasonic treatment attributed to the addition of colloidal silica binder in the slurry.

For the 2nd layer of coating, the samples were dipped in the slurry and the same procedure was adopted for the coated monoliths. The stepwise procedure followed for the preparation of zeolite coated structure catalyst using the dip coating method is shown schematically in Figures 3.4, 3.5 and 3.6.

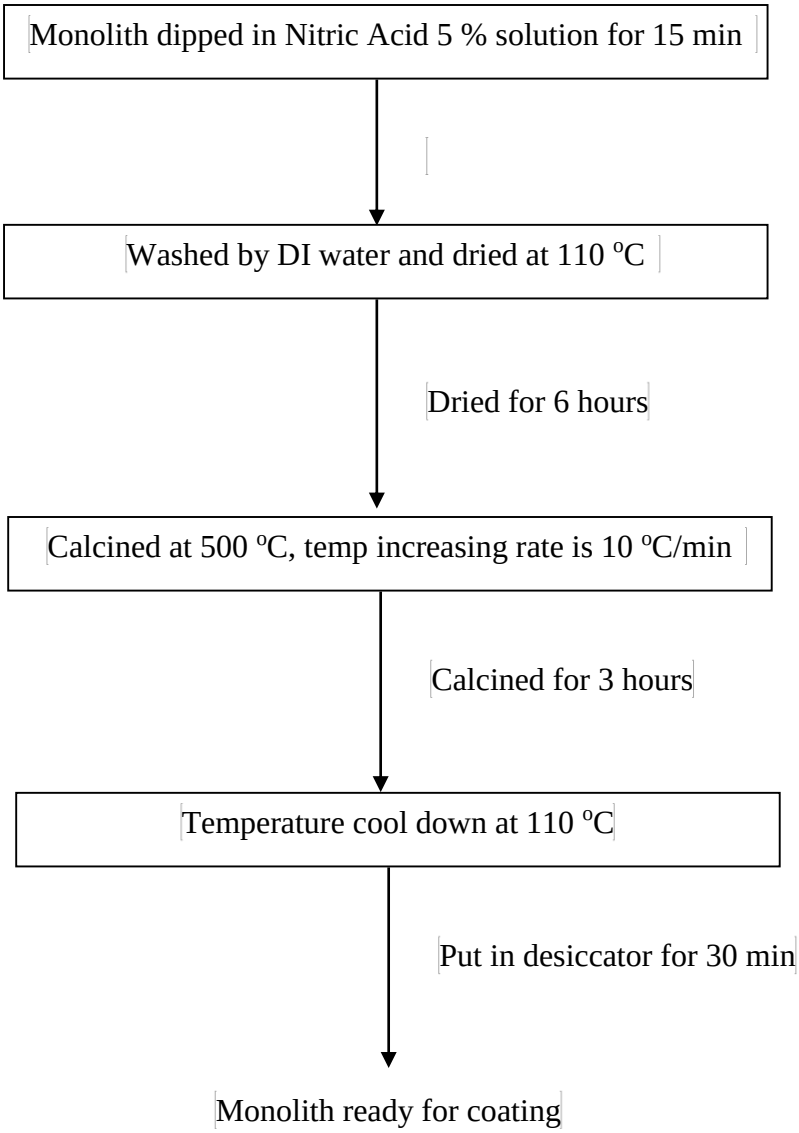

Figure 3-4: Cleaning/ washing of monolith before coating

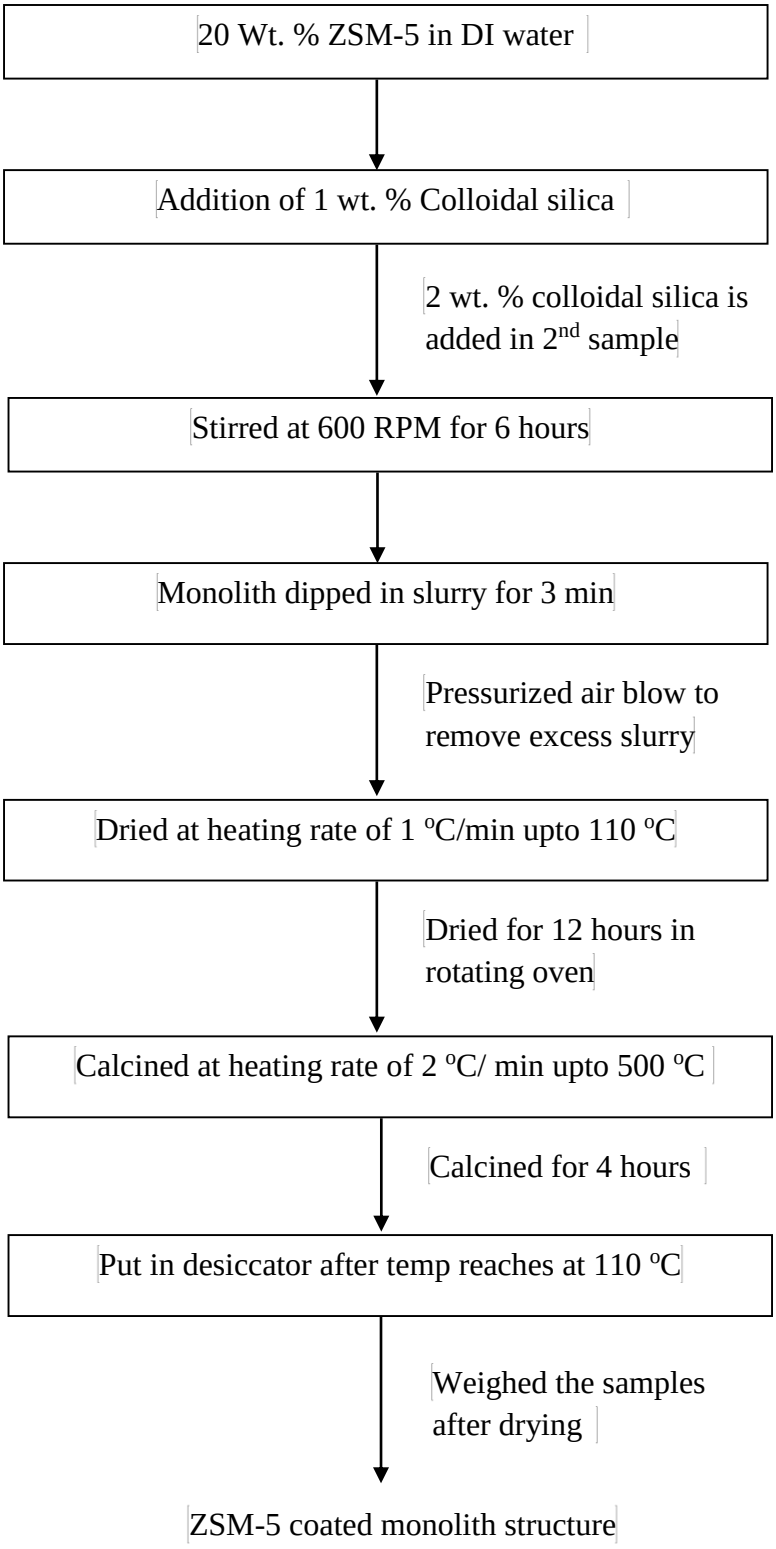

Figure 3-5: Preparation of zeolite coated monolith catalyst

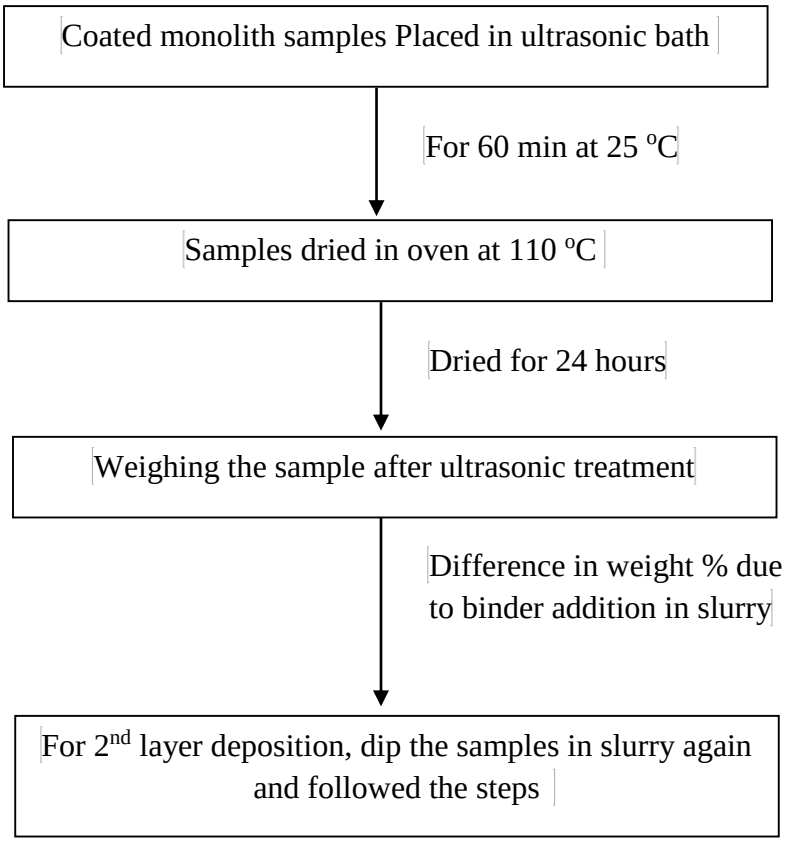

Figure 3-6: Adhesion testing of zeolite coated monolith catalyst

3.5 Catalyst Characterization

3.5.1 X-ray Diffraction (XRD)

XRD is the most widely used method to identify the crystallinity of zeolites. Moreover, it is the main characterization technique to examine the bulk structure of crystals. In zeolites, the active sites are formed on the solid surface and thus XRD is useful to probe its bulk structure.

The powder sample was made to be flat, compressed and then scanned at a predefined program. The X-rays diffracted from crystallographic planes in lattice structure of ample follow the well-known Bragg's equation:

$$\lambda = 2d \sin\theta$$

Where λ is the beam wavelength of incident X-rays, d is the interplanar spacing and θ is the Bragg angle. The peak intensities are calculated by subtracting the highest intensity of peak from the intensity of peaks under consideration. In crystallinity test, the higher and sharper diffraction peaks without any base line drift prove the better crystalline structure with an absence of impurities. Miniflex system was used for XRD and analysis was done by PDXL software which has provided by ICDD (International Center Diffraction Data).

3.5.2 Scanning Electron Microscopy (SEM)

It is the most widely used technique to examine the surface morphology of microporous materials. The main advantages of using SEM is its high lateral resolution (1 -10 nm) and large depth of focus (100mm at 1000 magnification) which are useful in achieving a high quality image. In SEM, a primary beam electrons is generated by a field emission electron gun. A high degree of vacuum is required for an uninterrupted path of electrons from source to sample. When the beam electrons accelerates and interact with the sample surface, it produces secondary and back-scattered the surface electrons. These electrons are picked up by an electron detector, processed electronically and converted to pixels on a cathode ray tube. The working distance, the electron probe current, convergence angle and electron beam accelerating voltage are the important parameters to control the magnification and clarity of the image achieve sharp and clear image. For this research, a Tescan Lyra-3 system has been used for SEM imaging at 20 kV.

3.5.3 Energy Dispersive X-ray (EDX)

EDX analysis can be carried out in SEM by an EDX Detector which is primarily an X-ray detector used for elemental analysis based on characteristic X-rays emitted from the sample. EDX analysis can be used for both qualitative and quantitative analysis. In order to prevent charging of the specimen surface a thin gold coating was applied using a spiller coater. Gold or Palladium sputter-coat can be used in low-resolution work less than 10,000 magnification. Chromium, tungsten or platinum sputter-coat under high vacuum conditions can be used in field-emission scanning for high resolution. EDX analysis functions

capturing the SEM image and then selection of particular area on the image for analysis. The approx. quantity of each element in the sample is plotted at its respective in both graphical & numerical formats in EDX.

3.5.4 Thermo Gravimetric Analysis (TGA)

Thermo gravimetric analysis equipment is used to study the working principle stability of the material used to determine the amount of coke deposits on spent catalyst. This test depends on the loss of sample weight during heating. Measurements in this equipment was done using inert gas or air flow and weight loss is recorded as a function of temperature. TGA analysis relies on a high degree of precision in three kinds of measurements: weight, temperature, and temperature shift. The equipment consist of a crucible which holds the sample, a very sensitive balance which continuously monitors the sample weight and a furnace which is used to heat the sample. In this work, TGA of the spent catalyst samples was carried out using a Netzsch Thermal Analyzer. The temperature range for analysis was programmed between 25 and 800 °C at a heating rate of 10 °C/ min.

3.5.5 Temperature Programmed Desorption (TPD)

Catalysts are often characterized by their interaction with gases. Thermal analyses are very useful to predict surface modifications and bulk reactions in catalysts. Temperature programmed reactions such as reduction (TPR), oxidation (TPO) and desorption (TPD) are

well known analyses for catalyst characterization. In this context, TPD is useful for surface analysis of the catalyst.

TPD is performed by chemisorptions of reactive gases such as CO, NH_3, and H_2 etc. It yields catalyst: the surface features that can be analysed using TPD include the extent of metal dispersion, active surface area, size of crystallites and surface acidity. The main objective of the chemisorptions is to deduce the number of active sites that can react with a fluid phase. Therefore, it is based on a chemical reaction which is performed by suitable reactive gas with the surface active site of the catalyst. The quantity of desorbed molecules from the surface when the surface temperature is increased. TPD technique includes the following steps: Catalyst pretreatment, Pre-adsorption of the adsorbate, Evacuation after pre-adsorption to remove physically adsorbed gas, Programmed desorption and Detection of the desorbed gas.

In this work, 100-250 mg of zeolite powder activated at 500 °C was used under the flow of nitrogen for 1 hour (75 ml/min) for TPD analysis. The samples were cooled to and kept at 150 °C for 30 minutes under flow of 2% NH_3 in helium (75 ml/min). Physisorbed ammonia was removed by flushing the sample with nitrogen at 150 °C for 2 hours (75 ml/min). Finally, the temperature of the oven was increased to 740 °C with heating rate of 10 °C/min under the flow of nitrogen (75 ml/min), and the desorbed ammonia was detected using TCD. The acid site density of the catalyst was calculated assuming adsorption of one ammonia molecule per acid site. The NH_3-TPD experiments were performed on Micrometrics Chemisorption Analyser.

3.5.6 N_2 Adsorption–Desorption Measurements (BET measurement)

Surface area of a catalyst has a definite effect on the activity of the catalyst and the amount of gas adsorbed. In this work, the surface area and pore volume were evaluated by the Braunauer, Emmett and Teller (BET) analysis of the catalyst. In this technique, the amount of nitrogen adsorbed at the sample surface at 77K is measured over a predefined pressure range below 1 atm. In this study, the analysis of the samples are carried out using Micromeritics model ASAP 2010. The weight of each sample used for analysis was approximately 150 mg. The samples were degassed under vacuum at 300 ^{o}C for 3 h approximately.

3.6 Catalyst Evaluation

The ZSM-5 catalyst pellet (0.5 -1.0 mm) and the prepared catalyst coated monoliths were evaluated in a fixed bed reactor setup. This reactor system and the online GC are explained in section 2.1. In this work, methanol feed varies from 0.16 - 0.48 ml/min. Nitrogen gas introduced in the reactor at 100ml/min initially for the purging but during reaction it is maintained at 44 ml/min. The experiments were performed over a temperature range between 350 – 500 ^{o}C.

The two pre-cautionary measures of the experiment requires vapour pressure of nitrogen and the sufficient quantity of methanol in the feed tank. It is also to be ensured that all thermocouples are at their correct position, valves on the panel are at correct position and power supply is available for the reactor & its accessories. Before the catalyst is loaded,

the reactor tube is unmounted from the reactor, pressurized air is blown for removing the small particles and then tube is washed thoroughly with tap water. The tube rinsed with DI water to remove any inorganic salts and then with acetone to remove any organic material. Reactor tube is then dried in oven at 100 ^{o}C for 2 hours.

3.6.1 Catalyst Loading

As shown in the reactor schematics in Figure 3.7, the lower part of the reactor is filled with Silicon carbide (SiC) bed and glass wool is placed above it. Then, required amount of catalyst mixed with small size of SiC is placed in such a way that it is at the center of the reactor, thermowell tip guides the location of the middle of the reactor which is mounted to provide the temperature at the middle of the catalyst bed, glass wool is places above the catalyst bed and at the top some amount of SiC is placed. After the reactor is filled, its top threads are polished with anti-sealant and then closed the reactor tube. Finally, the reactor tube is positioned at the right configuration and its tube connections are tightened manually.

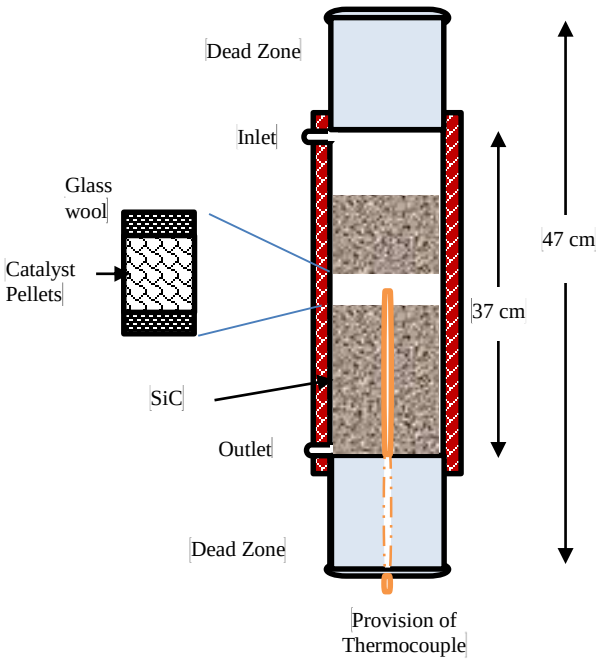

Figure 3-7: Schematic of reactor tube

3.6.2 Experiment Procedure

Once the catalyst is loaded, an inert nitrogen gas (e.g. N_2) is flown for approx. 30 min and the outlet gas flow rate is observed to ensure that there is no leakage in the system. The pressure of the system is adjusted if required by using back pressure regulator located at the downstream of separator. Afterwards, the heating furnace temperature controller is set at the desired heating program of ramping & steps and then followed by execution of the program. The vaporized temperature and all other heat tracing temperatures set at 100 ^{o}C are in the program. The methanol feed pump is manually purged to avoid pump cavitation which may be due to the entrapped air in the liquid system, the methanol pump also checked for its calibration by measuring the discharge volume. Once the reactor tube is calibrated at the required temperature, cooling water bath is then started. At the steady

condition of all temperatures set-points, the methanol feed is started and noted the start time of the experiment. During reaction, the product gas flowrates are recorded periodically after every 5 – 15 min. After 30 min of the reaction the first online course of the gas sample is injected in the GC and subsequent samples can be taken with the interval of 1 hour normally. Liquid samples are collected from the bottom of separator. Liquid samples are then weighed and separated using separating funnel. The upper layer is the aromatics layer and lower layer contains water and unreacted methanol. Weight of both of these separated layers are recorded while the lower liquid layer is analysed using the internal standard method of calculation used for unreacted methanol detection.

3.6.3 Internal Standard Method for Liquid Analysis

In this method, an internal standard (propanol in our case) is added to the sample and the ratio of the peak area of the methanol in the sample to the peak area of the propanol is compared to the similar ratio of each calibration standard. This ratio is termed as the (RF) response factor indicating that the target compound response is calculated relative to that of internal standard.

$$RF = \frac{A_x / A_{is}}{M_x / M_{is}}$$

Mx → Mass of the compound (Methanol)

Mis → Mass of the Internal Standard (Propanol)

A_x → Area of the compound

A_{is} → Area of the internal standard

In order to conduct the experiments using the internal standard method, GC is standardized using 11 variable standards of methanol and propanol (known weight rations), the developed calibration curve is shown in Figure 3.8. To determine the unknown quantity of the methanol in any sample (Mx), initially add the known quantity of propanol (Mis) and inject the sample in GC. Take the area of the peak of Methanol (Ax) and propanol (Ais). Calculate the ratio of Ax/Ais and determine the Mx/Mis by using the curve. Since the Ais is known Ax can be calculated which is our required mass of methanol in the sample.

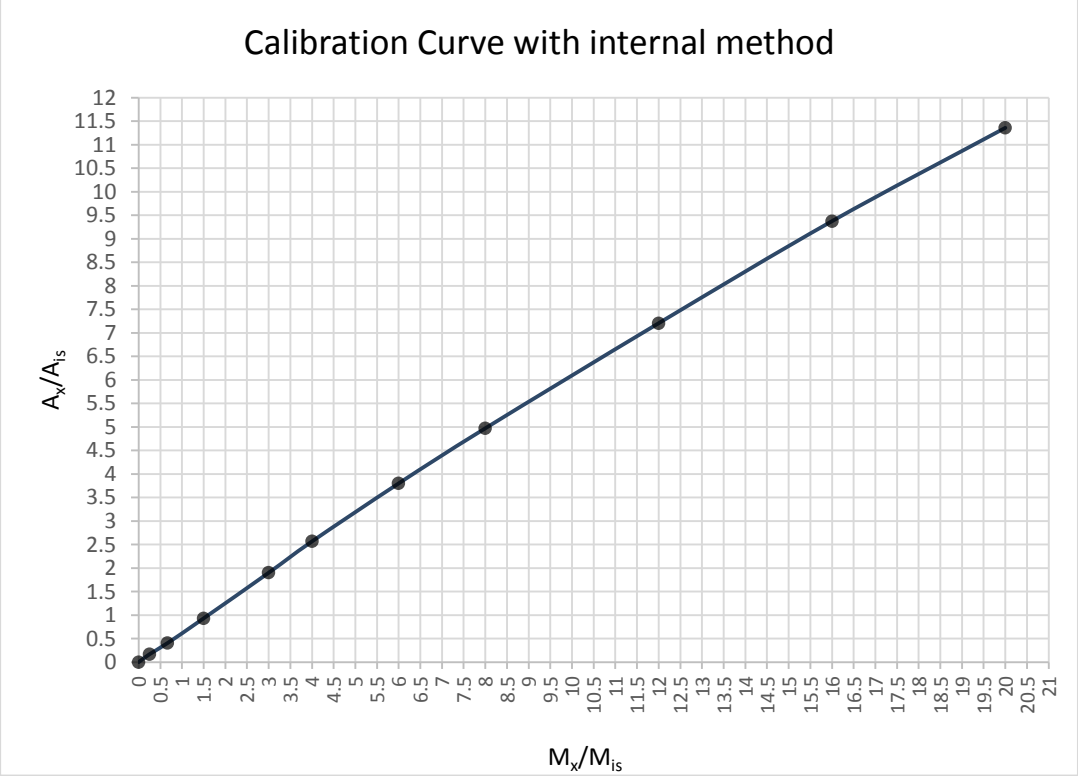

Figure 3-8: Calibration curve for liquid analysis

3.6.4 Conversion, Selectivity, and Yield Calculation

For the conversion of Methanol the "grams of Methanol (MeOH) in" is calculated from the feed flow rate available in ml/min, volumetric flowrate is converted into grams/ min and ultimately find the grams for the particular time of reaction normally 150 min. "grams of Methanol (MeOH) out" is the amount of methanol unreacted which is sort out by the internal method calculations of liquid streams. Conversion is calculated using the formulas:

$$Conversion\ (\%) = \frac{(g\ of\ MeOH\ in\ ) - (g\ of\ Methanol\ out)}{(g\ of\ MeOH\ in\ )} \times 100$$

The product selectivities are calculated based on the total amount of the gaseous phase products formed including alkanes and olefins. The formula used for the calculation of particular product in gaseous phase is as follows [91]

$$Selectivity\ (\%) = \frac{(g\ of\ product\ (gas))}{(100\ g\ of\ gaseous\ hydrocarbons)}$$

Yield of the Product is calculated using the formula:

$$Yield\ (\%) = \frac{g\ of\ product}{100\ g\ of\ Methanol\ feed}$$

CHAPTER 4

RESULTS AND DISCUSSION

This chapter begins with the discussion on base experiments in which suitable conditions are evaluated for the reactions on ZSM-5 catalyst with varying SiO_2/Al_2O_3 ratio. The effect of these reaction conditions on the conversion of methanol as well as yield and selectivity of propylene and propylene/ ethylene ratio is discussed in detail. The physical characterization results of pelletized zeolite catalyst are also included, which give an overview of the acidity, surface area, crystallinity, morphology and elemental composition of each sample. Furthermore, the same results have been presented for the coated structured catalyst in which a cordierite monolith has been coated by ZSM-5 zeolite with SiO_2/Al_2O_3 ratio of 280. The results for catalyst loading and adhesive strength of coating for four as prepared samples have also been discussed. The chapter concludes with the performance evaluation of the coated structure catalyst in a fixed bed reactor.

4.1 Base Experiments

Base experiments were carried out by varying the temperature, methanol flowrate, nitrogen flow rate, pressure, Weight hourly space velocity (WHSV) and catalyst/inert ratio. The effective time-on-stream (TOS) for the reactions is also selected at these conditions. On the basis of higher propylene selectivity at higher temperature, 500 ^oC was selected as a suitable reaction temperature. The higher selectivity of propylene is due to lower yield of

hydrocarbons at higher temperature, whereas increase in temperature can decrease the stability of catalyst so keeping in view the literature reported and higher selectivity of propylene all the reactions are carried out at 500 ^{o}C [92]. According to literature, the methanol to propylene process is run at atmospheric pressure [87,92–96]. The selectivity of the process is optimized towards propylene by high temperature and low pressure employed during the reaction. By changing the methanol feed flow rate with same amount of catalyst the effect of WHSV on propylene selectivity was studied. The reactions with particular SiO_2/Al_2O_3 ratios have different effect on WHSV so the catalysts are evaluated at a range of 11 h^{-1} to 19 h^{-1} WHSV in this study. Nitrogen is supplied as carrier gas in the reaction at a flow rate of 44 ml/min for all the reactions, initially this flow rate is calculated on the basis of nitrogen to methanol feed molar ratio. 1st gas sample is taken at 30 min and then after the interval of 60 min next two samples are collected. The reaction parameter selected as a result of base reactions are summarized in Table 4.1.

ZSM-5 catalysts with varying SiO_2/Al_2O_3 ratios are evaluated on the selected suitable operating conditions. The best chosen catalyst i.e. ZSM-5 with SiO_2/Al_2O_3 ratio of 280 is also tested at temperature range of 400 to 500 ^{o}C. The effect of temperature on the propylene selectivity and yield is shown in Figure 4.1. It can be seen that there is a progressive increase in propylene selectivity with corresponding increase in temperature. The cracking of heavy hydrocarbons to light olefins is significantly enhanced at 500 ^{o}C.

Table 4-1 : Suitable reaction conditions for catalyst evaluation

Temperature	500 ^{o}C
Pressure	1 bar
Nitrogen flow rate	44 ml/min
TOS	150 min
Methanol feed rate	0.24 – 0.4 ml/min
WHSV	11 – 19 h^{-1}
Catalyst : SiC	1 : 4

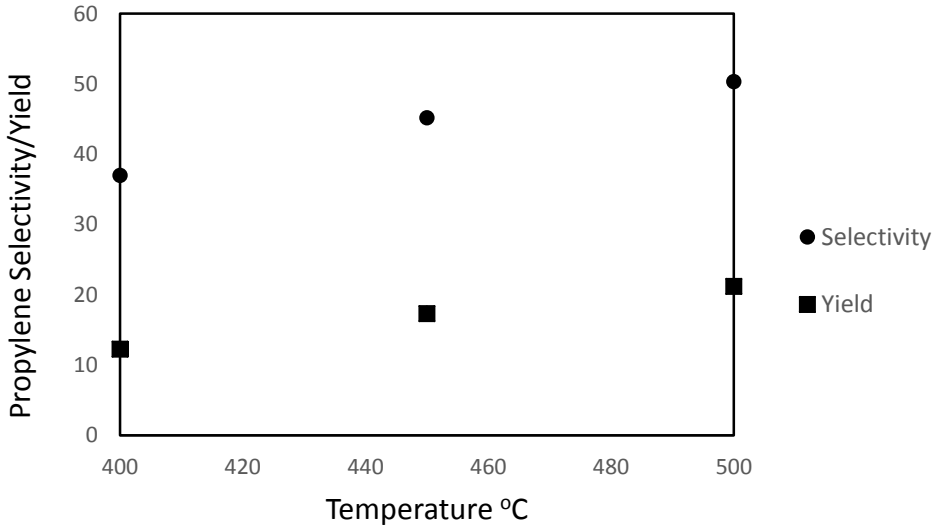

Figure 4-1: Effect of temperature on the selectivity and yield of propylene

4.2 Characterization of pelletized catalyst

4.2.1 X-Ray Diffraction (XRD)

The XRD analysis was conducted to identify the crystalline phase of ZSM-5 catalyst. Figure 4.2 shows the XRD pattern of the ZSM-5 catalyst with SiO_2/Al_2O_3 ratios of 30, 50, 80, 280 and 410. The prominent diffraction peaks appeared at 2θ = 8, 9, 15, 22 – 25 and 30, these peaks compared with JPDS card confirmed that the base powder is indeed ZSM-5 possess well crystalline MFI characteristics and they do not contain any detectable impurities or amorphous material [97]. The peak intensities show high degree of crystallinity.

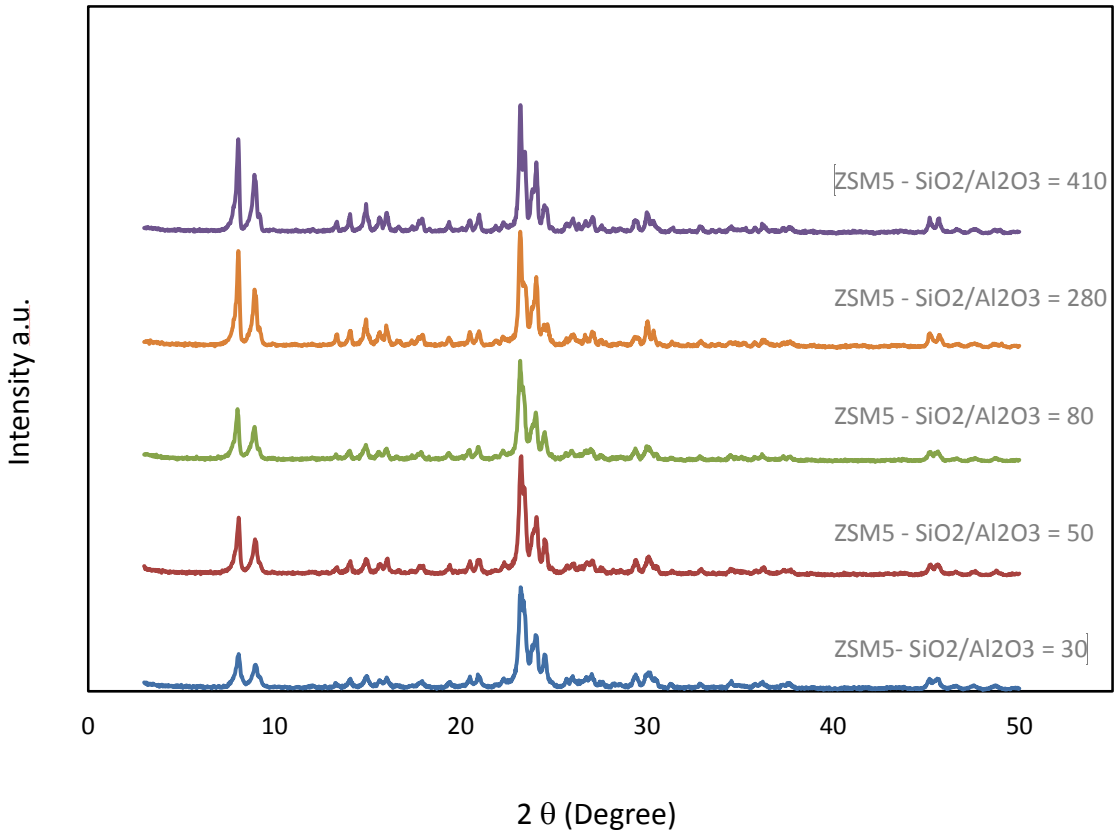

Figure 4-2: XRD pattern of ZSM-5 with SiO_2/Al_2O_3 ratio of 30, 50, 80, 280 and 410

4.2.2 NH_3 – TPD

NH_3 – TPD profiles are shown in Figure 4.3. The acidity of the sample with varying SiO_2/Al_2O_3 ratios was determined and the results are summarized in Table 4.2. The NH_3-TPD profile of ZSM-5 zeolite shows two well resolved peaks, lower temperature peak (LTP) around 220 ^oC and a high temperature peak (HTP) at around 420 ^oC. The lower temperature peak is assigned to ammonia desorbed from the weak acid Lewis site and the high temperature peak is ascribed to desorption from the more strongly acidic Bronsted sites [98].

As shown in Figure 4.3, the HTP intensity decreases as the SiO_2/Al_2O_3 ratio increases. This is attributable to the decrease in the aluminum framework content. It can also be observed that the desorption temperature of ammonia from strong acid sites is shifted to lower temperatures as the SiO_2/Al_2O_3 ratio increases. In Table 4.2, the total acidity reported shows that the total no. of acid sites increases with decrease in the SiO_2/Al_2O_3 ratio of ZSM-5. A similar observation is also reported in literature[99].

Table 4-2: NH_3-TPD adsorption for ZSM-5 with different molar ratio of SiO_2/Al_2O_3

ZSM- 5 SiO_2/Al_2O_3	Acidity (mmol g^{-1})
30	1.22
50	0.96
80	0.60
280	0.21
410	0.16

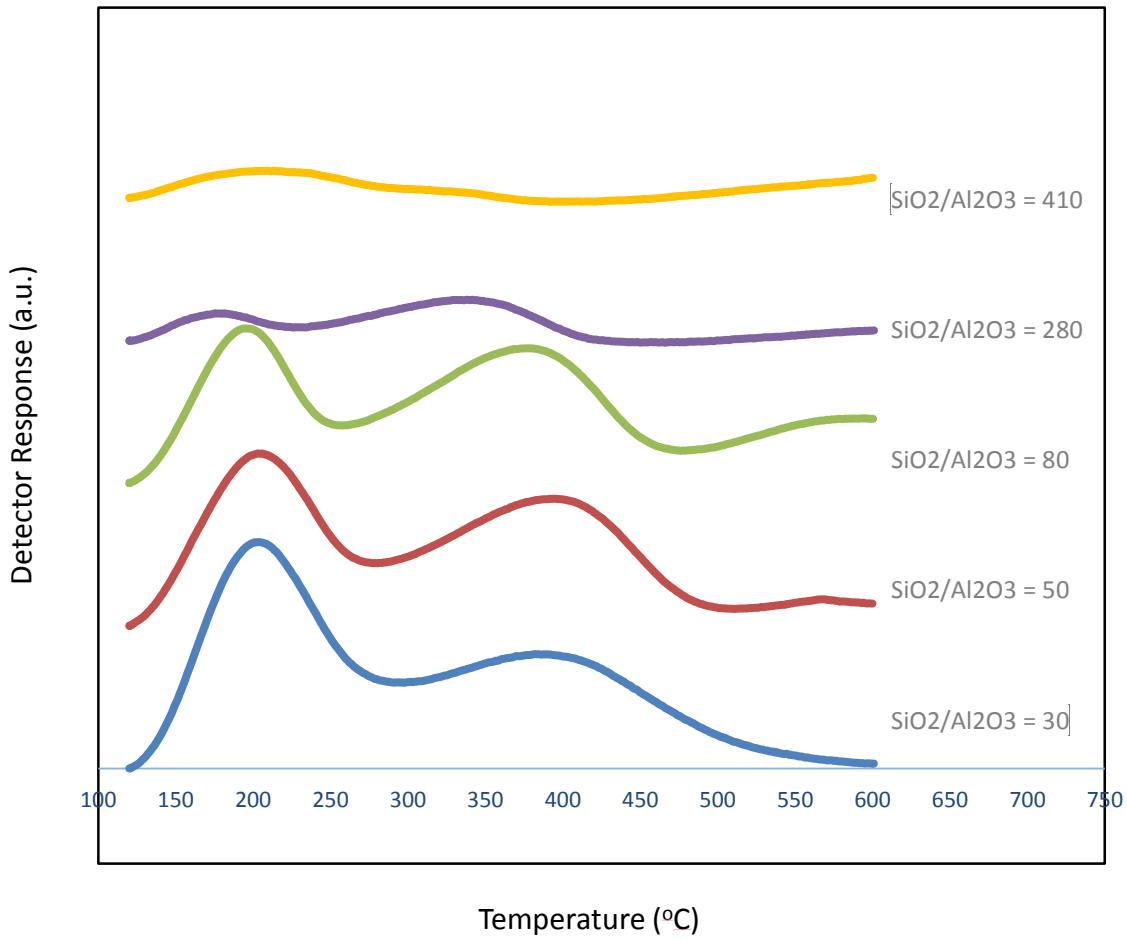

Figure 4-3: NH3-TPD profile of ZSM-5 samples with different SiO_2/Al_2O_3 ratios

4.2.3 SEM and EDX

The morphology of the ZSM-5 crystals with different molar ratios of SiO_2/Al_2O_3 is shown in Figures 4.4 – 4.9 (upper). All the samples are observed to possess different crystal morphologies, which are found to be elliptical, rectangular or cubical in shape with a uniform size distribution. They are found to be free of any amorphous substances or other crystalline impurities. In case of SiO_2/Al_2O_3 ratios of 30 and 50, a high degree of intergrowth and joining with a higher level of agglomeration is observed. It is also seen that at higher aluminum content of the sample, crystal size decreases. The approximate crystal sizes are 0.15, 0.2, 0.45, 0.7 and 0.8 μm for SiO_2/Al_2O_3 ratio of 30, 50, 80, 280 and 410 respectively. The electron micrographs clearly reveals that the size and morphology of the crystals depend on the SiO_2/Al_2O_3 molar ratio used.

The EDX analysis of all the catalyst samples is summarized in Table 4.3 and shown in Figures 4.4 - 4 .9 (lower) . The figures clearly reveals the presence of Silicon, Aluminium and Oxygen elements, the initial peaks basically represent the gold coating used in the FESEM technique. The EDX results confirm that there is no element present in the sample other than Si, Al and O, which are the primary constituting components of ZSM-5 catalyst.

Table 4-3: EDX elemental analysis of ZSM-5 catalyst samples

S #	Elemental Weight %		SiO_2/Al_2O_3
	Si	Al	ratio
1	36.41	2.22	32
2	30.24	1.16	50
3	31.74	0.77	79
4	45.12	0.28	311
5	45.37	0.21	417

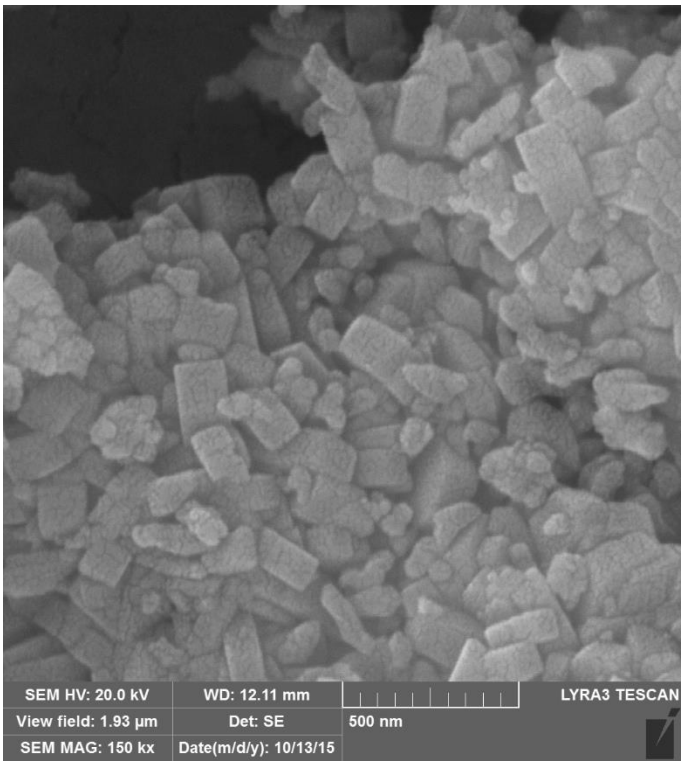

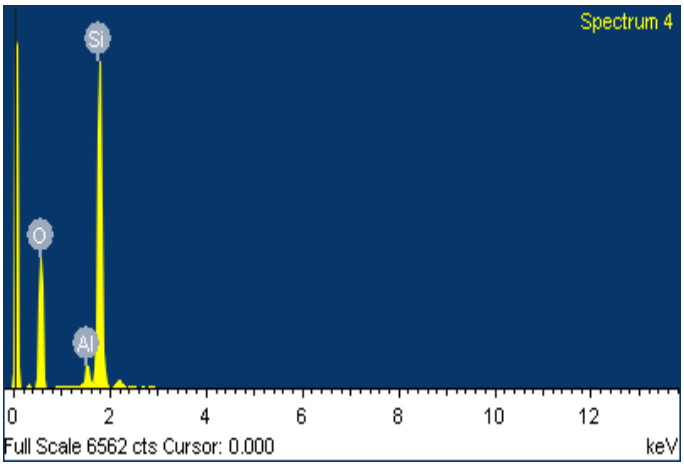

Figure 4-4: SEM image and EDX Spectrum of ZSM-5 sample (SiO_2/Al_2O_3 = 30)

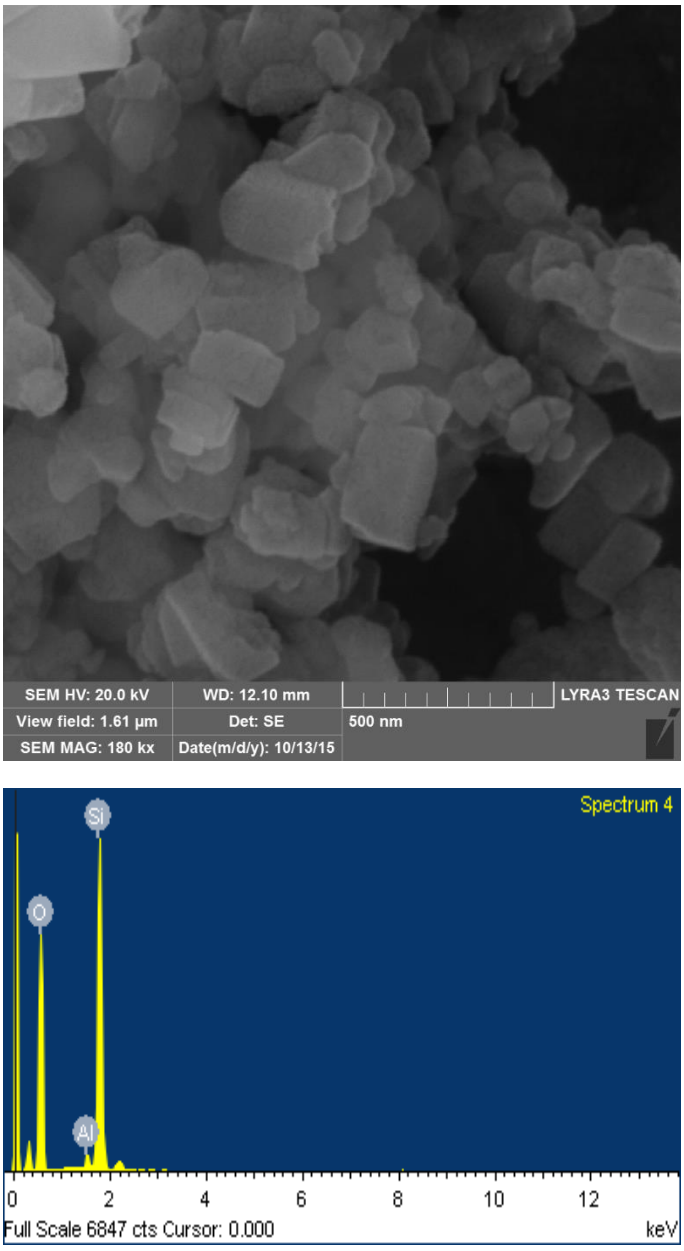

Figure 4-5: SEM image and EDX Spectrum of ZSM-5 sample (SiO_2/Al_2O_3 = 50)

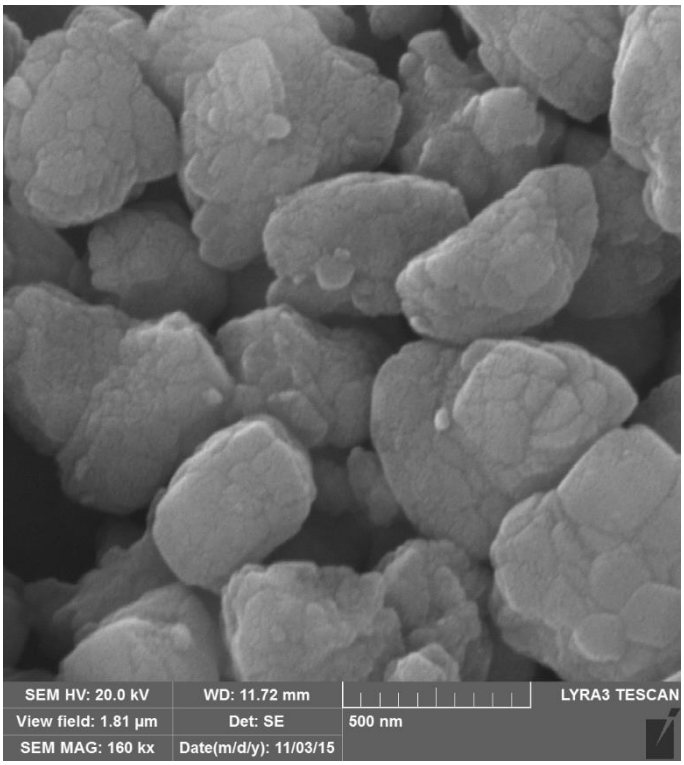

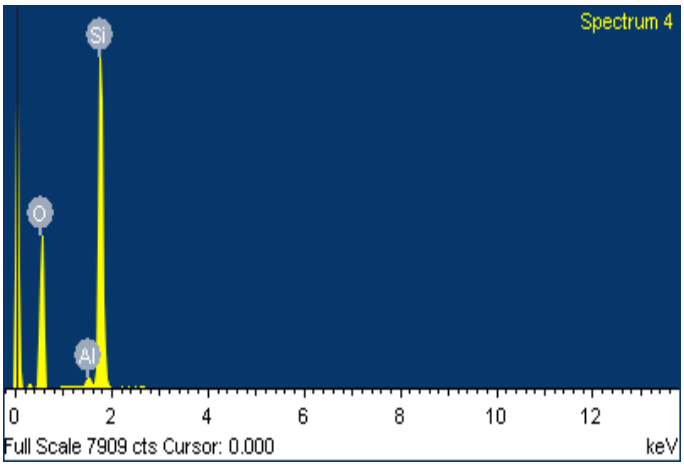

Figure 4-6: SEM image and EDX Spectrum of ZSM-5 sample (SiO_2/Al_2O_3 = 80)

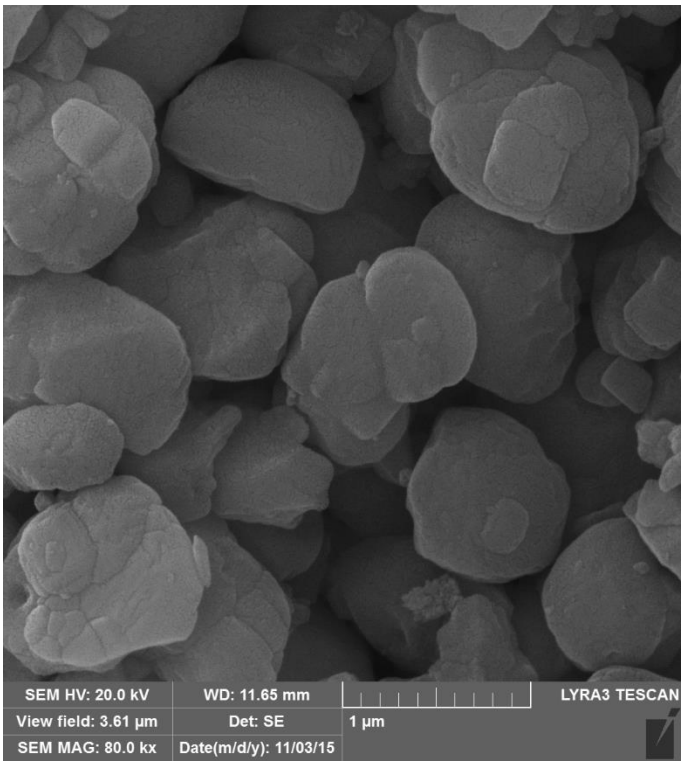

Figure 4-7: SEM image and EDX Spectrum of ZSM-5 sample (SiO_2/Al_2O_3 = 280)

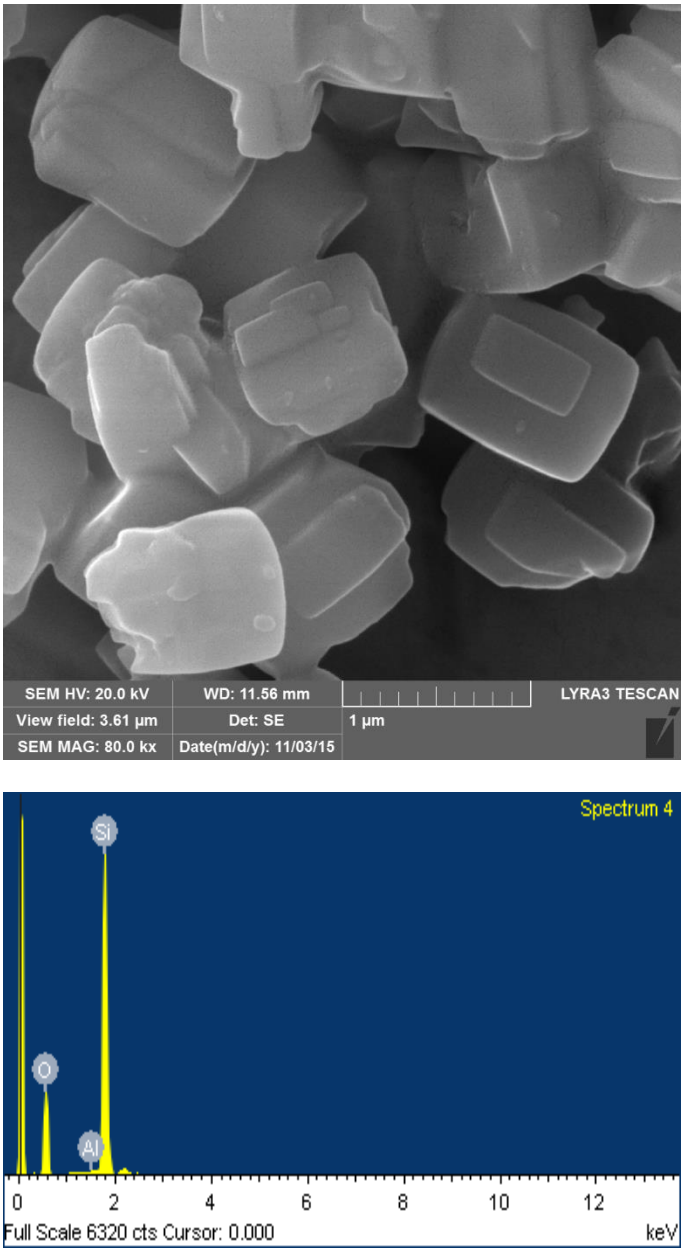

Figure 4-8: SEM image and EDX Spectrum of ZSM-5 sample (SiO_2/Al_2O_3 = 410)

4.2.4 BET Surface Area and Pore Volume

The N2 adsorption – desorption isotherm curves for each of the ZSM-5 catalyst samples are plotted in Figures 4.9 - 4.11 for all the catalyst samples individually. Nitrogen adsorption isotherms were measured over a relative pressure (p/po) range from 0.1 to 0.99. All the samples shows the type I + IV isotherm according to the classification of IUPAC correspondingly the presence of micro and mesoporosity. The hysteresis loop is of type H4 in most of the samples, hysteresis is obtained to occur due to the capillary condensation [100]. BET surface area and total volume of all the samples are calculated from the nitrogen adsorption isotherm data and summarized in Table 4.4. The BET surface area of all the samples are within the range of 321 to 361 m^2/g. The micrporous volume of ZSM-5 catalyst having the lower SiO_2/Al_2O_3 ratios i.e. 30, 50 and 80 are similar but in the case of 280 and 410 SiO_2/Al_2O_3 ratios the micropore pore volumes measured to be 0.03 and 0.05 cm^3g^{-1} respectively, which is lower from the other samples i.e. less SiO_2/Al_2O_3 ratio catalyst. This might be due to the defects in structure or may be due to the partial pore blockage of the ZSM-5 with a higher SiO_2/Al_2O_3 ratio [101].

Table 4-4: Surface properties of ZSM-5 catalyst samples

Sample Catalyst	S_{BET} (m^2/g)	V_{Total} ($cm^3\ g^{-1}$)
ZSM-5 (SiO_2/Al_2O_3 = 30)	327	0.12
ZSM-5 (SiO_2/Al_2O_3 = 50)	341	0.15
ZSM-5 (SiO_2/Al_2O_3 = 80)	361	0.12
ZSM-5 (SiO_2/Al_2O_3 = 280)	321	0.13
ZSM-5 (SiO_2/Al_2O_3 = 410)	329	0.07

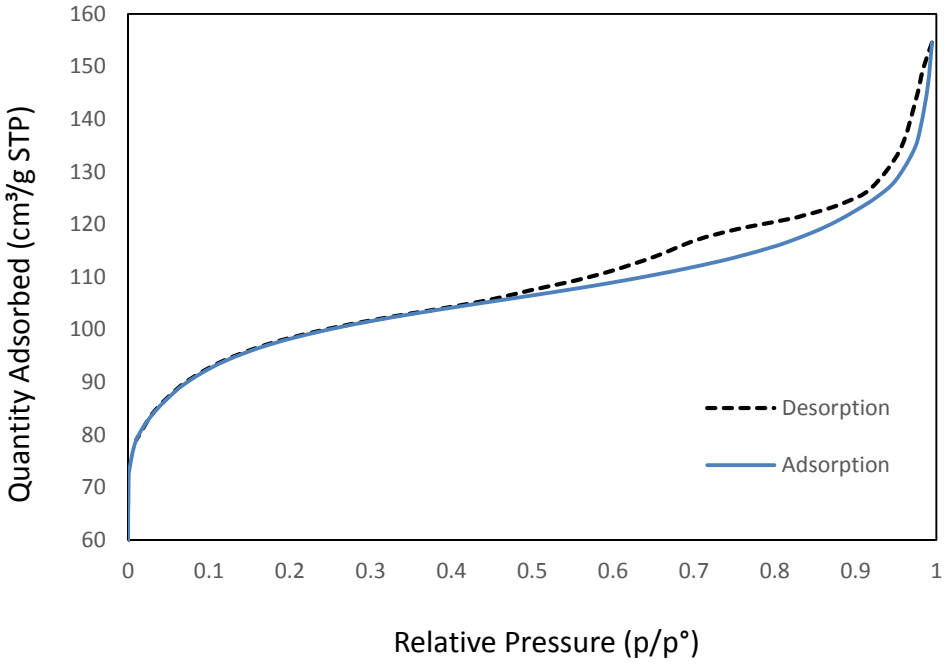

Figure 4-9: Adsorption desorption plot for ZSM-5 of 30 SiO_2/Al_2O_3 ratio.

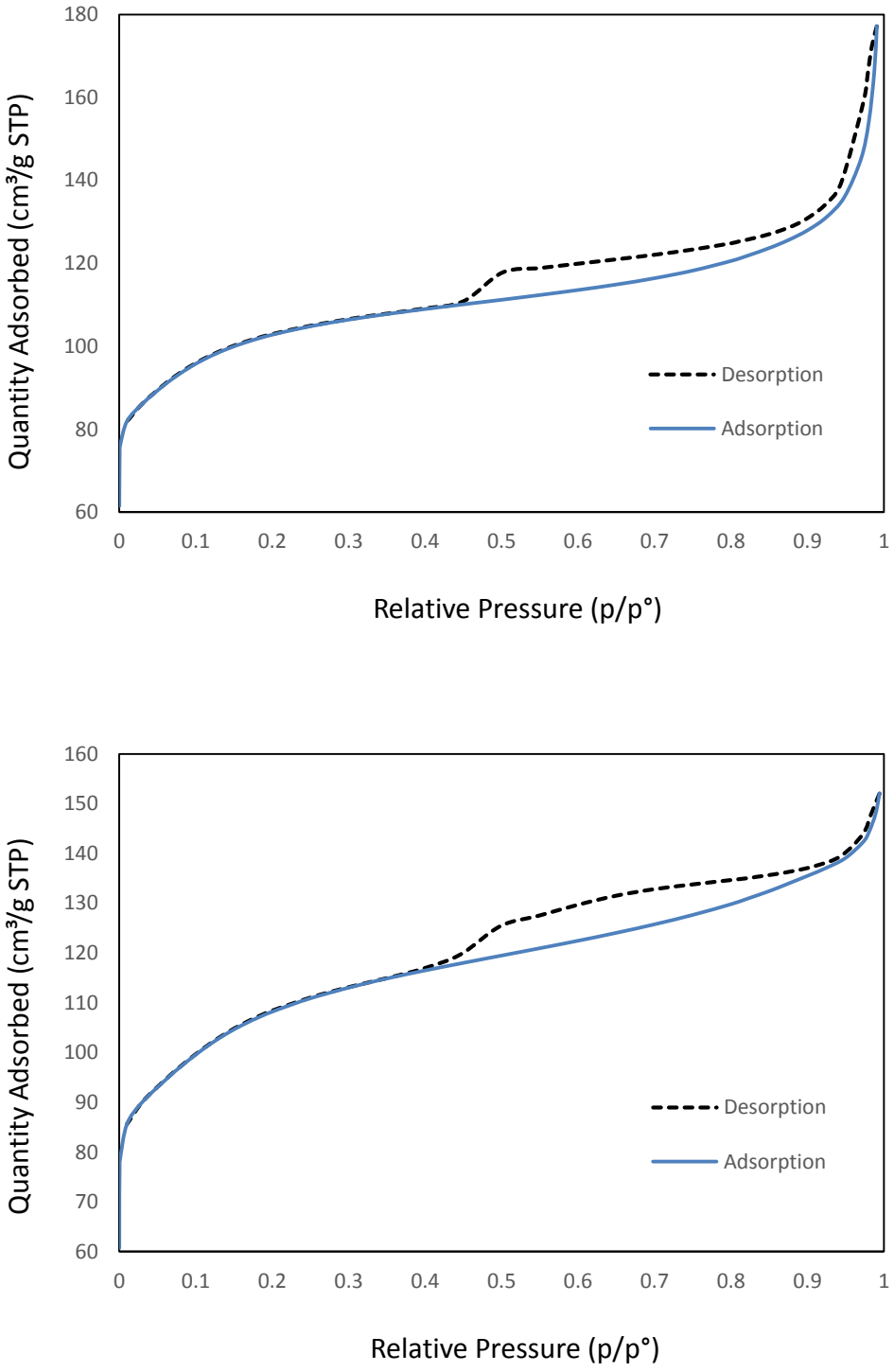

Figure 4-10: Adsorption desorption plot for ZSM-5 of 50 SiO_2/Al_2O_3 ratio (upper) and 80 SiO_2/Al_2O_3 ratio (lower)

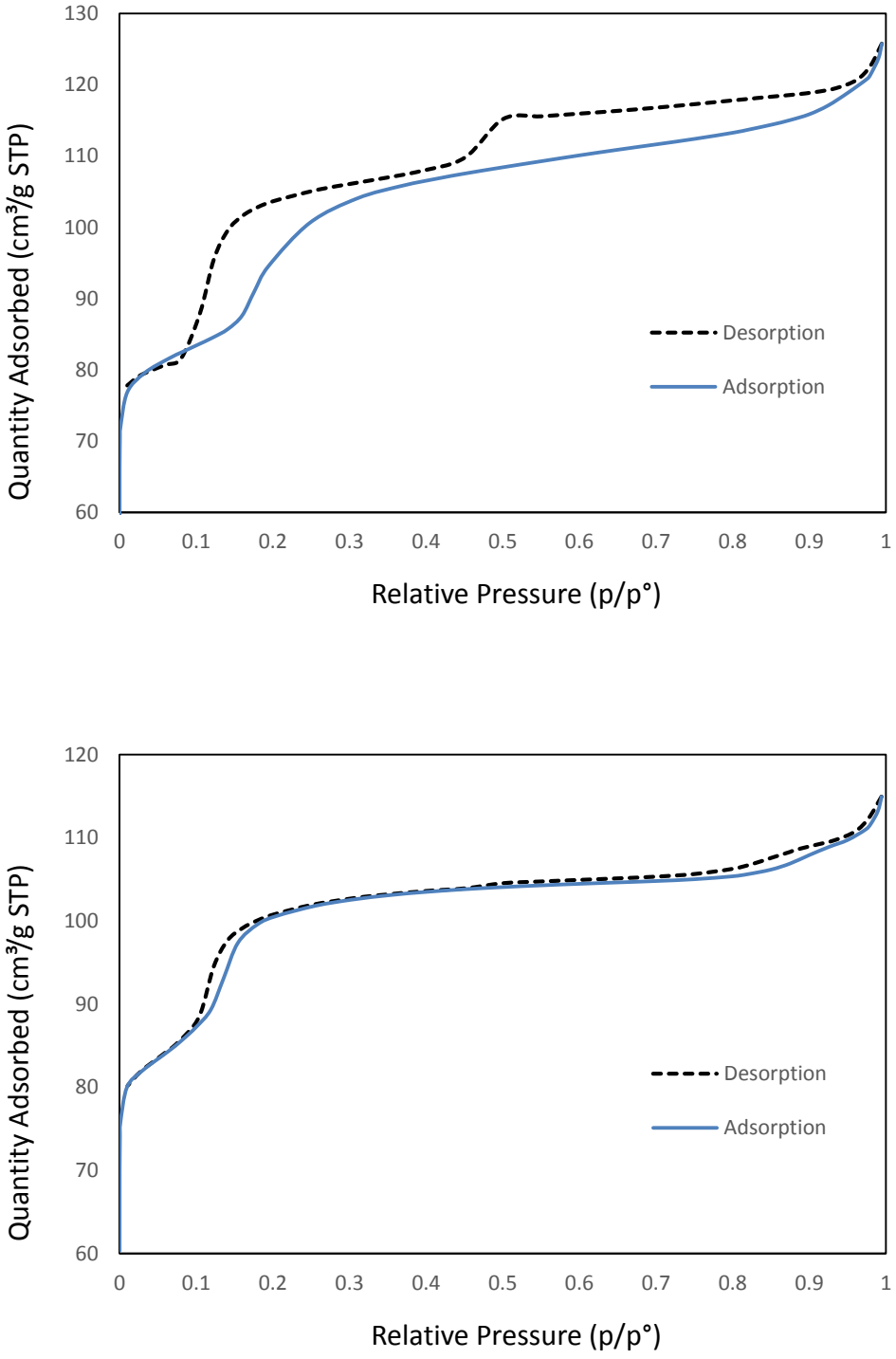

Figure 4-11: Adsorption desorption plot for ZSM-5 of 280 SiO_2/Al_2O_3 ratio (upper) and 410 SiO_2/Al_2O_3 ratio (lower)

4.3 Evaluation of Pelletized Catalyst

4.3.1 Blank run

Blank run test is carried out at 400, 450 and 500 ^{o}C with a methanol flow rate of 0.4 ml/min. The sample is analysed through online GC. Only ethane is observed in gaseous phase at 500 ^{o}C with the 4.2 % of methanol conversion. This conversion of methanol shows that reactor tube has almost negligible effect on the conversion of methanol into hydrocarbon reactions.

4.3.2 Effect of Reaction Conditions on Methanol Conversion

The methanol conversions over ZSM-5 catalyst with varying SiO_2/Al_2O_3 ratios and WHSV at 150 min TOS and 500 ^{o}C are presented in Figure 4.12. The experimental results of catalytic testing at these conditions with WHSV of 11 h^{-1}, 15 h^{-1} and 19 h^{-1} are reported in Table 4.6, 4.7 and 4.8, respectively. The product selectivities are calculated based on the total amount of the gaseous phase products formed including alkanes and olefins. In Figure 4.12, each catalyst with particular SiO_2/Al_2O_3 ratio is observed to show a different behavior towards the conversion of methanol whereas the conversion is maximum at WHSV of 15 h^{-1} for the catalyst with SiO_2/Al_2O_3 ratios of 30, 50, 80 and 280. At this WHSV, the catalyst with SiO_2/Al_2O_3 ratio of 410 is evaluated but it is observed that there is also a significant decrease in the conversion of methanol at these reaction conditions. The lower conversion of catalyst with SiO_2/Al_2O_3 ratio of 410 is attributable to its fast deactivation therefore it is

observed to result in lower overall conversion at a reaction time of 150 min. This apparent deactivation could be related to the lower number of Bronsted acid sites initially present on HZSM-5 [101].

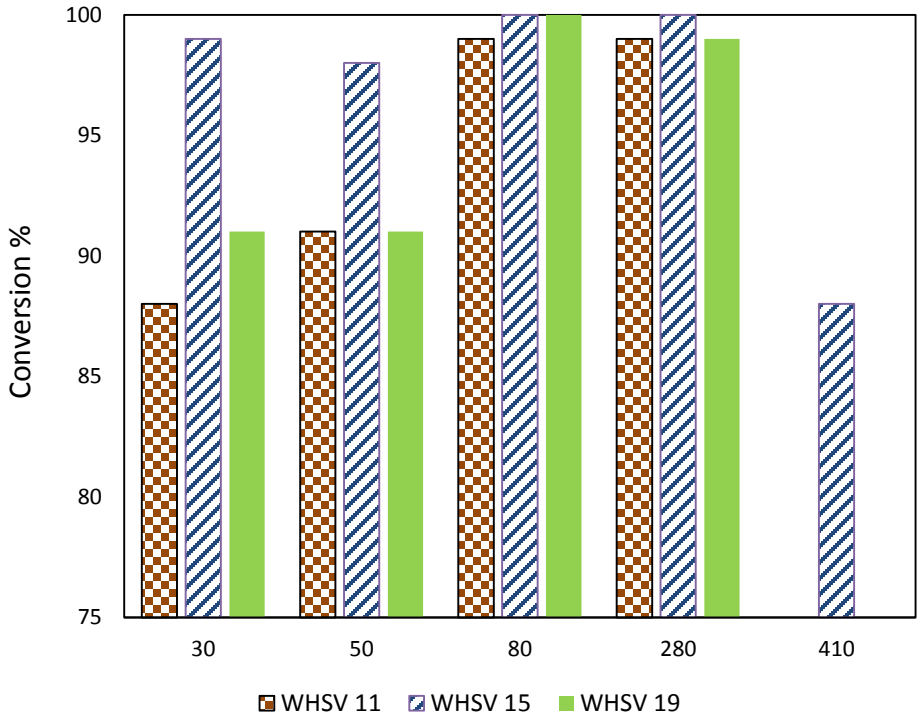

Figure 4-12: Methanol conversion at Reaction Temp = 500 ºC, TOS = 150 min

Table 4-5: Experimental results at WHSV = 11 h^{-1}, Temp = 500 ^{o}C, TOS = 150 min

SiO_2/Al_2O_3	**30**	**50**	**80**	**280**
Conversion %	88	91	99	99
Mass Balance %	94	96	96	97
Yield %				
Liquid HC	2.99	5.94	6.89	3.11
Water	62.17	62.47	55.09	54.33
Gases	34.84	31.59	38.02	42.56
Methane	8.47	4.04	2.91	0.29
Ethane	0.54	0.36	0.32	0.00
Ethylene	6.68	5.86	7.52	6.95
Propane	1.07	1.14	1.47	0.78
Propylene	9.19	10.53	14.18	20.32
Butylene	4.05	4.50	6.36	11.25
Alkanes C_4 +	4.84	5.16	5.26	2.97
Selectivity %				
Methane	24.32	12.78	7.66	0.69
Ethane	1.55	1.12	0.85	0.00
Ethylene	19.17	18.54	19.78	16.34
Propane	3.07	3.62	3.86	1.83
Propylene	26.38	33.33	37.30	47.73
Butylene	11.61	14.25	16.73	26.43
Alkanes C_4 +	13.90	16.35	13.82	6.98
Propylene/ Ethylene	1.38	1.80	1.89	2.92

Table 4-6: Experimental results at WHSV = 15 h^{-1}, Temp = 500 ^{o}C, TOS = 150 min

SiO_2/Al_2O_3	**30**	**50**	**80**	**280**	**410**
Conversion %	99	98	100	100	88
Mass Balance %	95	96	95	96	94
Yield %					
Liquid HC	4.52	8.00	5.95	3.16	1.69
Water	54.59	56.25	55.14	55.01	64.97
Gases	40.89	35.75	38.90	41.84	33.34
Methane	4.68	3.95	4.25	0.15	2.29
Ethane	0.88	0.69	0.38	0.10	0.00
Ethylene	9.67	8.48	7.31	6.84	4.94
Propane	3.12	2.51	1.10	0.86	0.00
Propylene	10.43	9.77	14.76	20.02	16.39
Butylene	3.76	3.03	7.00	10.93	9.72
Alkanes C_4 +	8.35	7.31	4.11	2.92	0.00
Selectivity %					
Methane	11.46	11.06	10.93	0.36	6.87
Ethane	2.14	1.93	0.97	0.24	0.00
Ethylene	23.65	23.73	18.78	16.36	14.83
Propane	7.62	7.03	2.83	2.05	0.00
Propylene	25.51	27.33	37.93	47.86	49.15
Butylene	9.21	8.47	17.99	26.14	29.15
Alkanes C_4 +	20.41	20.46	10.56	6.99	0.00
Propylene/ Ethylene	1.08	1.15	2.02	2.93	3.31

Table 4-7: Experimental results at WHSV = 19 h^{-1}, Temp = 500 ^{o}C, TOS = 150 min

SiO_2/Al_2O_3	**30**	**50**	**80**	**280**
Conversion %	91	91	100	99
Mass Balance %	95	94	95	96
Yield				
Liquid HC	6.12	7.38	7.57	3.91
Water	59.19	59.24	55.04	59.14
Gases	34.70	33.38	37.39	36.95
Methane	4.26	3.35	2.69	0.34
Ethane	0.55	0.36	0.37	0.10
Ethylene	7.69	6.59	8.74	6.43
Propane	1.53	1.40	1.81	0.65
Propylene	11.08	11.05	13.31	17.35
Butylene	3.00	4.88	7.15	9.89
Alkanes C_4 +	6.60	5.76	3.30	2.20
Selectivity %				
Methane	12.27	10.03	7.21	0.92
Ethane	1.60	1.08	1.00	0.27
Ethylene	22.15	19.74	23.39	17.40
Propane	4.40	4.20	4.85	1.76
Propylene	31.93	33.10	35.59	46.94
Butylene	8.63	14.61	19.13	26.76
Alkanes C_4 +	19.02	17.24	8.84	5.95
Propylene/ Ethylene	1.44	1.68	1.52	2.70

4.3.3 Effect of WHSV

Experiments are performed to investigate the effect of change in WHSV on reactions. All the catalyst are tested on WHSV of 11 h^{-1}, 15 h^{-1} and 19 h^{-1} at 500 ^{o}C as shown in Figure 4.13. WHSV is changed by varying the flow rate of methanol. The effect of WHSV on the conversion shows that there is a higher conversion of methanol at WHSV of 15 among all the tested samples. Within this range of WHSV the conversion is observed to almost remain the same for the case of catalyst with SiO_2/Al_2O_3 ratio of 80 & 280. In Figure 4.13 the effect of WHSV on propylene yield shows that the propylene yield decreases at higher WHSV for catalyst which results in an overall higher propylene yield i.e. 80 and 280 SiO_2/Al_2O_3 ratio catalyst. The propylene selectivity among the hydrocarbons is observed to be maximum for the case of catalyst with SiO_2/Al_2O_3 ratio of 280 and it remains almost constant at the range of WHSV, however it is noticed that at 19 h^{-1} WHSV; the Propylene/ ethylene ratio decreases which implies WHSV equal to 15 h^{-1} is the most suitable condition in term of propylene selectivity. In case of SiO_2/Al_2O_3 ratio of 30 and 50 the decrease in propylene selectivity at 19 h^{-1} is attributable to the higher production of butylene. The higher propylene yield at 15 h^{-1} is attributed to the higher conversion of methanol into gaseous hydrocarbons, whereas more than this particular WHSV the feed hold up decreases the overall conversion of methanol.

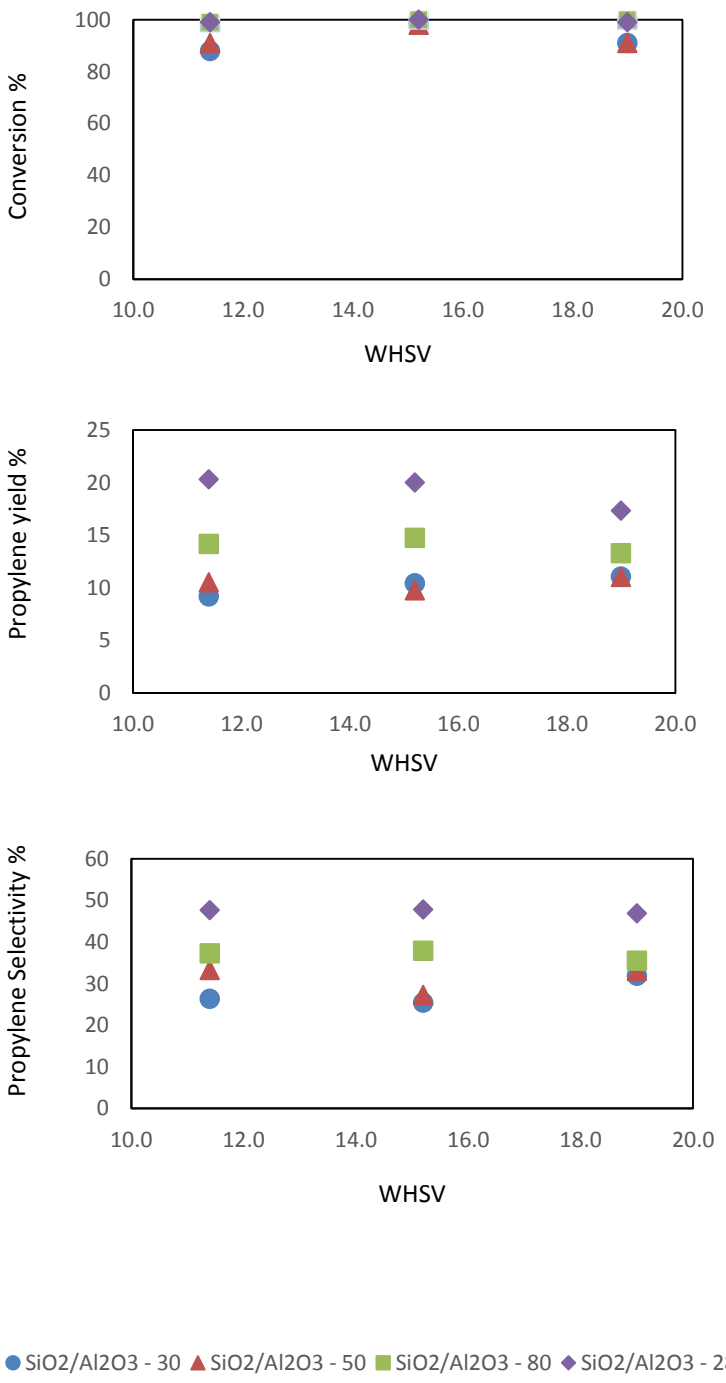

Figure 4-13: Effect of WHSV on conversion, propylene yield and propylene selectivity

4.4 Screening of Best Performing Catalyst

It has been reported in the above section that conversion is almost 98% – 100 % at WHSV of 15 h^{-1}. In this scenario, by analyzing the results at WHSV of 15 h^{-1} the selection criteria for the best catalyst with optimum performance can be regard as higher yield and propylene selectivity in gaseous phase.

4.4.1 Gaseous Product Selectivity

Figure 4.14 shows the selectivity plotted for all the catalysts with varying SiO_2/Al_2O_3 ratios at reactions conditions of 15 h^{-1} WHSV, 500 ^oC and TOS of 150 min. It can be observed that the percentage of alkanes in the gaseous product varies inversely with SiO_2/Al_2O_3 ratio as well as the overall olefins percentage. This behavior is attributable to the decrease in the rate of cracking reaction of higher olefins into paraffins/alkanes. The propylene selectivity can be observed to increase upto 47.86 % in case of SiO_2/Al_2O_3 ratio of 280 and upto 49.15 % in case of SiO_2/Al_2O_3 ratio of 410. The ethylene selectivity is 16.36 % and 14.86 % for SiO_2/Al_2O_3 ratios of 280 and 410 respectively. The selectivity for the propylene is observed to vary inversely with the total acidity. This similar behavior is also reported in [102], whereby decreasing the Bronsted acidity ZSM-5 results in an increase in propylene selectivity amongst the olefins.

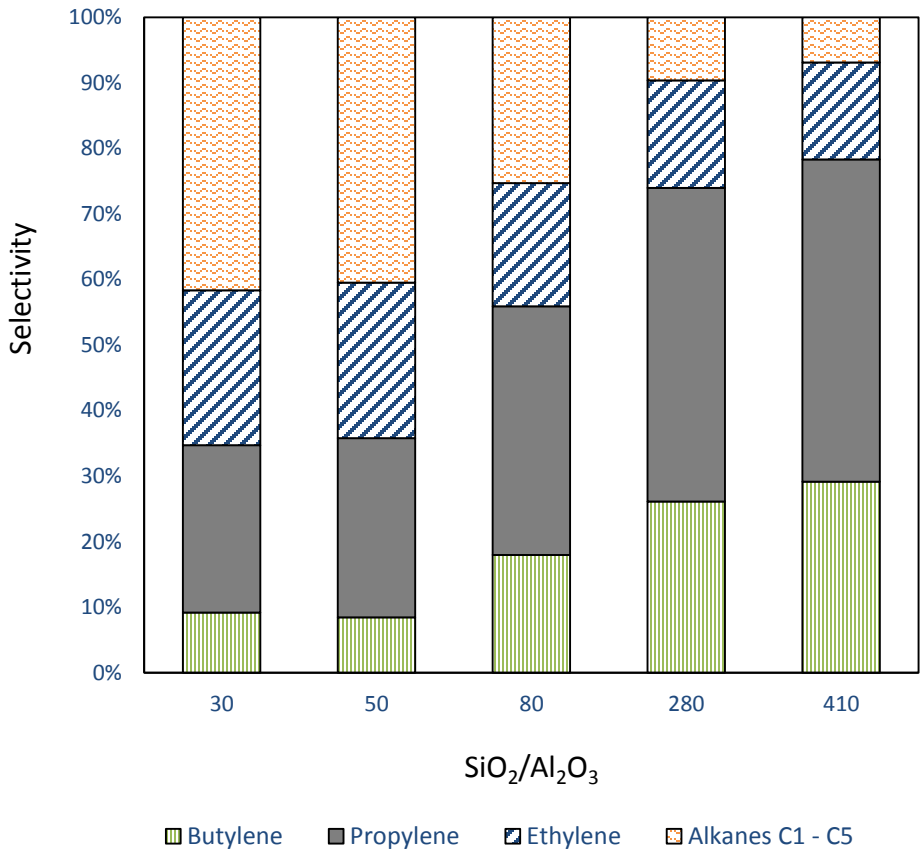

Figure 4-14: Selectivity at 15 h^{-1} WHSV and 500 ^{o}C temperature.

4.4.2 Product Distribution (Yield %)

Figure 4.15 shows the yield for all the catalysts with varying SiO_2/Al_2O_3 ratios at reactions conditions of 15 h^{-1} WHSV, 500 ºC and TOS of 150 min. The yield of gaseous product can be observed to vary from 33% to 42 %. The yield observed to be lowest at SiO_2/Al_2O_3 ratio of 410 and highest at SiO_2/Al_2O_3 ratio of 280. The propylene yield is particular observed to be the maximum at a SiO_2/Al_2O_3 ratio of 50 as shown in figure 4.16. The lower observed overall gaseous product yield in case of SiO_2/Al_2O_3 ratio of 410 attributable to its faster deactivation.

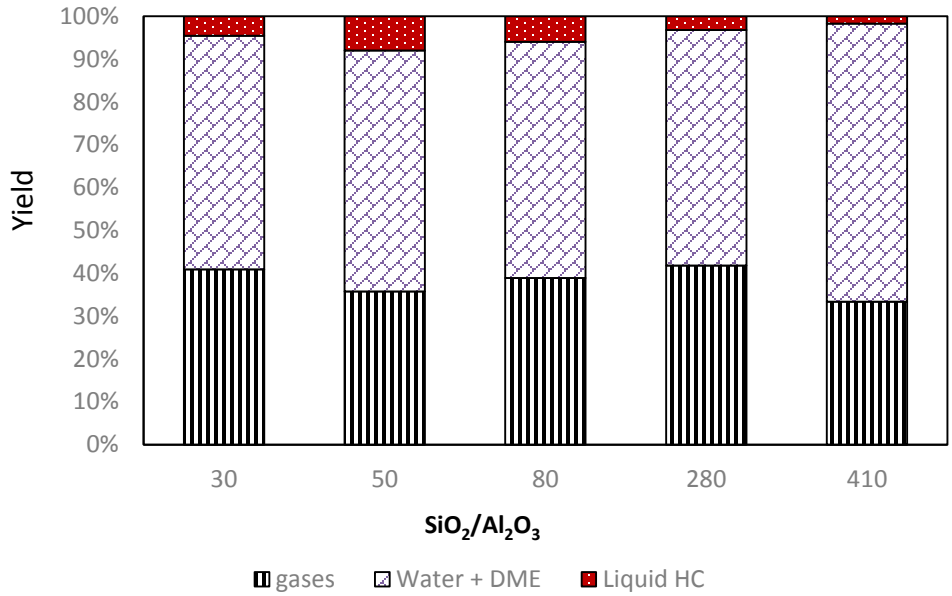

Figure 4-15: Overall yield at 15 h^{-1} WHSV and 500 °C temperature

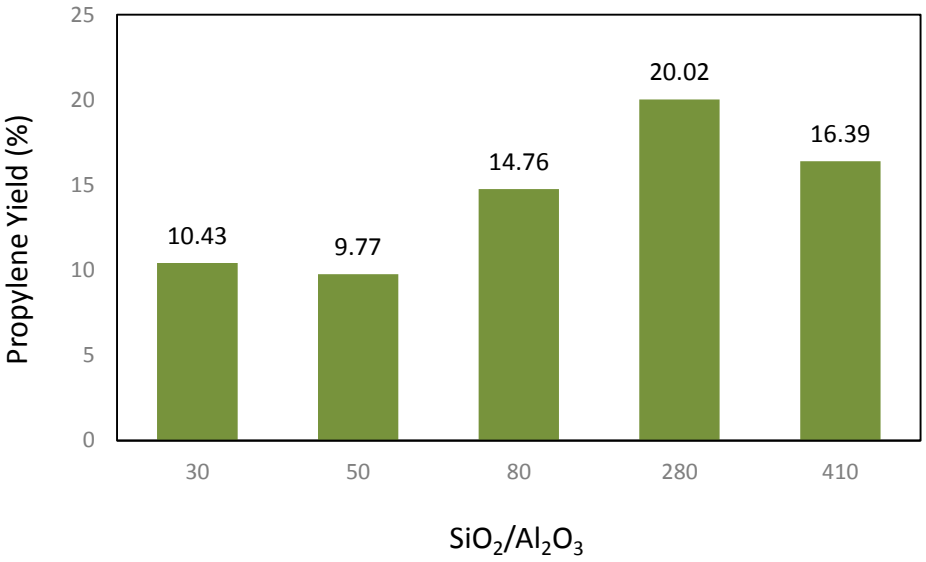

Figure 4-16: Propylene yield at 15 h^{-1} WHSV and 500 °C temperature

4.5 Preparation and Characterization of Monolith Coated Catalyst

4.5.1 Zeolite Coating and Adhesion Testing

The coating slurry contained 20 wt. % ZSM-5 in DI water with 1 wt. % binder for 1st sample and 2 wt. % binder for 2nd sample. Both of these samples were coated with a single layer and then tested in ultrasonic bath for 60 min. For the second coating, exactly the same testing procedure was adopted for the case of first coating. It was observed that the higher the amount of colloidal silica binder, the higher the amount of zeolite deposited on the structure [103]. According to Figure 4.17 the single coating layer is observed to be a 5.71 wt. % increase for the case of 1 wt. % binder and 7.51 wt. % increase for the case of 2 wt. % binder. A similar effect is also observed for the case of second coating layer. In Figure 4.18, the loss of weight % is also observed to be higher if the amount of binder used is reduced. This refers to the fact that adhesion of a higher zeolite particles to one another and to the support is enhanced when a higher amount of binder is used. However, an excessive increase in the amount of binder added is also observed to create difficulty in the removal of excess slurry from the monolith holes.

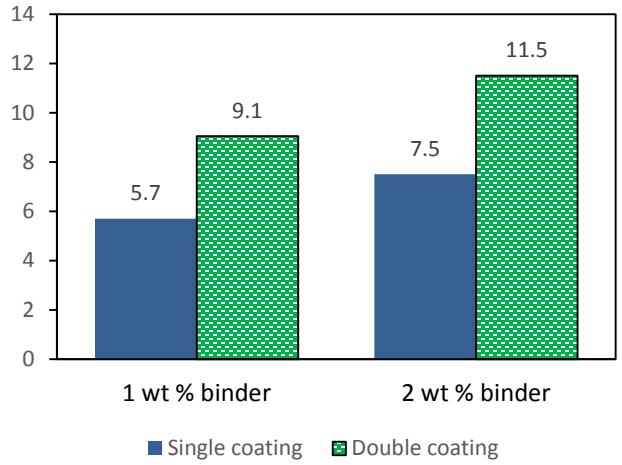

Figure 4-17: Catalyst loading (wt. %)

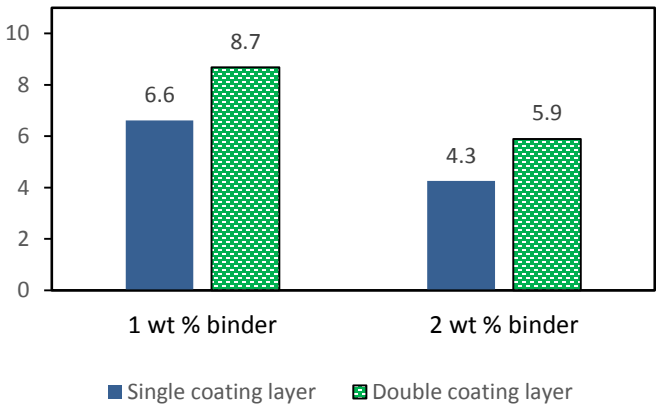

Figure 4-18: Loss in wt. % after ultrasonic treatment

4.5.2 X-Ray Diffraction (XRD)

The XRD analysis was carried out to confirm the presence of ZSM-5 catalyst on the cordierite monolith. Figure 4.19 shows the XRD spectra obtained for cordierite and the cordierite coated ZSM-5 catalyst. By comparing the cordierite spectra with those for the coated cordierite spectra it can be noticed that small intensity peaks appeared for value of 2θ between 13.5 and 18.0 for the cordierite coated spectra whereas clearly distinct peaks can be observed for 2θ between 23.0 and 26.0. The cordierite coated sample contains almost 11.5 % of the ZSM-5 catalyst.

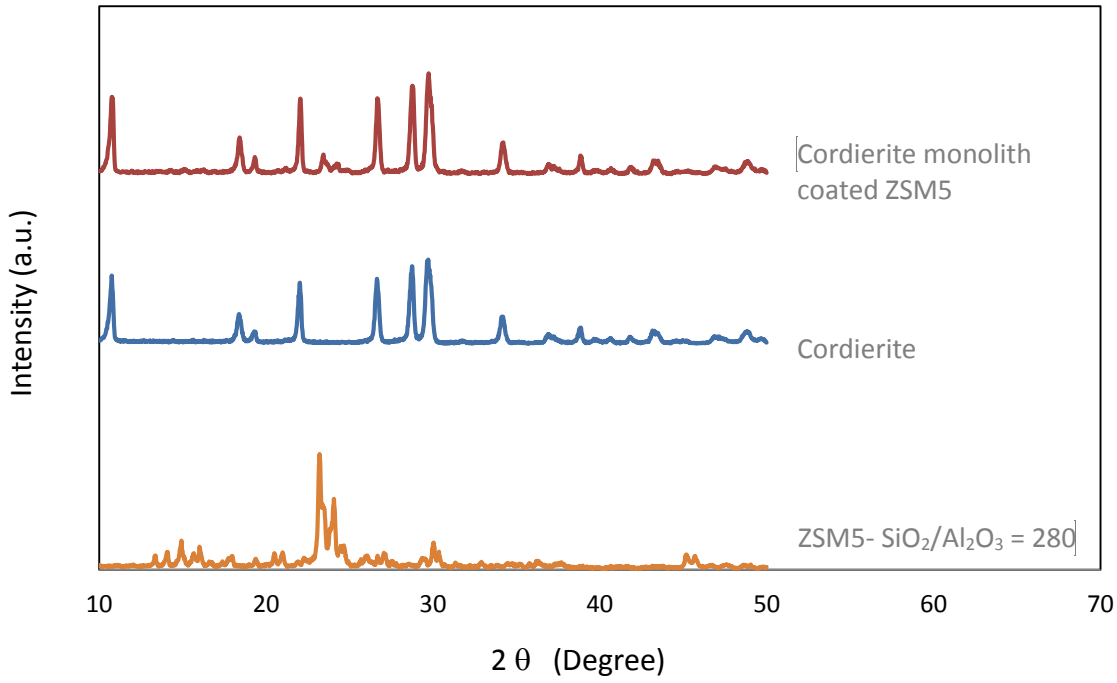

Figure 4-19: XRD pattern of ZSM-5 SiO_2/Al_2O_3 ratio of 280, cordierite and ZSM coated cordierite

4.5.3 Scanning Electron Microscopy (SEM)

SEM of coated structured catalyst was carried out to identify the morphology of coating layer as well as zeolite layer thickness after the single and double coatings. In Figure 4.20 (a) the SEM images of top view of the honeycomb monolith shown. Figure 4.20 (b) is the higher magnification of the cross sectional view of the uncoated monolith which show the uncovered monolith layer upon which the porous structure coating is visible. The crystal morphology of ZSM-5 (SiO_2/Al_2O_3 ratio equal to 280) shows that the crystals are elliptical in shape as shown in Figure 4.7, the same shape of zeolite crystals can be seen on the coating layer of sample prepared with 1 wt. % binder as shown in Figure 4.21 (a). Figure 4.21 (b) shows the clear zeolite deposition at the edge of the channels. In Figure 4.22 (a) the lower magnification image of the top view of sample prepared with 2 wt. % binder is shown, where it can be seen that the crystals are homogenously dispersed in the underlying matrix, on comparison with the images shown for the uncoated sample in Fig 4.20 (a), we can conclude that a uniform layer of catalyst has been deposited on coating the monolith surface and the roughness in surface is physically changed in a smooth surface. Figure 4.22 (b) shows the cross sectional image of the zeolite coating on the corners of the channels.

Figure 4.23 (a) shows the wall thickness calculated for the uncoated 400 cpi honeycomb monolith wall thickness calculation. It can be noticed that the average wall thickness of the monolith sample is approx. 195 μm while the average distance between the walls (channels) is approx. 1006 μm. According to Figure 4.23 (b) the wall thickness of zeolite coated monolith is approx. 230 μm, which means that the coating thickness of the sample prepared with 2 wt. % binder is approx. 18 μm.

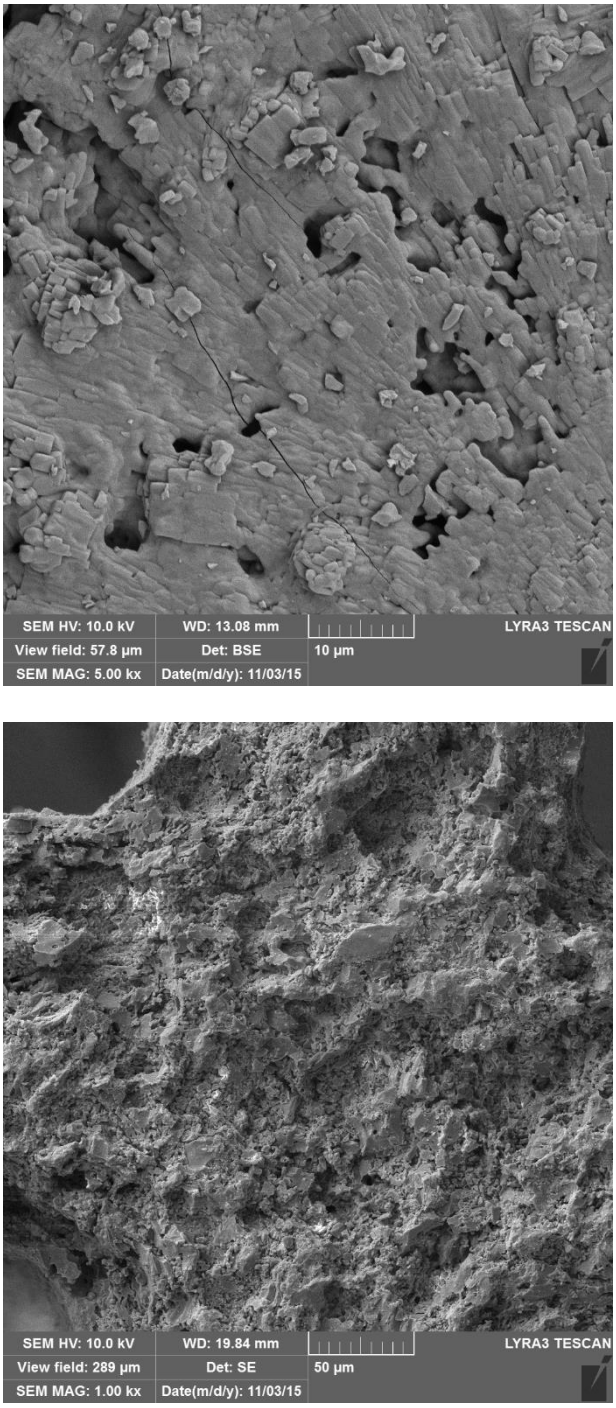

Figure 4-20: SEM images of top view of blank monolith (upper), cross sectional view of blank monolith (lower)

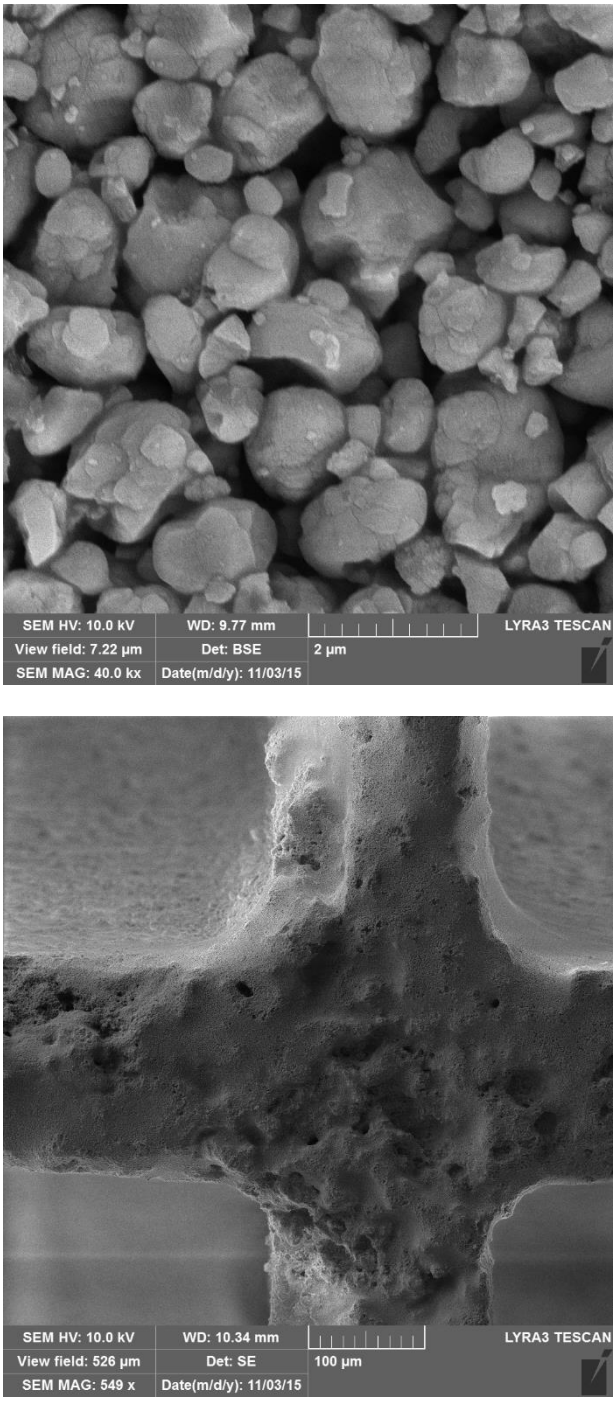

Figure 4-21: SEM images of top view of 1 wt. % binder prepared sample (upper), cross-sectional view (lower)

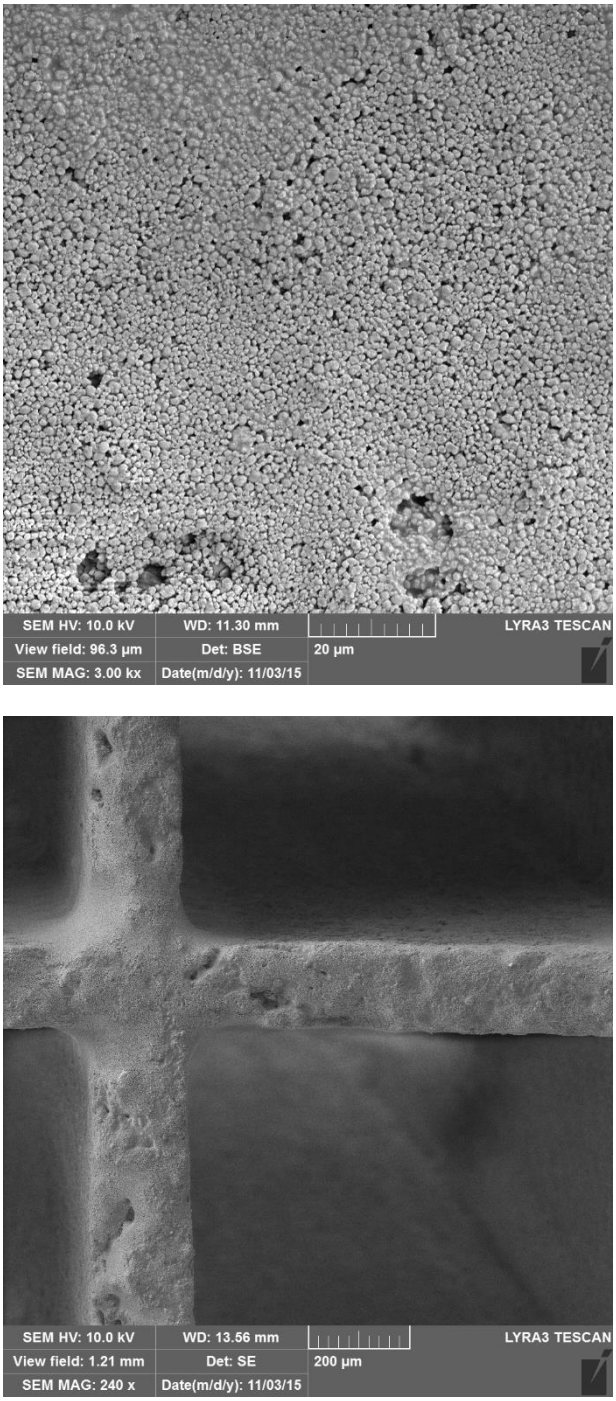

Figure 4-22: SEM images of top view of 2 wt. % binder prepared sample (upper), cross-sectional view (lower)

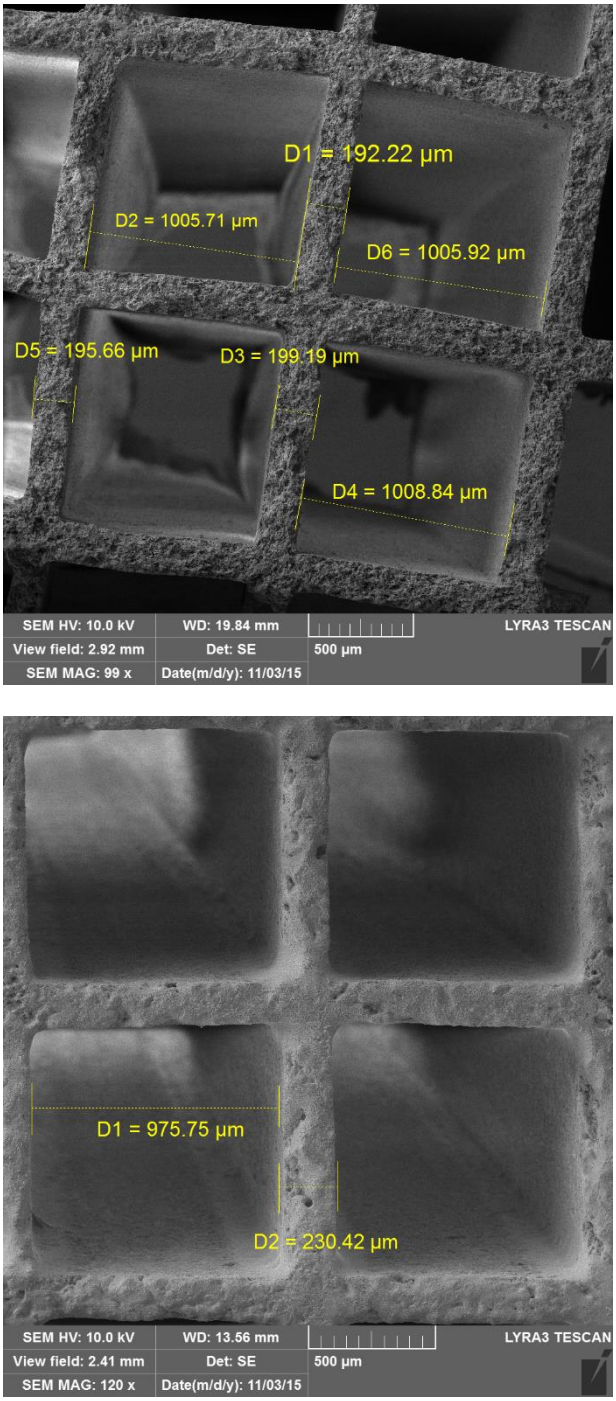

Figure 4-23: SEM images for the coating thickness measurement

4.6 Monolith coated catalyst evaluation

The structured catalyst was prepared from ZSM-5 with SiO_2/Al_2O_3 ratio of 280 coated on a cordierite monolith. This structured catalyst with double coating of zeolite was then evaluated in the fixed bed flow reaction system. The catalyst evaluation results at WHSV of 15 and 19 h^{-1} are summarized in Table 4.9. In case of pelletized catalyst, the highest propylene yield (20.02 %) and maximum conversion was achieved for SiO_2/Al_2O_3 ratio of 280 and WHSV of 15 h^{-1}. Hence, the SiO_2/Al_2O_3 ratio results for the coated catalyst can be compared with those of the uncoated catalyst at the same WHSV and other conditions. At a temperature of 500 ^oC a 100% conversion rate is observed for all the coated catalyst, whereas for pelletized catalyst it was observed to be in the range of 99 – 100% for SiO_2/Al_2O_3 ratio of 280. It has been observed that coated catalyst shows good performance regarding propylene yield and selectivity. Moreover, a negligible amount of aromatics were observed to produce during the reactions. As shown in Figure 4.24 the gaseous product yield increased from 42 % for pelletized to 47 % for the coated catalyst. Less amount of water is observed to be produced in coated catalyst, whereas almost negligible amount of aromatics/ liquid hydrocarbons observed in the liquid phase. The gas phase product selectivity comparison is shown in Figure 4.25, it can be observed that the propylene selectivity increased from 48 % to 52 %. It can be seen that butylene is also produced in higher quantity in case of coated catalyst, whereas alkanes production is minimized.

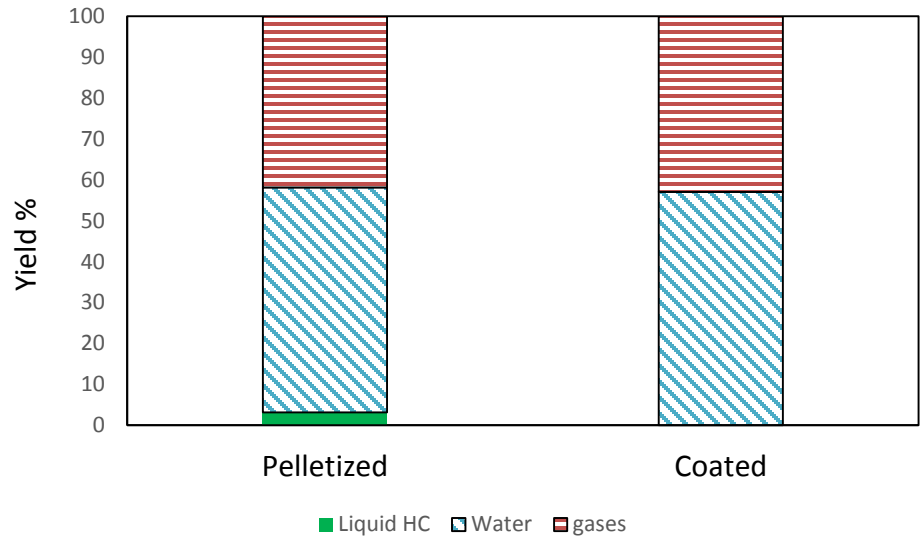

Figure 4-24: Total yield comparison between pelletized and coated catalyst at WHSV 19 h^{-1}

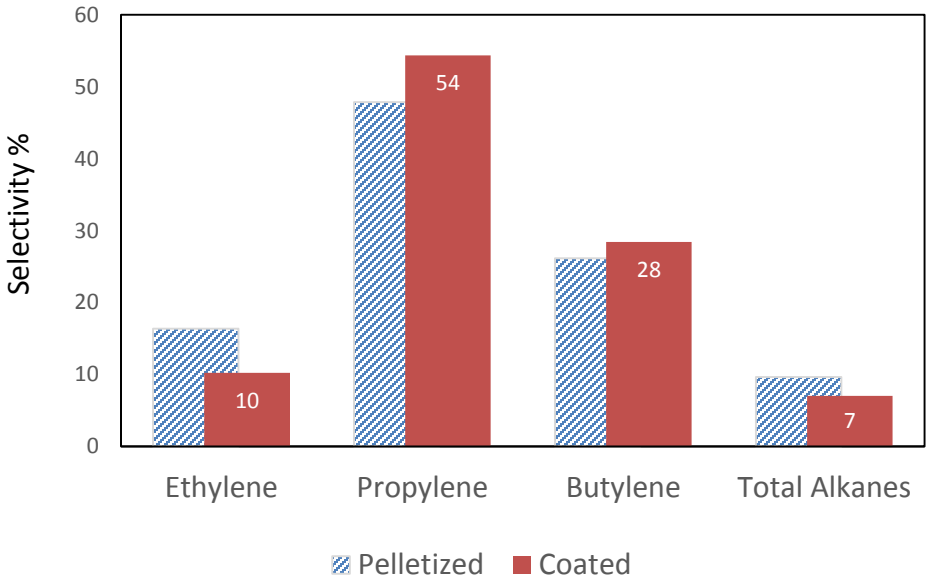

Figure 4-25: Comparison between the selectivity of gaseous products formed in pelletized catalyst and coated catalyst

Table 4-8: Experimental results at Temp = 500 °C, TOS = 150 min

WHSV (h^{-1})	15	19
Conversion %	100	100
Mass Balance %	99	98
Yield %		
Liquid HC	0.00	0.00
Water	52.85	57.10
Gases	47.15	42.90
Methane	0.00	0.00
Ethane	0.00	0.00
Ethylene	5.23	4.38
Propane	0.58	0.49
Propylene	24.60	23.31
Butylene	14.07	12.19
Alkanes C_4 +	2.66	2.52
Selectivity %		
Methane	0.00	0.00
Ethane	0.00	0.00
Ethylene	11.10	10.21
Propane	1.24	1.15
Propylene	52.17	54.34
Butylene	29.84	28.41
Alkanes C_4 +	5.65	5.88
Propylene/ Ethylene	4.70	5.32

4.7 Effect of SiO_2/Al_2O_3 Ratio and Coating on Product Selectivity

The product selectivities are calculated on the basis of total amount of gaseous product formed including methane, ethane, ethylene, propane, propylene, butylene and alkanes (C4+). All the alkanes products has been merged in the analysis in order to achieve a clear identification of the required olefin product. A WHSV of 15 h^{-1}, TOS of 150 min and a temperatureof 500 ^oC have been utilized to generate the plots shown in Figure 4.26.

The selectivity of propylene is observed to be almost same for SiO_2/Al_2O_3 ratio of 30 and 50, but continuously increases for the higher SiO_2/Al_2O_3 ratios. For monolith coated reaction system, the short diffusional path and lesser inter and intracrystalline diffusional resistances as compared to a fixed bed reactor results in a higher amount of olefins and a lower amount of paraffins. Hence, an approx. 4.31% increase in propylene selectivity and a 3.7 % increase in butylene selectivity are observed in case of coated monolith structure. The highest propylene selectivity in this study is observed to be 52 %.

Ethylene selectivity among the gaseous products ratios is observed to be almost the same for catalyst with lower SiO_2/Al_2O_3 ratios of 30 & 50. Since the ethylene is formed predominantly from aromatics and the hydrogen transfer reaction takes place preferably on strong acidic sites, a decrease in the production of ethylene is observed for higher SiO_2/Al_2O_3 ratios which favour lesser number of strong acid sites [104]. For the coated catalyst the ethylene selectivity was observed to decrease further from 16 % to 11 %. Since propylene selectivity is prioritized over ethylene selectivity, this ratio of propylene to ethylene is successfully achieved upto 4.7 % as shown in Figure 4.27.

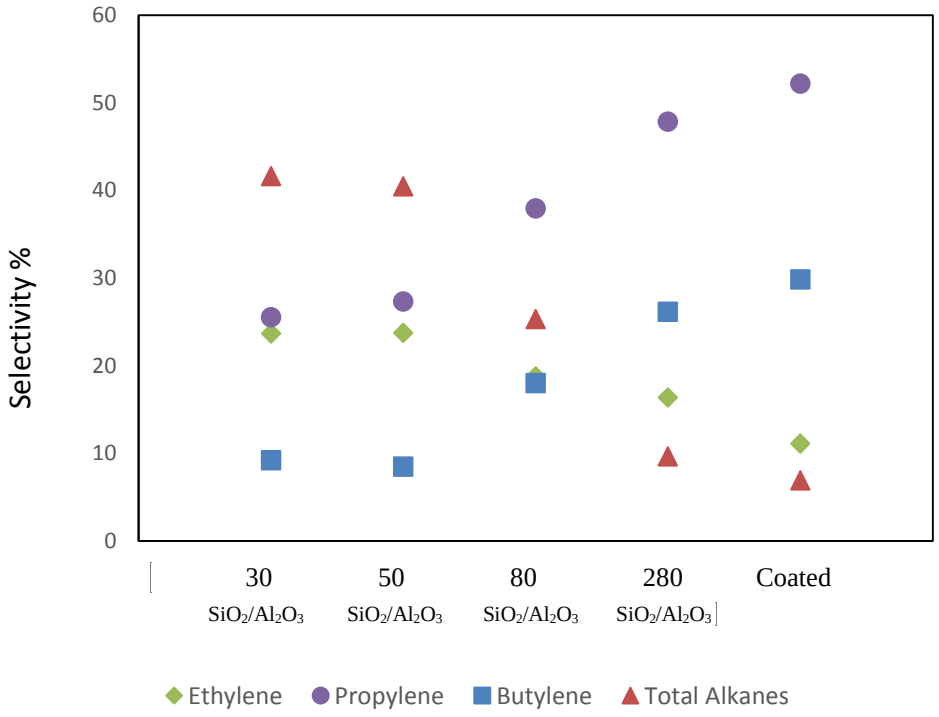

Figure 4-26: Product Selectivity trend at different SiO_2/Al_2O_3 ratio and Coating

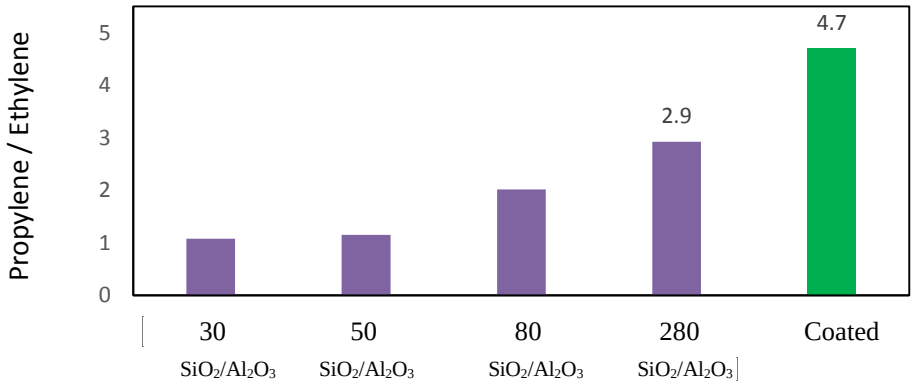

Figure 4-27: P/E ratio at WHSV of 15 h^{-1}

4.8 Stability Test

The catalytic performance of pelletized and monolith coated structure catalyst as a function of time are shown in Figure 4.28 and 4.29, in this figure the comparison among the yield, selectivity and conversion in pelletized and monolith coated catalyst is presented. For this analysis, the single coated structured catalyst was prepared and the same amount of loaded catalyst on the monolith is then tested in the reactor as pelletized catalyst. The coated catalyst leads to distinct improvement in the stability of methanol conversion. The conversion drops to 67 % after 42 hours when pelletized catalyst are evaluated. In case of monolith catalyst evaluation the methanol conversion after 42 hours is 80 %. The deactivation of zeolite catalyst in Methanol to hydrocarbon reactions is due to coke formation. It can be seen in the Figure 4.28 and 4.29 that ZSM-5 coated on monolith structure provide improved stability towards deactivation in comparison to the fixed bed of ZSM-5 pellets. Monolith catalyst shows higher propylene yield and selectivity. When the monolith catalyst is used the less crystalline diffusional resistance successfully suppress the side reactions formation which are responsible for the coke formation on the zeolite catalyst. The selectivity of propylene was slightly increased after some time indicating that catalytic deactivation by coke formation also suppress the formation of alkanes in gaseous phase.

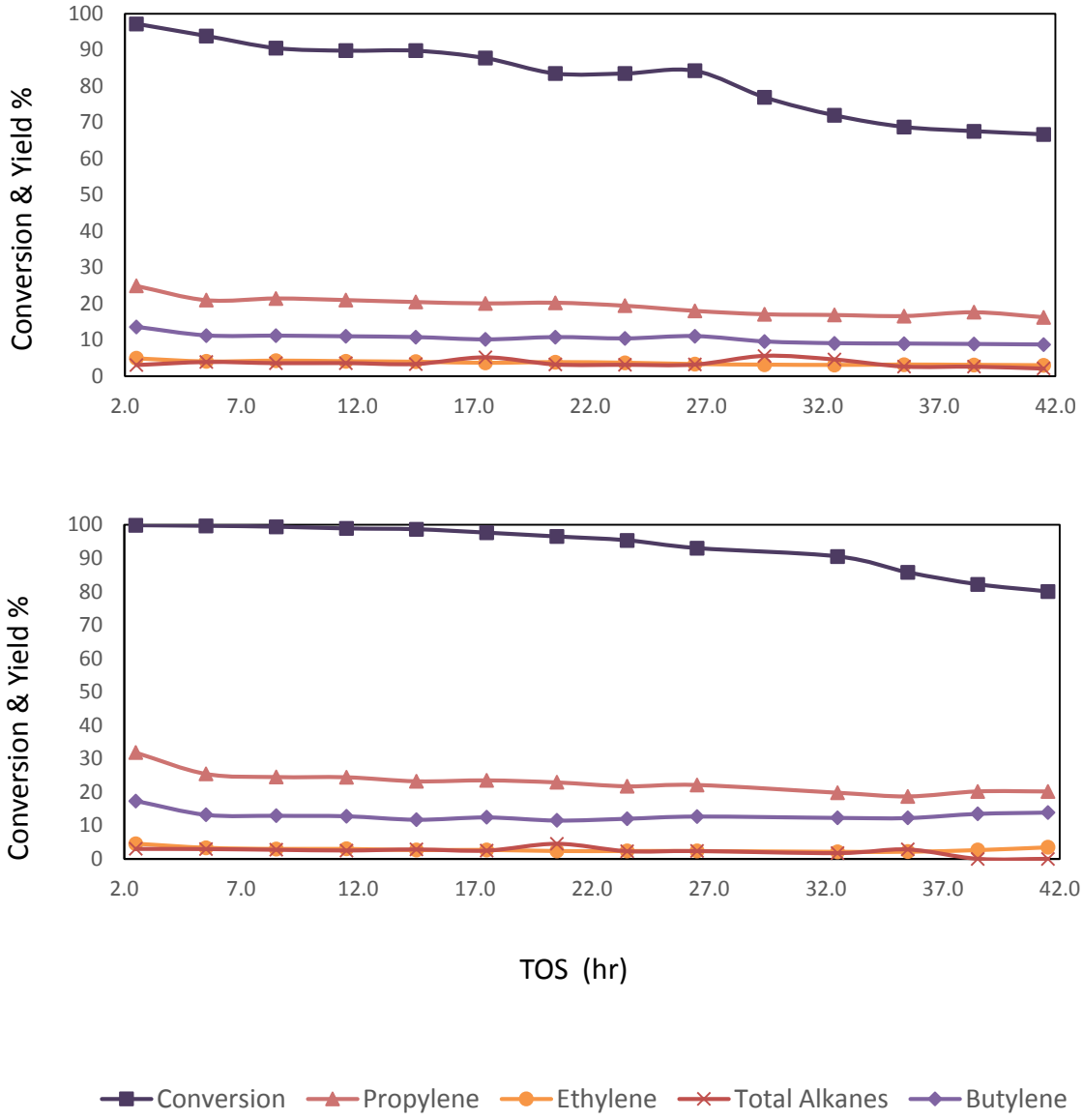

Figure 4-28: Effect of TOS on Conversion and Yield, Pelletized catalyst (upper) and Structure catalyst (lower)

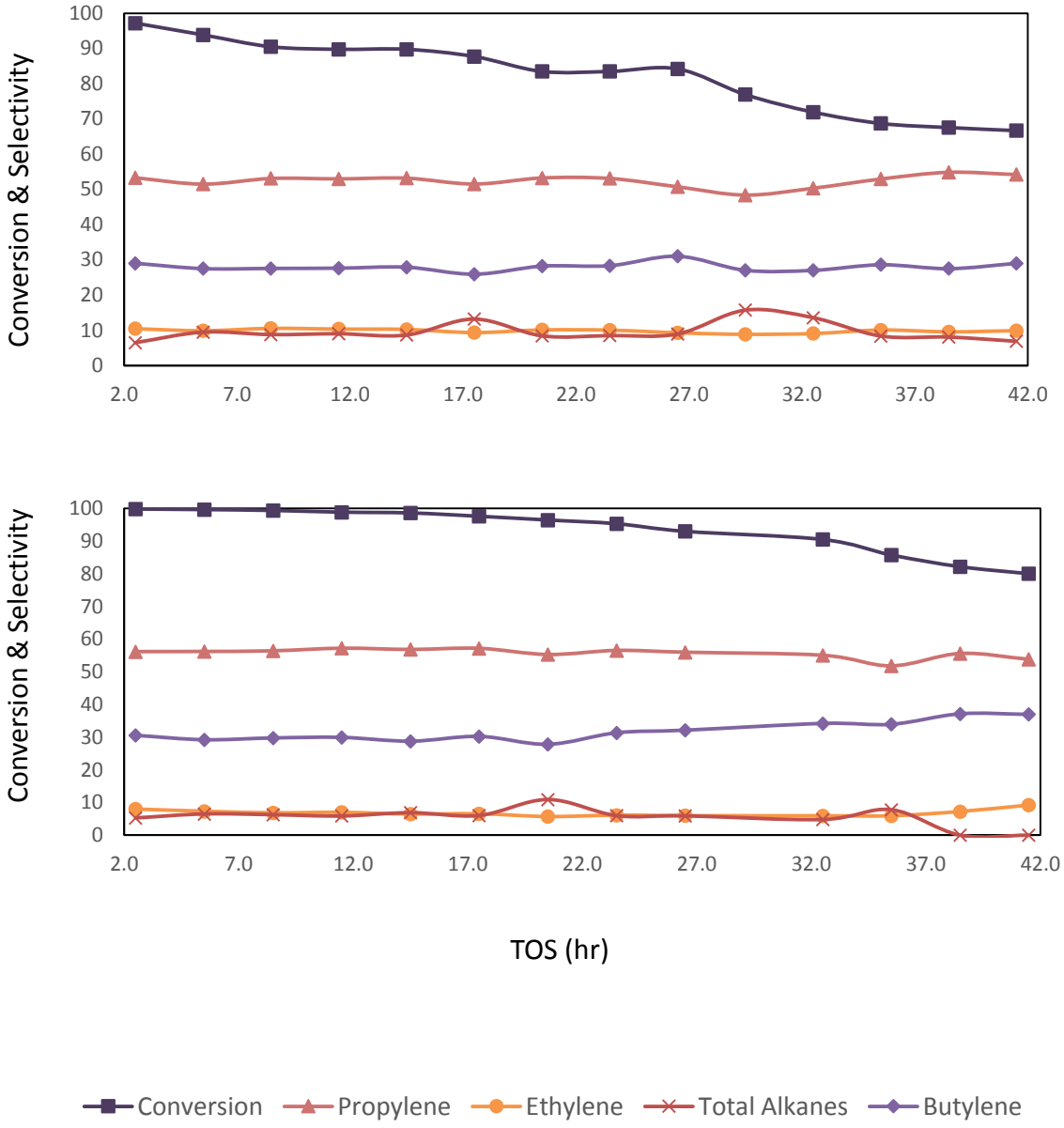

Figure 4-29: Effect of TOS on Conversion and Selectivity, Pelletized catalyst (upper) and Structure catalyst (lower)

CHAPTER 5

CONCLUSION AND RECOMMENDATIONS

5.1 Conclusion

A continuous flow fixed bed system used for the production of propylene through methanol over zeolite based catalyst having different catalytic properties was successfully investigated. Following are the conclusion of this study:

- ZSM-5 pelletized catalyst with varying SiO_2/Al_2O_3 molar ratios are evaluated and it was found that SiO_2/Al_2O_3 molar ratios of 280 showed the highest propylene yield and selectivity at 500 ^oC and atmospheric pressure.
- With the increase in the SiO_2/Al_2O_3 molar ratio the acidity of the catalyst decreases which increase the lighter olefins yield and decreased the formation of aromatics and paraffins.
- The catalyst deactivation at much higher SiO_2/Al_2O_3 molar ratio is due to total amount of acid sites on the catalyst surface is very low, even a small amount of acid site covered by the coke formation would lead towards an obvious decrease in the activity.
- Monolith coated catalyst performed better for higher propylene and butylene yield, the higher diffusivity of olefin products supress the secondary reactions.

- In monolith catalyst the aromatization reaction is significantly supressed and propylene become the predominant products, alkanes production decreased and almost negligible amount of aromatics are formed.
- On comparison of pelletized and monolith catalyst results, enhancement of propylene selectivity was achieved over monolith catalyst from 48% to 54 %.
- In monolith catalyst the minimization of diffusional resistances favours the production of propylene more than ethylene. Hence, increase in propylene/ethylene ratio from 2.9 to 4.7
- Monolith catalyst is more stable towards the deactivation of the catalyst, the deactivation is due to the coke formation on zeolite catalyst.

5.2 Recommendations

- Other structured substrates i.e. glass, SS, SiC foams can be used to prepare coated catalysts
- Metal impregnated ZSM-5 zeolite can be used to prepare the coated monolith catalysts.
- Use in-situ hydrothermal crystallization processes for the preparation of structured catalyst.
- Investigate the catalytic performance with different methanol/water ratio in feed.

References

[1] Z. Liu, C. Sun, G. Wang, Q. Wang, G. Cai, New progress in R&D of lower olefin synthesis, Fuel Process. Technol. 62 (2000) 161–172. doi:10.1016/S0378-3820(99)00117-4.

[2] IHS, IHS Chemical Economics Handbooks, (n.d.). www.ihs.com/products/chemical/planning/ceh/index.aspx?pu=1&rd=chemihs.

[3] S.M. Auerbach, K.A. Carrado, P.K. Dutta, Handbook of Zeolite Science and Technology, CRC Press, 2003. https://books.google.com/books?hl=en&lr=&id=iIi08k1iF4gC&pgis=1 (accessed October 21, 2015).

[4] Inc, IHS Global, (n.d.). www.ihs.com.

[5] T. Mokrani, M. Scurrell, Gas Conversion to Liquid Fuels and Chemicals: The Methanol Route- Catalysis and Processes Development, 2009. doi:10.1080/01614940802477524.

[6] https://www.kbr.com/, (n.d.). www.kbr.com.

[7] C.E. Kliewer, Zeolite Chemistry and Catalysis, (2009) 7–13. doi:10.1007/978-1-4020-9678-5.

[8] M. Stöcker, Methanol-to-hydrocarbons: catalytic materials and their behavior, Microporous Mesoporous Mater. 29 (1999) 3–48. doi:10.1016/S1387-1811(98)00319-9.

[9] M. Stöcker, Gas phase catalysis by zeolites, Microporous Mesoporous Mater. 82 (2005) 257–292. doi:10.1016/j.micromeso.2005.01.039.

[10] O. Paper, Catalytic Applications of Zeolites in Chemical Industry, (2009) 888–895. doi:10.1007/s11244-009-9226-0.

[11] K. Pangarkar, T.J. Schildhauer, J.R. van Ommen, J. Nijenhuis, F. Kapteijn, J.A. Moulijn, Structured Packings for Multiphase Catalytic Reactors, Ind. Eng. Chem.

Res. 47 (2008) 3720–3751. doi:10.1021/ie800067r.

[12] A.Q. Wang, D.B. Liang, T. Zhang, A novel method for synthesis of ZSM-5 coatings on monolithic cordierite substrate, Chinese J. Chem. 19 (2001) 227–232. http://www.scopus.com/inward/record.url?eid=2-s2.0-0039436622&partnerID=tZOtx3y1.

[13] M. a. Ulla, R. Mallada, J. Coronas, L. Gutierrez, E. Miró, J. Santamaría, Synthesis and characterization of ZSM-5 coatings onto cordierite honeycomb supports, Appl. Catal. A Gen. 253 (2003) 257–269. doi:10.1016/S0926-860X(03)00498-8.

[14] C. CHANG, The conversion of methanol and other O-compounds to hydrocarbons over zeolite catalysts, J. Catal. 47 (1977) 249–259. doi:10.1016/0021-9517(77)90172-5.

[15] J.F. Haw, W. Song, D.M. Marcus, J.B. Nicholas, The Mechanism of Methanol to Hydrocarbon Catalysis, Acc. Chem. Res. 36 (2003) 317–326. doi:10.1021/ar020006o.

[16] Conversion of methanol to products comprising gasoline boiling components, (1976). https://www.google.com/patents/US3969426 (accessed November 12, 2015).

[17] G. Ertl, H. Knozinger, F. Schuth, J. Weitkamp, eds., Handbook of Heterogeneous Catalysis, Wiley-VCH Verlag GmbH & Co. KGaA, Weinheim, Germany, 2008. doi:10.1002/9783527610044.

[18] J.Q. Chen, A. Bozzano, B. Glover, T. Fuglerud, S. Kvisle, Recent advancements in ethylene and propylene production using the UOP/Hydro MTO process, Catal. Today. 106 (2005) 103–107. doi:10.1016/j.cattod.2005.07.178.

[19] L.D. Hickman, D.A., Schmidt, Production of syngas by direct catalytic oxidation of methan, Science (80-.). 259 (1993) 343–346. doi:10.1126/science.259.5093.343.

[20] W.-Y. Wen, Mechanisms of Alkali Metal Catalysis in the Gasification of Coal, Char, or Graphite, Catal. Rev. 22 (2006) 1–28. doi:10.1080/03602458008066528.

[21] D. Sutton, B. Kelleher, J.R.H. Ross, Review of literature on catalysts for biomass

gasification, Fuel Process. Technol. 73 (2001) 155–173. doi:10.1016/S0378-3820(01)00208-9.

[22] J. Kim, C.A. Henao, T.A. Johnson, D.E. Dedrick, J.E. Miller, E.B. Stechel, et al., Methanol production from CO2 using solar-thermal energy: process development and techno-economic analysis, Energy Environ. Sci. 4 (2011) 3122. doi:10.1039/c1ee01311d.

[23] G.A. Olah, A. Goeppert, G.K.S. Prakash, Chemical recycling of carbon dioxide to methanol and dimethyl ether: from greenhouse gas to renewable, environmentally carbon neutral fuels and synthetic hydrocarbons., J. Org. Chem. 74 (2009) 487–98. doi:10.1021/jo801260f.

[24] www.methanol.org, (n.d.). www.methanol.org.

[25] H. Koempel, W. Liebner, Natural Gas Conversion VIII, Proceedings of the 8th Natural Gas Conversion Symposium, Elsevier, 2007. doi:10.1016/S0167-2991(07)80142-X.

[26] U. Olsbye, S. Svelle, M. Bjørgen, P. Beato, T.V.W. Janssens, F. Joensen, et al., Conversion of Methanol to Hydrocarbons: How Zeolite Cavity and Pore Size Controls Product Selectivity, Angew. Chemie Int. Ed. 51 (2012) 5810–5831. doi:10.1002/anie.201103657.

[27] B. Gerhard, H. Koempel, W. Liebner, H. Bach, Method and device for producing lower olefins from oxygenates, (2011). https://www.google.com/patents/US7923591 (accessed November 13, 2015).

[28] H. Koempel, W. Liebner, M. Wagner, Lurgi's gas to chemicals (GTC?): Advanced technologies for natural gas monetisation, Gastech Conf. Proc. (2005) 38.

[29] A. Corma, Inorganic Solid Acids and Their Use in Acid-Catalyzed Hydrocarbon Reactions, Chem. Rev. 95 (1995) 559–614. doi:10.1021/cr00035a006.

[30] IZA Commission of Natural Zeolites, (n.d.). www.iza-online.org.

[31] R.M. Barrer, Zeolites and clay minerals as sorbents and molecular sieves, (1978). http://agris.fao.org/agris-search/search.do?recordID=US201300556262 (accessed November 12, 2015).

[32] J. Jiang, J. Yu, A. Corma, Extra-large-pore zeolites: bridging the gap between micro and mesoporous structures., Angew. Chem. Int. Ed. Engl. 49 (2010) 3120–45. doi:10.1002/anie.200904016.

[33] D.S. Coombs, A. Alberti, T. Armbruster, G. Artioli, C. Colella, E. Galli, et al., Recommended nomenclature for zeolite minerals: report of the subcommittee on zeolites of the International Mineralogical Association, Commission on new Minerals and Mineral names, Can. Mineral. 35 (1997) 1571–1606. doi:10.1180/minmag.1997.061.405.13.

[34] A. Stewart, An Introduction to Zeolite Molecular Sieves by Alan Dyer. Wiley, Chichester, 1988. 164 pages. Price: £29.50. ISBN 0471 91981 0, Surf. Interface Anal. 14 (1989) 213–213. doi:10.1002/sia.740140410.

[35] J. Weitkamp, Zeolites and catalysis, Solid State Ionics. 131 (2000) 175–188. doi:10.1016/S0167-2738(00)00632-9.

[36] F. Di Renzo, Zeolites as tailor-made catalysts: Control of the crystal size, Catal. Today. 41 (1998) 37–40. doi:10.1016/S0920-5861(98)00036-4.

[37] M. Ackley, Application of natural zeolites in the purification and separation of gases, Microporous Mesoporous Mater. 61 (2003) 25–42. doi:10.1016/S1387-1811(03)00353-6.

[38] R.E. Morris, Ionic liquids and microwaves--making zeolites for emerging applications., Angew. Chem. Int. Ed. Engl. 47 (2008) 442–4. doi:10.1002/anie.200704888.

[39] A. Corma, L.T. Nemeth, M. Renz, S. Valencia, Sn-zeolite beta as a heterogeneous chemoselective catalyst for Baeyer-Villiger oxidations., Nature. 412 (2001) 423–5. doi:10.1038/35086546.

[40] M.E. Davis, Ordered porous materials for emerging applications., Nature. 417 (2002) 813–21. doi:10.1038/nature00785.

[41] A. Corma, State of the art and future challenges of zeolites as catalysts, J. Catal. 216 (2003) 298–312. doi:10.1016/S0021-9517(02)00132-X.

[42] J.A. Rabo, M.W. Schoonover, Early discoveries in zeolite chemistry and catalysis at Union Carbide, and follow-up in industrial catalysis, Appl. Catal. A Gen. 222 (2001) 261–275. doi:10.1016/S0926-860X(01)00840-7.

[43] J.A. Moulijn, M. Makkee, A.E. van Diepen, Chemical Process Technology, John Wiley & Sons, 2013. https://books.google.com/books?hl=en&lr=&id=3pQVEnGKvDgC&pgis=1 (accessed November 12, 2015).

[44] Introduction to Zeolite Science and Practice | 978-0-444-82421-9 | Elsevier, (n.d.). https://www.elsevier.com/books/introduction-to-zeolite-science-and-practice/van-bekkum/978-0-444-82421-9 (accessed November 12, 2015).

[45] B. Smit, T.L.M. Maesen, Towards a molecular understanding of shape selectivity., Nature. 451 (2008) 671–8. doi:10.1038/nature06552.

[46] Verified Synthesis of Zeolitic Materials | 978-0-444-50703-7 | Elsevier, (n.d.). https://www.elsevier.com/books/verified-synthesis-of-zeolitic-materials/robson/978-0-444-50703-7 (accessed November 13, 2015).

[47] P.M. Slangen, J.C. Jansen, H. van Bekkum, The effect of ageing on the microwave synthesis of zeolite NaA, Microporous Mater. 9 (1997) 259–265. doi:10.1016/S0927-6513(96)00119-8.

[48] K.E. Hamilton, E.N. Coker, A. Sacco, A.G. Dixon, R.W. Thompson, The effects of the silica source on the crystallization of zeolite NaX, Zeolites. 13 (1993) 645–653. doi:10.1016/0144-2449(93)90137-R.

[49] N.N. Feoktistova, S.P. Zhdanov, W. Lutz, M. Büllow, On the kinetics of crystallization of silicalite I, Zeolites. 9 (1989) 136–139. doi:10.1016/0144-2449(89)90063-8.

[50] H. Kacirek, H. Lechert, Growth of the zeolite type NaY, J. Phys. Chem. 79 (1975) 1589–1593. doi:10.1021/j100582a024.

[51] C.S. Cundy, P.A. Cox, The hydrothermal synthesis of zeolites: Precursors, intermediates and reaction mechanism, Microporous Mesoporous Mater. 82 (2005) 1–78. doi:10.1016/j.micromeso.2005.02.016.

[52] T. Kunieda, J.-H. Kim, M. Niwa, Source of Selectivity of p-Xylene Formation in the Toluene Disproportionation over HZSM-5 Zeolites, J. Catal. 188 (1999) 431–433. doi:10.1006/jcat.1999.2686.

[53] Integration of p-xylene production and subsequent conversion process, (2000). https://www.google.com/patents/US6133470 (accessed November 12, 2015).

[54] S. Fujiyama, S. Seino, N. Kamiya, K. Nishi, K. Yoza, Y. Yokomori, Adsorption structures of non-aromatic hydrocarbons on silicalite-1 using the single-crystal X-ray diffraction method., Phys. Chem. Chem. Phys. 16 (2014) 15839–45. doi:10.1039/c4cp01860e.

[55] A. Zamaniyan, Y. Mortazavi, A.A. Khodadadi, H. Manafi, Tube fitted bulk monolithic catalyst as novel structured reactor for gas–solid reactions, Appl. Catal. A Gen. 385 (2010) 214–223. doi:10.1016/j.apcata.2010.07.014.

[56] S. Roy, T. Bauer, M. Al-Dahhan, P. Lehner, T. Turek, Monoliths as multiphase reactors: A review, AIChE J. 50 (2004) 2918–2938. doi:10.1002/aic.10268.

[57] R.M. Heck, S. Gulati, R.J. Farrauto, The application of monoliths for gas phase catalytic reactions, Chem. Eng. J. 82 (2001) 149–156. doi:10.1016/S1385-8947(00)00365-X.

[58] P. Avila, M. Montes, E.E. Miró, Monolithic reactors for environmental applications, Chem. Eng. J. 109 (2005) 11–36. doi:10.1016/j.cej.2005.02.025.

[59] R.K. Edvinsson, A.M. Holmgren, S. Irandoust, Liquid-Phase Hydrogenation of Acetylene in a Monolithic Catalyst Reactor, Ind. Eng. Chem. Res. 34 (1995) 94–100. doi:10.1021/ie00040a007.

[60] C. Moreno-Castilla, A.F. Pérez-Cadenas, Carbon-based honeycomb monoliths for environmental gas-phase applications, Materials (Basel). 3 (2010) 1203–1227. doi:10.3390/ma3021203.

[61] J.G. Speight, Structured Catalysts and Reactors, 2006.

[62] H. Bode, ed., Materials Aspects in Automotive Catalytic Converters, Wiley-VCH Verlag GmbH & Co. KGaA, Weinheim, FRG, 2002. doi:10.1002/3527600531.

[63] H. Sun, X. Quan, S. Chen, H. Zhao, Y. Zhao, Preparation of well-adhered γ-Al2O3 washcoat on metallic wire mesh monoliths by electrophoretic deposition, Appl. Surf. Sci. 253 (2007) 3303–3310. doi:10.1016/j.apsusc.2006.07.044.

[64] W. Fei, S.C. Kuiry, Y. Sohn, S. Seal, Sol Gel Alumina Coating On Fe–Cr–Al–Y Fibre Media for Catalytic Converters, Surf. Eng. 19 (2003) 189–194. doi:10.1179/026708403225006249.

[65] J.L. Williams, Monolith structures , materials , properties and uses ଌ, 69 (2001) 3–9.

[66] E. García-Bordejé, F. Kapteijn, J.. Moulijn, Preparation and characterisation of carbon-coated monoliths for catalyst supports, Carbon N. Y. 40 (2002) 1079–1088. doi:10.1016/S0008-6223(01)00252-4.

[67] D. Zhao, P. Yang, B.F. Chmelka, G.D. Stucky, Multiphase Assembly of Mesoporous−Macroporous Membranes, Chem. Mater. 11 (1999) 1174–1178. doi:10.1021/cm980782j.

[68] Structured Catalysts and Reactors, CRC Press, 1997. https://books.google.com/books?hl=en&lr=&id=WRbXJgaTCyIC&pgis=1 (accessed November 21, 2015).

[69] T. Boger, A.K. Heibel, Heat transfer in conductive monolith structures, Chem. Eng. Sci. 60 (2005) 1823–1835. doi:10.1016/j.ces.2004.11.031.

[70] H. Liu, J. Zhao, C. Li, S. Ji, Conceptual design and CFD simulation of a novel metal-based monolith reactor with enhanced mass transfer, Catal. Today. 105 (2005) 401–406. doi:10.1016/j.cattod.2005.06.060.

[71] J.. Richardson, D. Remue, J.-K. Hung, Properties of ceramic foam catalyst supports: mass and heat transfer, Appl. Catal. A Gen. 250 (2003) 319–329. doi:10.1016/S0926-860X(03)00287-4.

[72] A.-M. Hilmen, E. Bergene, O.A. Lindvåg, D. Schanke, S. Eri, A. Holmen, Fischer–Tropsch synthesis on monolithic catalysts of different materials, Catal. Today. 69 (2001) 227–232. doi:10.1016/S0920-5861(01)00373-X.

[73] F. Kapteijn, T.. Nijhuis, J.. Heiszwolf, J.. Moulijn, New non-traditional multiphase

catalytic reactors based on monolithic structures, Catal. Today. 66 (2001) 133–144. doi:10.1016/S0920-5861(00)00614-3.

[74] T.A. Nijhuis, A.E.W. Beers, T. Vergunst, I. Hoek, F. Kapteijn, J.A. Moulijn, Preparation of monolithic catalysts, Catal. Rev. (2007). http://www.tandfonline.com/doi/abs/10.1081/CR-120001807 (accessed November 22, 2015).

[75] C. Agrafiotis, A. Tsetsekou, A. Ekonomakou, The effect of particle size on the adhesion properties of oxide washcoats on cordierite honeycombs, J. Mater. Sci. Lett. 18 (n.d.) 1421–1424. doi:10.1023/A:1006675524692.

[76] T. Vergunst, F. Kapteijn, J.A. Moulijn, Monolithic catalysts — non-uniform active phase distribution by impregnation, Appl. Catal. A Gen. 213 (2001) 179–187. doi:10.1016/S0926-860X(00)00896-6.

[77] D.S.C. Chairman, A. Alberti, T. Armbruster, G. Artioli, C. Colella, E. Galli, et al., Recommended nomenclature for zeolite minerals: report of the subcommittee on zeolites of the International Mineralogical Association, Commission on New Minerals and Mineral Names, Mineral. Mag. 62 (1998) 533–571. doi:10.1180/002646198547800.

[78] R. DESSAU, On the mechanism of methanol conversion to hydrocarbons over HZSM-5, J. Catal. 78 (1982) 136–141. doi:10.1016/0021-9517(82)90292-5.

[79] R. DESSAU, On the H-ZSM-5 catalyzed formation of ethylene from methanol or higher olefins, J. Catal. 99 (1986) 111–116. doi:10.1016/0021-9517(86)90204-6.

[80] I.M. Dahl, S. Kolboe, On the Reaction Mechanism for Hydrocarbon Formation from Methanol over SAPO-34, J. Catal. 161 (1996) 304–309. doi:10.1006/jcat.1996.0188.

[81] I.M. Dahl, S. Kolboe, On the reaction mechanism for propene formation in the MTO reaction over SAPO-34, Catal. Letters. 20 (1993) 329–336. doi:10.1007/BF00769305.

[82] I. Dahl, On the Reaction Mechanism for Hydrocarbon Formation from Methanol over SAPO-34 I. Isotopic Labeling Studies of the Co-Reaction of Ethene and Methanol, J. Catal. 149 (1994) 458–464. doi:10.1006/jcat.1994.1312.

[83] W. Wang, A. Buchholz, M. Seiler, M. Hunger, Evidence for an initiation of the methanol-to-olefin process by reactive surface methoxy groups on acidic zeolite catalysts., J. Am. Chem. Soc. 125 (2003) 15260–7. doi:10.1021/ja0304244.

[84] W. Wang, Y. Jiang, M. Hunger, Mechanistic investigations of the methanol-to-olefin (MTO) process on acidic zeolite catalysts by in situ solid-state NMR spectroscopy, Catal. Today. 113 (2006) 102–114. doi:10.1016/j.cattod.2005.11.015.

[85] U. Olsbye, M. Bjørgen, S. Svelle, K.-P. Lillerud, S. Kolboe, Mechanistic insight into the methanol-to-hydrocarbons reaction, Catal. Today. 106 (2005) 108–111. doi:10.1016/j.cattod.2005.07.135.

[86] M. Kaarsholm, B. Rafii, F. Joensen, R. Cenni, J. Chaouki, G.S. Patience, Kinetic modeling of methanol-to-olefin reaction over ZSM-5 in fluid bed, Ind. Eng. Chem. Res. 49 (2010) 29–38. doi:10.1021/ie900341t.

[87] W. Wu, W. Guo, W. Xiao, M. Luo, Dominant reaction pathway for methanol conversion to propene over high silicon H-ZSM-5, Chem. Eng. Sci. 66 (2011) 4722–4732. doi:10.1016/j.ces.2011.06.036.

[88] N. Hadi, A. Niaei, S.R. Nabavi, A. Farzi, M.N. Shirazi, Development of a new kinetic model for methanol to propylene process on Mn/H-ZSM-5 catalyst, Chem. Biochem. Eng. Q. 28 (2014) 53–63. http://www.scopus.com/inward/record.url?eid=2-s2.0-84898932030&partnerID=tZOtx3y1.

[89] A.E.W. Beers, T.A. Nijhuis, N. Aalders, F. Kapteijn, J.A. Moulijn, BEA coating of structured supports — performance in acylation, 243 (2003) 237–250.

[90] J. Lefevere, M. Gysen, S. Mullens, V. Meynen, J. Van Noyen, The benefit of design of support architectures for zeolite coated structured catalysts for methanol-to-olefin conversion, Catal. Today. 216 (2013) 18–23. doi:10.1016/j.cattod.2013.05.020.

[91] S. Ahmed, Methanol to olefins conversion over metal containing MFI-type zeolites, 19 (2012) 111–117. doi:10.1007/s10934-011-9454-0.

[92] A.T. Aguayo, D. Mier, A.G. Gayubo, M. Gamero, J. Bilbao, Kinetics of methanol transformation into hydrocarbons on a HZSM-5 zeolite catalyst at high

temperature (400-550 °c), Ind. Eng. Chem. Res. 49 (2010) 12371–12378. doi:10.1021/ie101047f.

[93] D. Mier, A.T. Aguayo, A.G. Gayubo, M. Olazar, J. Bilbao, Catalyst discrimination for olefin production by coupled methanol/n-butane cracking, Appl. Catal. A Gen. 383 (2010) 202–210. doi:10.1016/j.apcata.2010.05.052.

[94] T. Park, G.F. Froment, Kinetic Modeling of the Methanol to Olefins Process . 2 . Experimental Results , Model Discrimination , and Parameter Estimation, (2001) 4187–4196.

[95] P. Kumar, J.W. Thybaut, S. Svelle, U. Olsbye, G.B. Marin, Single-event microkinetics for methanol to olefins on H-ZSM-5, Ind. Eng. Chem. Res. 52 (2013) 1491–1507. doi:10.1021/ie301542c.

[96] S. Svelle, P.O. Rønning, U. Olsbye, S. Kolboe, Kinetic studies of zeolite-catalyzed methylation reactions. Part 2. Co-reaction of [12C]propene or [12C]n-butene and [13C]methanol, J. Catal. 234 (2005) 385–400. doi:10.1016/j.jcat.2005.06.028.

[97] C. Mei, P. Wen, Z. Liu, H. Liu, Y. Wang, W. Yang, et al., Selective production of propylene from methanol: Mesoporosity development in high silica HZSM-5, J. Catal. 258 (2008) 243–249. doi:10.1016/j.jcat.2008.06.019.

[98] L. Shirazi, E. Jamshidi, M.R. Ghasemi, The effect of Si/Al ratio of ZSM-5 zeolite on its morphology, acidity and crystal size, Cryst. Res. Technol. 43 (2008) 1300–1306. doi:10.1002/crat.200800149.

[99] C. Costa, I.. Dzikh, J.M. Lopes, F. Lemos, F.R. Ribeiro, Activity–acidity relationship in zeolite ZSM-5. Application of Brönsted-type equations, J. Mol. Catal. A Chem. 154 (2000) 193–201. doi:10.1016/S1381-1169(99)00374-X.

[100] K.S.W. Sing, Reporting physisorption data for gas/solid systems with special reference to the determination of surface area and porosity (Recommendations 1984), Pure Appl. Chem. 57 (1985) 603–619. doi:10.1351/pac198557040603.

[101] F. Ferreira Madeira, K. Ben Tayeb, L. Pinard, H. Vezin, S. Maury, N. Cadran, Ethanol transformation into hydrocarbons on ZSM-5 zeolites: Influence of Si/Al ratio on catalytic performances and deactivation rate. Study of the radical species role, Appl. Catal. A Gen. 443-444 (2012) 171–180. doi:10.1016/j.apcata.2012.07.037.

[102] C.D. Chang, Methanol Conversion to Light Olefins, Catal. Rev. 26 (2007) 323–345. doi:10.1080/01614948408064716.

[103] C.J. Brinker, G.C. Frye, A.J. Hurd, C.S. Ashley, Fundamentals of sol-gel dip coating, Thin Solid Films. 201 (1991) 97–108. doi:10.1016/0040-6090(91)90158-T.

[104] M. BJORGEN, S. SVELLE, F. JOENSEN, J. NERLOV, S. KOLBOE, F. BONINO, et al., Conversion of methanol to hydrocarbons over zeolite H-ZSM-5: On the origin of the olefinic species, J. Catal. 249 (2007) 195–207. doi:10.1016/j.jcat.2007.04.006.

Vitae

Name	Muhammad Haris
Nationality	Pakistani
Date of Birth	6/18/1985
Email	haris_amjad@yahoo.com
Contact #	+92-333-7838013
Address	House # 76/71 Al-Bagh manzil, Barkhan, District Barkhan, 84400, Balochistan, Pakistan
Educational Qualification	**B.Sc. Chemical Engineering**, (2005-2009) University of the Punjab, Lahore, Pakistan. **M.S Chemical Engineering**, (2013 - 2015) KFUPM, Dhahran, Saudi Arabia.
Industrial Experience	Internships at Fertilizer Plant, Natural Gas Distribution Company and Power Plant. 1.5 year in Process/Operation Department of Natural Gas Sweetening and Dehydration Plant. 2 years as Engineer (Operations) at well head gas compression facility